

**TRANSDUCTION OF VIRULENCE FACTORS BY ALPHAVIRUSES
IN VERTEBRATE AND INVERTEBRATE MODELS OF INFECTION**

by
John R. Clayton

A dissertation submitted to The Johns Hopkins University in conformity
with the requirements for the degree of Doctor of Philosophy

Baltimore, Maryland
October, 2010

© 2010 John R. Clayton
All rights reserved

Abstract

Arthropod-borne viruses (arboviruses) cause morbidity and mortality worldwide. Sindbis virus (SV) is an arbovirus and the prototype alphavirus. Recombinant alphaviruses were constructed to express cellular and virus-derived virulence factors in a vertebrate host, *Mus musculus*, and an invertebrate host, *Aedes aegypti*. Mosquitoes are responsible for transmitting numerous pathogens of public health importance, including dengue and yellow fever viruses and the malaria parasite.

Understanding the host response to virus infection will aid in developing novel disease control strategies. We developed a prime-challenge model of infection in mosquitoes to determine whether the anti-viral response mounted during a virus infection affects the outcome of a subsequent hyper-virulent infection by a related virus (SV-B2). Mosquitoes primed with SV were completely protected from a subsequent hyper-virulent challenge. Acquired resistance to SV-B2 is rapidly established and persists throughout life. Acquired protection is completely dependent on a productive primary infection, as neither UV-inactivated SV nor replication incompetent SV were able to elicit the protective phenotype. However, replication competent infectious RNA is sufficient to both initiate an infection and produce protection. Protection observed against a “killer” virus following a prime from an innocuous strain of the virus demonstrates acquired immunity to virus infection in a non-chordate animal, the potency of which illustrates the functional capacity of the mosquito anti-viral response.

The *Drosophila* death gene *reaper* was evaluated as a candidate biopesticide effector molecule. Reaper is an important regulator of programmed cell death responsible

for activating caspases by binding inhibitors of apoptosis and targeting them for degradation. Mosquitoes infected *per os* with an insect-derived strain of SV expressing Reaper displayed enhanced mortality compared to controls, indicating the feasibility of this strategy to kill insects. The NSs protein from the Orthobunyavirus San Angelo virus is an important virulence determinant that bears sequence similarity to Reaper. NSs is presumed to exert its virulence by inhibiting host gene expression, but the mechanism of NSs toxicity remains unknown. Mice infected with SV-NSs display enhanced mortality that is dependent on residues shared with Reaper. Expression of virulence factors in distinct infection models highlights similarities and differences in requirements for virulence in animals *in vivo*.

Thesis Readers

Dr. J. Marie Hardwick (Primary Advisor)
Professor
Department of Molecular Microbiology and Immunology
Johns Hopkins Bloomberg School of Public Health

Dr. Gary Ketner
Professor
Department of Molecular Microbiology and Immunology
Johns Hopkins Bloomberg School of Public Health

Dr. Terry Brown
Professor
Department of Biochemistry and Molecular Biology
Johns Hopkins Bloomberg School of Public Health

Dr. Valeria Culotta
Professor
Department of Biochemistry and Molecular Biology
Johns Hopkins Bloomberg School of Public Health

*Dedicated to my wonderful mother and father,
for their unwavering and unconditional support.
I could not ask for better parents.*

Acknowledgements

There are so many people to thank. Of course, I am eternally grateful and indebted to my thesis advisor, Marie, for her patience, support and understanding during trouble-free and difficult times alike. Of the many things I have learned in Marie's laboratory, the thing I consider most valuable is the capacity I have gained to critically evaluate scientific data. Marie is correct about things most of the time, regardless of whether I realize it.

Starting at the beginning, I would like to thank some of my earliest teachers. I was never the best student, but I hold in my mind certain individuals who helped me at even the earliest stages of my personal and professional development. Namely, Lou Ann Lester, my third and fourth grade teacher, whose kindness and compassion made a difficult transitional period in my young life much more bearable. I must also thank Toni Majers-Andersen for her exceptional talents teaching Spanish and for kindling my interest in linguistics in general. From high school, I would like to thank my journalism teacher, Tom Brennan, from whom I learned that teachers are actually real human beings. I would also like to thank my high school biology teacher, Chuck Copeland, who gave me the only "C" I got in high school (which I deserved), for teaching me about Mendelian inheritance.

I would like to thank my undergraduate advisor, Brent Mishler, who allowed me to work in his lab even though I had no idea what I was doing. Brent also facilitated my first scientific meeting by helping me get my first travel grant. Through Brent I learned to view all of biology in an evolutionary framework or as Dobzhansky famously wrote, "Nothing in biology makes sense except in the light of evolution."

To my supervisor at CDC, Mark Benedict, I owe my initiation into the vector

biology field as well as my first taste of what Richard Feynman called “The kick in the discovery,” that narcotic sense of experiencing an experimental result that no one has ever seen or done before you; the feeling that keeps us going the rest of the time. Mark was also great about allowing me to pursue my professional development. I must also thank my colleagues from that important time, including Bill Collins, Gena Groner, Fernando Monteiro, Martin Donnelly, Audrey Lenhart, Cristina Rafferty and Debbie Deppe.

To Fotis Kafatos, my supervisor at EMBL, I owe a special thank-you. Fotis took a chance on me when he didn’t have to. He fought for me to be regarded as a staff member and all of the benefits that come with that status, rather than as a temporary employee. He and the other members of the lab, including Gareth Lycett, Stephan Meister, Stéphanie Blandin, Jennifer Volz, Claudia Blass, Giorgos Christophides and Elena Levashina facilitated my career development and general outlook on the scientific endeavor profoundly. I owe Fotis a debt of gratitude that I will never be able to repay.

At JHSPH, I would like to thank the many students who impacted me along the way. In particular, I would like to thank Amy Baker-Greer, Mike Overstreet, Mark Siracusa, Tara Martinez, Judy Easterbrook, Mike Smeaton, Matt Beattie, Lindsey Garver, Kristen Gibson, Martin Devenport, Heidi Galonek, Jennifer Drummond, Chris Cirimotich and Kelly Leach. I would also like to thank all members of the Hardwick lab, past and present, for their help and support along the way.

I must thank my family members for their continued support after all these years. In particular, I would like to thank my uncle Dan and aunt Idelle. We have been out of touch, but they have always been there. Aunt Carrie and uncle Tony are two of the finest people I have ever had the pleasure of knowing. I must also give thanks to my brother and sister, who can be a real pain in the ass, but who will always be my brother and sister.

Finally, I thank my thesis advisory committee members and readers, past and present, for their thoughtful and insightful comments, advice and help over the years.

Contents

Abstract	ii
Dedication	iv
Acknowledgements	v
Contents	vii
List of Figures	xii
Chapter 1 Introduction	1
Introduction to the Alphaviruses	1
Alphaviruses and vector-borne disease	1
Alphavirus structure, genome and replication	3
Pathogenesis of alphaviruses in vertebrates	4
Sindbis virus pathogenesis in invertebrates	6
Superinfection exclusion	7
Cell death in virus infection	9
Programmed cell death	9
Viral factors affecting extrinsic cell death pathways	11
Viral factors affecting the intrinsic cell death pathway	14
Viral factors affecting caspase activation	16

Virulence determinants used in this work	17
Flock House virus B2	17
Drosophila Reaper	18
Bunyavirus NSs	18
Questions addressed and hypotheses tested	19
Chapter 2 Specific acquired resistance to virus infection in the Yellow Fever mosquito <i>Aedes aegypti</i>	21
Introduction	21
Arboviruses and vector control	21
RNAi is an essential component of insect anti-viral immunity	22
Homologous interference among alphaviruses	23
The prime-challenge model of infection	23
Acquired resistance to Sindbis virus infection	24
Materials and methods	25
Cell lines	25
Insect rearing	25
Virus constructs	26
In vitro transcription of infectious virus	27
Rescue of recombinant virus	28
Plaque assays	28
SV infection of BHK cells	29
Microscopy	29
The prime-challenge model and virus infections	29
Quantitative RT-PCR	30
Results	31
Replication of hypervirulent SV in Aedes aegypti	31

Priming with avirulent SV protects against subsequent hypervirulent challenge	33
Protection develops rapidly and persists throughout life	35
Acquired protection is sequence specific	37
Priming virus replication is necessary for acquired protection	41
Discussion	42
Chapter 3 Evaluating recombinant Sindbis virus expressing <i>reaper</i> for use as a biopesticide	57
Introduction	57
Mosquitoes as disease vectors	57
Biopesticides for insect control	58
Drosophila Reaper as a biopesticide effector	58
Alphaviruses as gene expression vectors	59
Materials and methods	60
Cell lines	60
Insect rearing	61
Virus constructs	62
Cell counts and viability stains	63
In vitro transcription of infectious virus	63
Rescue of recombinant virus	64
Plaque assays	64
Western blotting	65
Microscopy	65
Virus injections	66
Feeding <i>per os</i>	67
Virus decay assay	67

Results	68
Vertebrate-adapted SV expressing reaper enhances mosquito cell death in a manner dependent on the IAP-binding motif	68
An orally infectious clone of Sindbis virus expressing <i>reaper</i> enhances cell death in an IBM-dependent manner	69
Imaging mosquitoes infected by MRE16-GFP <i>in vivo</i>	71
Disseminated infection with SV-Rpr kills mosquitoes in an age dependent manner when injected	73
Infection of adult <i>Aedes aegypti</i> <i>per os</i> with MRE16-SV in sucrose or a bloodmeal	75
Discussion	77
Chapter 4 Functional analysis of San Angelo virus NSs in the Sindbis virus neurovirulence model	85
Introduction	85
Bunyavirus NSs	85
Similarities between NSs and Reaper	86
Functional analysis of NSs by heterologous expression in SV	87
Materials and methods	88
Cell lines	88
In vitro transcription of NSs mRNAs	89
Transfection of NSs RNAs	90
NSs co-transfection assay	90
Cell counts and viability stains	90
Immunofluorescence imaging	91
Live cell imaging	91
Protein blotting	92

Virus constructs	92
In vitro transcription of infectious virus	93
Rescue of recombinant virus	94
Plaque assays	94
Virus injections	95
Results	95
NSs toxicity in vertebrate cells	95
NSs protein suppresses GFP expression in <i>trans</i>	96
Localization of NSs mutants	100
Survival Analysis	103
Discussion	104
Conclusions and general discussion	109
References	113
Appendix I Oligonucleotide and probe sequences	129
Appendix II Perl script for comparing identity blocks	134
Curriculum vitae	138

List of Figures

Figure 1-1	Arbovirus transmission cycle	2
Figure 1-2	Replication cycle of Sindbis virus	5
Figure 1-3	Adult female <i>Aedes aegypti</i> , lateral aspect	7
Figure 1-4	Cell death signaling during virus infection	12
Figure 2-1	Hypervirulent Sindbis Virus kills adult <i>Aedes aegypti</i>	34
Figure 2-2	Infection with SV induces protection against a subsequent hypervirulent challenge by SV-B2	36
Figure 2-3	Acquired protection to hypervirulent SV is sequence-dependent	39
Figure 2-4	Determining the minimum molecular requirements for protection	43
Figure 2-5	A model for sequence-specific anti-viral protection in insects	45
Figure 2-6	Replication of SV constructs in BHK cells	47
Figure 2-7	Correlation of molecular and functional readouts of virus replication	48
Figure 2-8	Priming with SV-GFP protects against challenge with SV-Rpr	49
Figure 2-9	Comparison of nucleotide identity blocks between alphaviruses	50
Figure 2-10	Replication of VEEV constructs (PFU/mosquito)	51
Figure 2-11	Replication of VEEV constructs (RNA copies/mosquito) . .	52
Figure 2-12	VEEV-B2 does not kill mosquitoes	53
Figure 2-13	Killing by dsTE12Q-B2 in animals inoculated with MRE16 SV	54
Figure 2-14	Killing by SV-B2 in VEEV-infected mosquitoes	55
Figure 2-15	SV-B2 enhances virulence in four day old CD1 mice	56

Figure 3-1	Alphavirus expression constructs used in the study	61
Figure 3-2	Recombinant, vertebrate-adapted Sindbis viruses (dsTE12Q) expressing Reaper enhance mosquito cell death in an IAP-dependent manner	70
Figure 3-3	An orally infectious clone of Sindbis virus (dsMRE16) expressing Reaper enhances mosquito cell death in an IAP-dependent manner	72
Figure 3-4	Infection <i>per os</i> of <i>Aedes aegypti</i> by MRE16-SV gives rise to a systemic infection	74
Figure 3-5	Disseminated infection with SV-Rpr kills mosquitoes in an age dependent manner <i>in vivo</i> when injected	76
Figure 3-6	Infection <i>per os</i> of adult <i>Aedes aegypti</i> with MRE16-SV . . .	78
Figure 3-7	Reduction in viability of C7-10 cells infected with SV-Rpr . .	81
Figure 3-8	Tricine-SDS-PAGE protein blot from HeLa lysates with α -HA antibody	82
Figure 3-9	MRE16-Rpr does not kill 3-day old mosquitoes by 15 days when injected	83
Figure 3-10	Stability of MRE16-Rpr after incubation for one or two hours at 37°C	84
Figure 4-1	Alphavirus expression constructs used	89
Figure 4-2	NSs RNA is toxic to HeLa cells	97
Figure 4-3	Functional NSs protein inhibits EGFP expression in <i>trans</i> . .	99
Figure 4-4	Expression of NSs mutants in BHK and HeLa cells	101
Figure 4-5	Sub-cellular localization of NSs in HeLa cells.	102
Figure 4-6	Survival of CD1 mice infected with NSs mutants	106
Figure 4-7	Functional NSs protein inhibits EGFP expression in <i>trans</i> . .	107
Figure 4-8	Survival of CD1 mice infected with NSs mutants	108

Chapter 1

Introduction

Introduction to the Alphaviruses

Alphaviruses and vector-borne disease

Viruses are obligate intracellular pathogens. The alphaviruses are a genus of neurotropic RNA viruses of the *Togaviridae* virus family that can cause encephalitis, arthritis and febrile illness in a variety of vertebrate hosts including humans, horses and birds. Alphaviruses include the etiological agents of infectious viral outbreaks such as Eastern Equine Encephalitis virus (EEEV), Chikungunya virus (CHIKV) and O'nyong'nyong virus (ONNV) and are distributed across all continents [1]. Alphaviruses cycle between vertebrate hosts, usually birds, and invertebrate hosts, usually mosquitoes, and both hosts are essential for alphavirus propagation in nature [2]. Hematophagous insects obtain nutrients to produce eggs by drawing blood from vertebrate animals which are therefore essential for completion of the mosquito life cycle. Transmission of pathogens to the insect vector occurs when a susceptible mosquito takes a bloodmeal from an infected vertebrate host. Conversely, arthropod-borne viruses (or Arboviruses, a polyphyletic grouping encompassing several virus

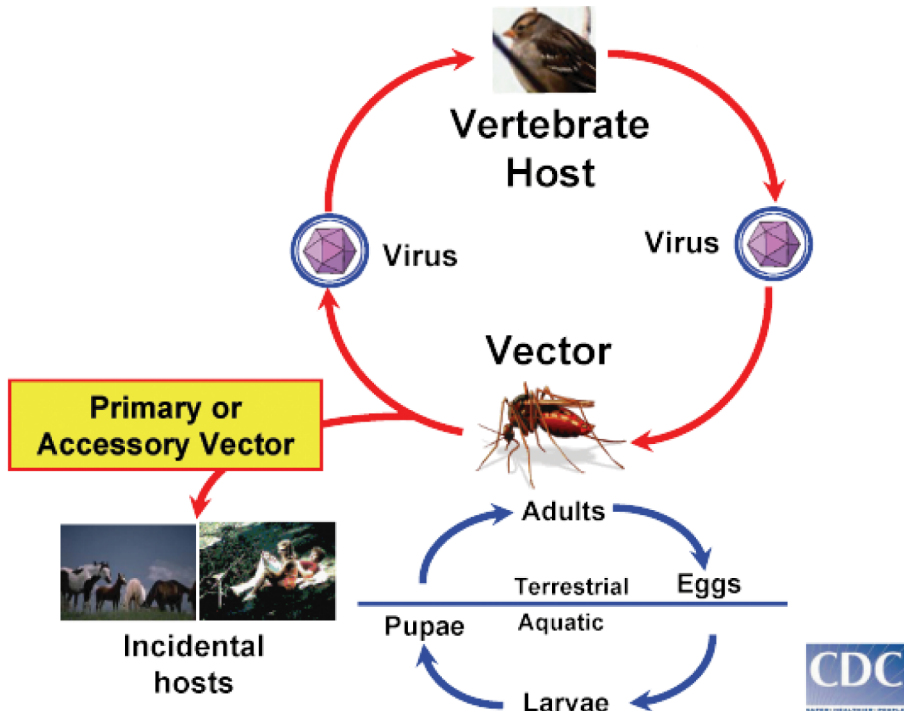


Figure 1-1. Arbovirus transmission cycle. Infection of incidental hosts can occur through transmission by the primary vector responsible for maintenance of the virus in nature or from an accessory vector less important in the enzootic transmission cycle. Adapted from *CDC.gov* [4].

families) are transmitted to susceptible vertebrate hosts during bloodfeeding by an infected insect. Transmission from the mosquito back to the vertebrate host occurs after an incubation period dependent on both extrinsic and intrinsic factors, such as the virus strain, species of mosquito and environmental conditions [3]. Infectious agents transmitted in this manner are said to be vector-borne. Such pathogens require productive infections in both the vertebrate and insect hosts for their transmission and maintenance in nature. Often, humans are incidental or “dead-end” hosts for these normally enzootic viruses, where the principal amplifying host (or reservoir) is another vertebrate such as a bird (Figure 1-1) [2].

Alphavirus structure, genome and replication

Sindbis virus (SV) is the prototype alphavirus, possessing a non-segmented, single-stranded RNA genome of positive polarity. The 11.7 kb RNA genome mimics a cellular mRNA with both a 5'-terminal cap and a 3'-terminal poly-adenine tail (Figure 2-1A) [5]. The virion particle consists of the encapsidated genome surrounded by a host-derived phospholipid envelope embedded with virus-encoded glycoprotein spikes in an icosahedral symmetry essential for cellular invasion [1, 6, 7]. Upon entry into the host cell endosome, a pH reduction causes a conformational change in the glycoprotein spikes, resulting in fusion of the viral membrane (envelope) to the pre-lysosomal membrane and release of the nucleocapsid into the cytoplasm, where it rapidly uncoats and is translated on cellular ribosomes, first producing the non-structural proteins (Figure 1-2) [8–10]. Four non-structural proteins (nsP1-4) are synthesized as a single polyprotein (nsP1234) comprising the N-terminal two-thirds of the virus genome to form the replication complex [1]. A series of proteolytic cleavages of the replication complex by nsP2 result in the synthesis of minus-strand RNA and its subsequent cessation [11]. The viral replicase complex produces a negative-sense anti-genome (minus strand replication intermediate) that serves as the template for both full-length genomes and a high-abundance subgenomic RNA that is translated into the structural proteins of the virus, which are encoded in the 3' third of the viral genome [1, 6]. The subgenomic RNA encodes the structural proteins of the virus that are cleaved from a single polyprotein by viral capsid (C) and cellular proteases into several proteins (C, E3, E2, 6K and E1) [1, 6]. The subgenomic promoter on the negative-sense anti-genome is used by the virus RNA-dependent RNA polymerase (RdRp) complex to synthesize large amounts of the structural protein mRNA [12] (see Figure 2-1A, 3-1 and 4-1). It is this powerful subgenomic promoter, combined with a broad cellular tropism, which enables the use of SV as a recombinant viral expression vector for genes of interest [13, 14]. After replicating its genome and producing the structural proteins necessary

to assemble new virions, infectious SV particles bud from the plasma membrane [9].

Pathogenesis of alphaviruses in vertebrates

Alphaviruses replicate in a wide variety of vertebrate tissues *in vivo* as well as many cultured cell lines *in vitro* [6, 13]. Susceptible host cell types include epidermal dendritic cells (Langerhans cells), lymphoid cells, skeletal muscle, brown fat and neurons [1]. After extravascular deposition in the dermis by the bite of a mosquito, the virus is taken into the bloodstream and lymphoid tissues, probably by Langerhans cells, where it has access to the numerous target tissues permissive for replication and amplification [6]. Virions circulating in the bloodstream are subsequently acquired by naïve mosquitoes during bloodfeeding. Humans are generally considered to be incidental dead-end hosts in the transmission cycle, not producing sufficient viremia to transmit an infection to mosquitoes [15]. Infection of amplifying vertebrate hosts, therefore, is critical for the maintenance of transmission [16]. In the laboratory, newborn mice exhibit enhanced susceptibility to virus infection compared to adult mice, making SV infection of neonatal mice an attractive neurovirulence model for pediatric viral encephalitis [17, 18]. Infection of vertebrate cells by SV *in vitro* is generally characterized by an acute replication phase followed by cell death 24-48 hours post-infection. The cytopathology observed in the acute infection of cultured cells bears the hallmarks of apoptosis, including chromatin condensation, DNA cleavage (laddering) and membrane blebbing [19, 20]. Furthermore, overexpression of human Bcl-2 in some cell lines is sufficient to rescue cells from death induced by infection with SV, resulting in a persistent infection that likely mimics the situation in the brain [20]. Endogenous and exogenously expressed Bcl-2 (via SV-Bcl-2) in mice has a similar protective effect, significantly increasing the survival of SV-infected neonatal mice [21]. While inhibiting apoptosis clearly affects the outcome of infection, the signals upstream that mediate its onset are less well characterized. Cellular perturbations

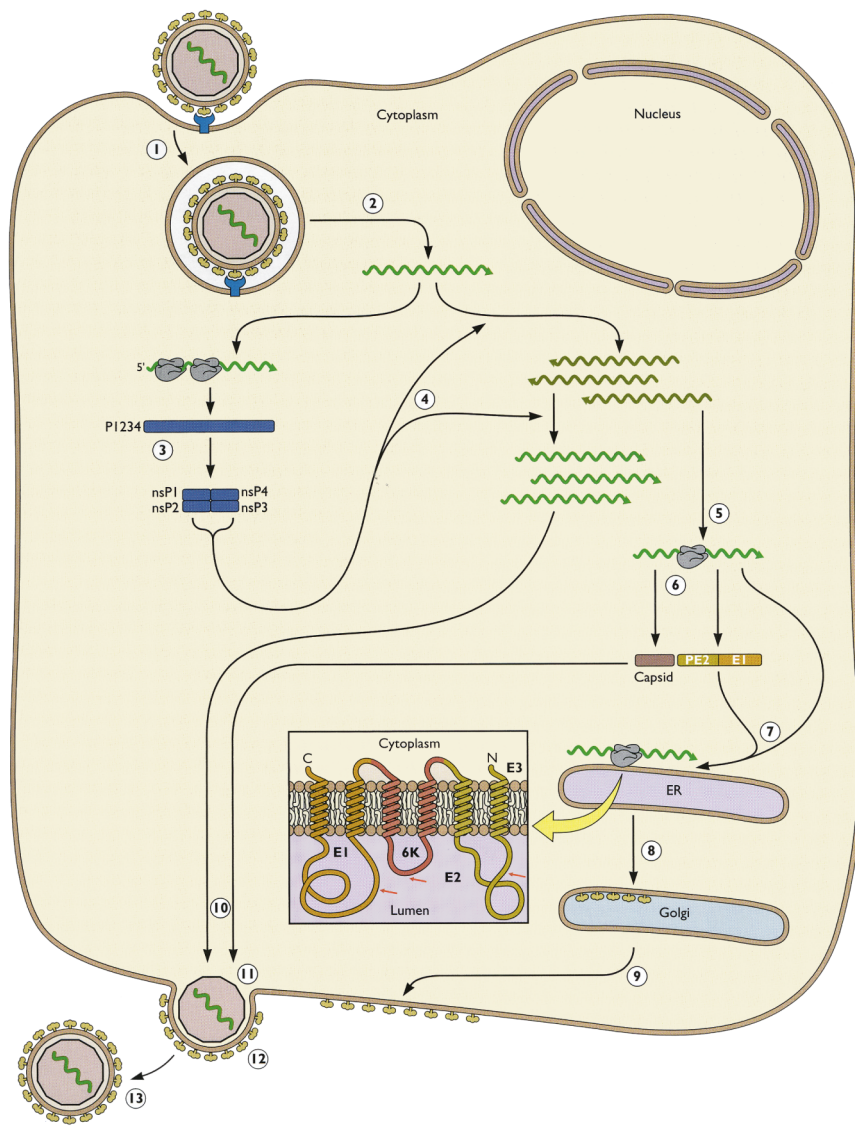


Figure 1-2. Replication cycle of Sindbis virus. (1) Receptor-mediated endocytosis of the virion. (2) Fusion of the virion from the endosome and uncoating of the virus genome. (3) Genomic RNA is immediately translated on cellular ribosomse to produce the non-structural polyprotein. (4) Processing of the replication complex formed by the non-structural proteins results in the production of minus-sense anti-genomes (early) and plus-sense full length genomes (late). (5) Further processing of the replication complex gives rise to the sub-genomic RNA transcript encoding the structural proteins. The virus envelope glycoproteins are translated at the ER (7) and migrate through the Golgi apparatus (8) before being transported to the plasma membrane (9). The capsid protein associates with full-length positive- polarity genomes (10) and progeny virions bud from the plasma membrane (11,12). Proteolytic maturation of the glycoprotein spikes gives rise to the infectious virus particle (13). Adapted from Enquist [7].

caused by SV that precede cell death include inhibition of cellular protein translation, the depletion of cellular NAD stores and the activation of caspases resulting in the cleavage and inactivation of poly-ADP-ribose polymerase (PARP) by caspase-3 [22]. However, virus-parasitized cells that are actively synthesizing viral macromolecules from limited cellular resources are likely to be compromised in their usual functions, ultimately leading to cell suicide.

Sindbis virus pathogenesis in invertebrates

Sindbis virus infection of cultured mosquito cells is characterized by a non-lytic acute replication phase followed by a persistent replication phase [23]. As in vertebrates, SV displays a wide tissue tropism in mosquitoes *in vivo*, infecting both the luminal and basal surfaces of the gut, musculature, circulating hemocytes, fat body, salivary glands and central nervous system, including the brain.(Figure 1-3) [23–26]. Despite this pan-tropic tissue distribution, mosquitoes infected with SV and other alphaviruses are not generally thought to display enhanced mortality relative to uninfected animals, although this varies by strain. This belief has lead to the general feeling that infection of the insect host is relatively innocuous [1]. This is not always the case, however, as reductions in fitness have been observed in some vector-pathogen combinations [27–29]. Primary infection of the gut epithelia occurs after the uptake of a virus-containing bloodmeal by the arthropod host [30, 31]. Viruses that bud from the basal surface of the gut epithelia subsequently cross the basal lamina into the circulation of the hemocoel [32]. Once disseminated into the circulation, the virus has access to the acinar cells of the salivary glands, which it must invade to be transmitted during a subsequent bloodfeeding. Productive infection of the salivary gland cells persists and the insect is infectious for the remainder of its life [33].

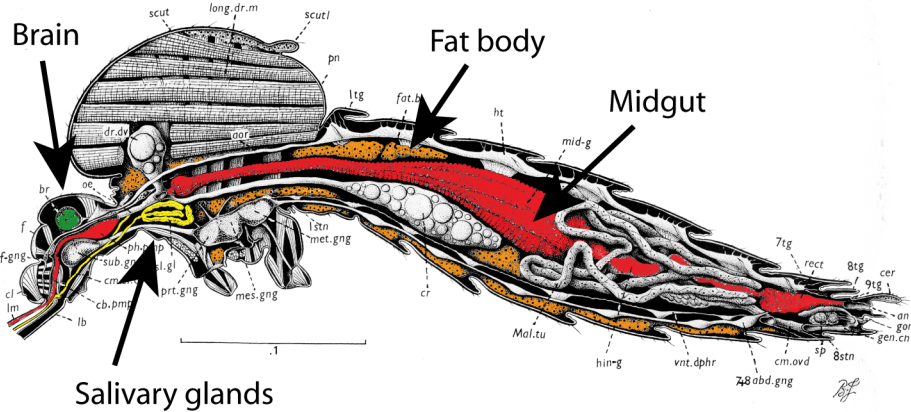


Figure 1-3. Adult female *Aedes aegypti*, lateral aspect. Selected tissues relevant to arbovirus infection are highlighted. Viruses are acquired during bloodfeeding and infect the epithelia of the midgut. Viruses released from the basal surface of the midgut enter the circulation and establish a disseminated, systemic infection of peripheral tissues. The distribution of tissues susceptible to infection varies by virus species and strain, but all arboviruses must ultimately infect the salivary glands to be transmitted to a naive host during a subsequent feeding. Adapted from Jobling [34].

Superinfection exclusion

Homologous interference, or superinfection exclusion, describes a phenomenon in which cells infected with a particular virus become refractory to infection by a related virus at a later time [1]. Superinfection exclusion has been described for many distinct groups of viruses and is thought to be a common strategy by which individual virus strains facilitate their own spread and transmission, preventing co-infection by and hence competition with closely related viruses [35–41]. Exclusion of superinfecting Sindbis virus in chicken embryo (CE) cells is completely established within one hour of primary infection [38]. The exclusion phenotype is conditional in the temperature-sensitive mutant *ts-24*, which possesses a mutation (G736S) in nsP2 that destroys its protease activity and prevents proteolytic processing of the non-structural proteins [42, 43]. It was also shown that while non-structural proteins of the superinfecting virus are translated, minus-strand synthesis is blocked [44]. Exclusion of the second incoming virus is suggested to occur when the first virus infection has progressed to a point

where the nsP2 protease is cleaved from its nsP23 polyprotein to release a more active protease capable of cleaving substrates in *trans*. Thus, nsP2 protease produced by the first virus is suggested to cleave prematurely the precursor nsP123 polyprotein of the incoming second (superinfecting) virus, before the production of minus strand replication intermediates of the second incoming viral genome. Because the nsP123 + nsP4 replication complex is required specifically for production of minus strand intermediates, successful replication of the second incoming virus is greatly impaired due to premature proteolytic processing of its nsP123 by the nsP2 of the first virus [1, 11].

Homologous (same virus species) and heterologous (related virus species) interference have been shown to operate in mosquito cells, although the phenomenon is less well characterized in that system [45, 46]. Although the available data do not disprove the hypothesis of a *trans*-acting nsP2 protease, there are unsatisfying elements of the model as described above, particularly in the invertebrate system. While superinfection exclusion in vertebrate cells appears to develop rapidly, requiring only the expression of non-structural proteins, this is not the case in mosquito cells, which synthesize minus-strand RNA continuously and require 10 hours or more to develop the exclusion phenotype [11, 44, 45]. Furthermore, it was also shown in mosquito cells that while homologous SV was effectively excluded, heterologous EEEV was not, suggesting that related but sufficiently diverged viruses are incapable of excluding each other [46]. Nor is another New World serogroup alphavirus, VEEV, capable of excluding SV (see Chapter 2) in mosquitoes *in vivo*. Both of these viruses belong to the VEE/EEE species complex. Another study showed that SV was indeed capable of excluding three heterologous alphaviruses: Aura virus, also from the SIN species complex, and Semliki Forest and Ross River viruses, of the SF species complex [47, 48]. The available data suggest, therefore, that SV is capable of excluding members of two predominantly Old World subgroups of alphaviruses (SF and SIN complexes) but not the related

viruses of the New World serogroup, VEEV and EEEV. The kinetics of developing the superinfection exclusion phenotype are also markedly different, taking 10 times longer to develop in insect cells than in vertebrate cells and longer than the entire replication cycle of the virus, suggesting the involvement of a host-mediated response to virus infection in arthropods [6, 45]. Insects use the endogenous RNA-interference machinery to recognize and degrade infectious non-self nucleic acids, such as virus and transposable element replication intermediates, in a sequence dependent manner [49, 50]. It is reasonable to suggest and consistent with the available data that the phenomenon of homologous interference (or superinfection exclusion) in mosquito cells is actually an induced, host-encoded, phenotypic manifestation of the insect response to virus infection.

Cell death in virus infection

Programmed cell death

Any process by which cells participate in their own death can be defined as programmed cell death. Cell suicide programs are facilitated by the actions of gene products encoded by the cell destined to die. These death-promoting genes evolved, at least in part, for the purpose of orchestrating cell-autonomous death [51]. The term apoptosis describes the morphology of naturally occurring programmed cell death during development and following certain pathological stimuli [52, 53]. In contrast to this deliberate cell death, the term necrosis describes cell morphology that was assumed until recently to be due exclusively to non-programmed, accidental cell death caused by acute injury [52]. However, new gene-directed (programmed) cell death pathways (including some accidental death, e.g. ischemic injury following trauma) are currently being delineated [54]. These pathways are dependent on lysosomal proteases, non-apoptotic

caspases and more recently, the kinase activity of RIPK1 that mediates necroptosis [55]. Apoptosis can also be used as a mechanistic term that refers to all types of programmed cell death, but is more commonly reserved to describe caspase-dependent cell death, as caspases are now known to be responsible for many of the morphological and biochemical features of classical apoptosis [51]. In multicellular organisms, programmed cell death is essential for development, tissue homeostasis and regulating immune responses [51]. In humans, it is estimated that billions of cells normally die per day by programmed death and insufficient or excessive cell death characterizes most human disease states, including virus infections [56]. Classical apoptosis is characterized by numerous morphological and biochemical changes, including condensation of chromatin, cleavage of DNA between nucleosomes (DNA laddering), plasma membrane blebbing, exposure of phosphatidyl-serine on the outer leaflet of the plasma membrane (detected by annexin V binding), and fragmentation/division of mitochondria [56, 57]. These events are caused by the activity of a subset of intracellular proteases known as caspases. Caspases are a family of cysteine proteases that cleave after specific aspartate residues in several hundred cellular proteins [58, 59]. A second subset of caspases includes the proteases that activate inflammatory mechanisms and may promote non-apoptotic programmed cell death [60]. Any perturbation of the cell can potentially lead to activation of programmed cell death as a host defense mechanism to eliminate aberrant, damaged or tumorigenic cells. Similarly, virus infection of a cell usually triggers the activation of programmed cell death, and failure of this defense mechanism is likely due to specific virus-encoded strategies to manipulate the host cell [56, 61]. The ability of cells to recognize intruding viruses and to activate cell suicide provides an important host defense mechanism for eliminating viruses and other intracellular pathogens by eliminating virus-infected cells. Some viruses, such as Baculoviruses, cause pathogenesis by inhibiting apoptosis [62], while other viruses, such as Sindbis virus, cause disease primarily by inducing host cell death [21, 56, 63]. As such, viruses

have developed a myriad of mechanisms to adapt to and regulate cellular death processes.

Viral factors affecting extrinsic cell death pathways

Of the multiple pathways leading to cell death, caspase-dependent apoptosis is the best characterized. There are two general pathways for activating caspases, the receptor-activated (extrinsic) pathway and the mitochondria-dependent (intrinsic) pathway [51]. Different viruses regulate multiple steps in both of these pathways (Figure 1-4). Receptor-mediated pathways for the activation of caspases can be further subdivided into two groups, cell surface death receptors of the TNFR (tumor necrosis factor receptor) superfamily, and the intracellular pattern recognition receptors that activate primarily inflammatory caspases [64–66]. The cytoplasmic portions of death receptors recruit and activate long pro-domain caspases (for example, caspase-8). In turn, caspase-8 cleaves and activates the short pro-domain caspases (for example, caspase-3) [58, 59]. Caspase-3 is responsible for cleaving most of the known cellular substrates to facilitate apoptotic cell death [51, 59]. Death receptor pathways are regulated by both viral and cellular FLICE-interacting proteins (FLIPs) that bind to receptor complexes in a manner that prevents caspase activation [56, 63, 65]. Viral FLIP proteins (vFLIPs) encoded by herpesviruses modulate the activation of caspase-8 by mimicking the death effector domain (DED) of caspases and competitively binding with the DED domain of FADD, thereby preventing the oligomerization of preformed caspase-8-containing complexes [65, 67]. Cellular counterparts of vFLIPs were later identified to function as negative regulators and mimics of full-length pro-caspase-8 and -10, except that they are catalytically inactive. Short cFLIPs are similar to viral FLIPs and consist of only two DED domains, corresponding to the two DED domains in the pro-domain of caspase-8 [68, 69].

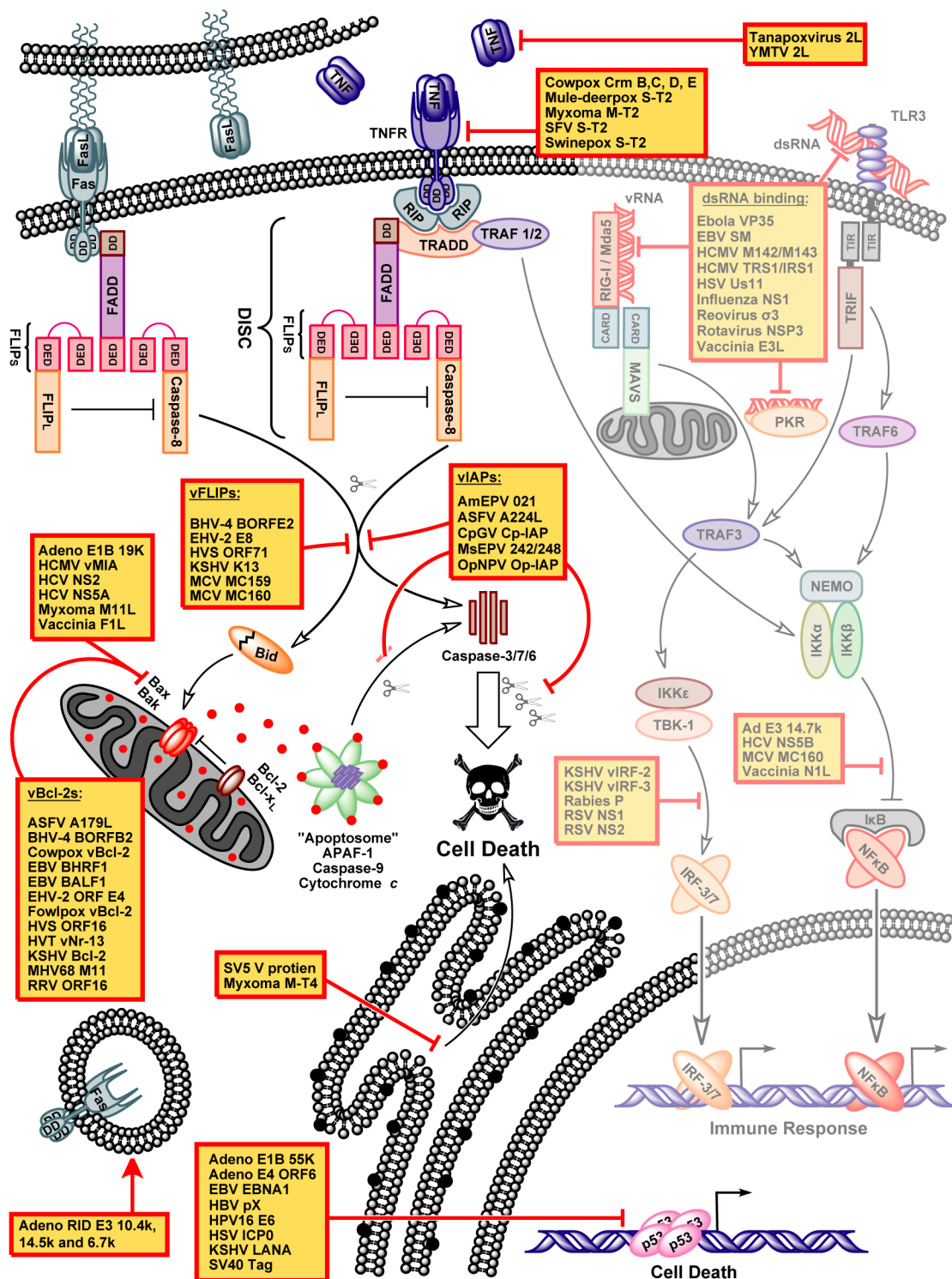


Figure 1-4. Cell death signaling during virus infection. Virus-encoded factors are boxed in red. Grayed areas indicate innate immune signaling. Adapted from Clayton [70].

The second receptor subgroup includes the pattern recognition receptors (PRRs), which can be further subdivided into three groups: the plasma membrane Toll-like receptor (TLR) family that detects extracellular pathogens [71, 72] and two cytosolic receptor families, the NLRs (NOD-like receptors) [73, 74] and the pattern recognition helicases RIG-I and Mda5 (RLH) [75, 76], all of which are capable of detecting non-self nucleic acids and initiating a cellular response to them. NLRs are activators of the inflammasome, which contains activated caspase-1 (ICE) that cleaves the pro-cytokine IL-1 β in addition to indirectly activating IRF-3 and NF- κ B [73, 77]. The cytosolic RLH receptors recognize viral nucleic acids and trigger the activation of IRF-3 and IRF-7 as well as NF- κ B [78]. Similarly, TLR-3, -7 and -9 signal the detection of extracellular pathogen-associated molecular patterns (PAMPs) via endosomes to activate IRF-3, IRF-7 and NF- κ B [76]. Although often considered the mediators of survival due to their induction of cell death inhibitors, pro-inflammatory transcription factors also contribute to “pyroptosis”, or inflammatory apoptosis, the end result of which is the production of cytokines with concomitant dismantling of the cell [79]. Recent advances in anti-viral pattern recognition have yielded the discovery of the helicases RIG-I and MDA5 as well as their downstream signaling partner, the CARD-containing mitochondrial anti-viral signaling protein (MAVS) [80, 81]. The wide variety of viruses that encode proteins to obstruct RLH signaling during early infection underscores its important role. The protease NS3/4A from the flavivirus hepatitis C virus (HCV) cleaves and inactivates MAVS, thereby short-circuiting virus recognition and signaling through the CARD [82, 83]. Meanwhile, the same protease also cleaves the toll/interleukin-1 receptor (TIR) domain-containing adaptor-inducing IFN- β (TRIF) and short-circuits TLR signaling as well [84]. Vaccinia virus A46R contains a TIR domain to sequester TRIF away from TLR3, thus preventing the recognition of viral antigens [85, 86]. RNA binding proteins encoded by both RNA viruses (influenza [87, 88], Ebola virus [89–91], reovirus [92]) and DNA viruses (Vaccinia

virus [93], Epstein Barr virus [94] and Herpes Simplex virus [95, 96]) have also been implicated in modulating cellular RNA levels. The virus-associated interfering RNA (VAI) encoded by adenovirus acts at least in part by forming dsRNA structures that can be loaded into the RNA-induced silencing complex and act as competitive inhibitors for Dicer endonuclease and also producing virus-derived effector siRNAs [97–99].

Viral factors affecting the intrinsic cell death pathway

The mitochondrial pathway for activating caspases is triggered when cytochrome *c* and other factors are released from the intermembrane space of mitochondria into the cytoplasm [100]. Cytosolic cytochrome *c* and a molecule of ATP bind to Apaf-1 resulting in oligomerization of Apaf-1 to form the apoptosome [101]. This complex recruits and activates caspase-9 by a yet unclarified mechanism [102]. Like the dimerization-induced activation of caspase-8 by death receptors, dimerization of caspase-9 via the DED-like CARD (caspase-recruitment domain) in the N-terminal pro-domain of caspase-9 is thought to activate the caspase-9 protease [103]. New evidence indicates that full activation of upstream initiator caspases (for example, caspase-8 and -9) requires both oligomerization and proteolytic processing of the pro-caspases into their active subunits [104]. In contrast, downstream effector caspases (for example, caspase-3 and -7) are activated when they are proteolytically cleaved by the upstream initiator caspases. Like caspase-8, activated caspase-9 also cleaves and activates caspase-3 to mediate apoptotic cell death [105, 106].

Initiation of the mitochondrial pathway is regulated by pro- and anti-apoptotic cellular Bcl-2 family proteins that promote or inhibit cytochrome *c* release [107]. Multi BH-domain pro-apoptotic Bcl-2 family members Bax and Bak are widely believed to homo-oligomerize in the mitochondrial outer membrane to form the pores that release

cytochrome *c* and other factors [108]. This function of Bax and Bak is inhibited by anti-apoptotic Bcl-2 family members Bcl-2, Bcl-x_L and others [51]. Anti-apoptotic members work by directly binding pro-death family members and by binding and inhibiting the activators of Bax and Bak (Bid, Bim, and possibly PUMA) [109–111]. A second subclass of pro-death Bcl-2 family members (e.g. BAD, Bmf, Hrk) are thought to directly antagonize the anti-apoptotic Bcl-2 proteins in response to specific cell stress stimuli [109, 112, 113]. Cross-talk between the extrinsic and intrinsic pathways potentially serves to amplify the apoptotic signals from the extrinsic pathway by involving the mitochondrial pathway. This occurs when receptor-activated caspase-8 cleaves and activates the pro-death protein Bid, which in turn activates Bax- or Bak-mediated cytochrome *c* release [114, 115]. Although Bid is the most widely studied caspase-cleaved Bcl-2 family member, our lab first demonstrated this phenomenon by showing that Bcl-2 and Bcl-x_L can be cleaved by caspases to convert their anti-death activities into pro-death activity [116–118]. In contrast, virus-encoded Bcl-2 homologs are refractory to conversion into pro-death factors [119]. Three-dimensional structure determinations have revealed that the vaccine strain of vaccinia virus encodes 9 ORFs (8 unique proteins) with Bcl-2-like structure, although these proteins lack significant amino acid sequence similarity [106]. However, few if any of these viral Bcl-2-like proteins appear to regulate apoptosis.

In contrast to the mainstream hypothesis for Bcl-2 family proteins described above, our lab has reported many examples where anti-death and pro-death Bcl-2 family proteins can exhibit opposite cell death/survival functions, challenging prevailing opinions [65]. This was initially revealed by inserting Bax into the Sindbis virus vector and infecting mice, where Sindbis virus predominantly replicates in neurons of brain. Although Bax was expected to increase neuronal death during infection, Bax (and Bak) unexpectedly protects neurons and dramatically increases mouse survival rates [120–122]. In contrast to mice, cell lines infected with SV-Bax or SV-Bak

exhibit increased cell death compared to control viruses [123]. These unexpected findings in SV-Bax/Bak-infected mice were further verified for endogenous proteins by infecting knockout mice lacking either Bax or Bak. Although these knockout mice were previously shown to have only minor (*bax*^{-/-}) or no (*bak*^{-/-}) known phenotypes, they exhibit significantly reduced survival rates following Sindbis virus infection compared to littermate controls [120, 122]. Thus, endogenous Bax and Bak increase the survival of young mice, contrary to expectations. These *in vivo* studies were confirmed using *in vitro* cultured organotypic tissue slices of brains from mice deficient for these genes. These and other studies led to the emerging viewpoint that Bcl-2 family proteins have alternative functions in healthy cells [122, 124].

Viral factors affecting caspase activation

Viruses also modulate caspase activity, encoding inhibitors of both pro-apoptotic and pro-inflammatory caspases [125, 126]. The baculovirus P35 protein is a caspase pseudosubstrate and effectively inhibits caspases by binding into the caspase active site [127, 128]. In addition to being the first molecule of its kind to be discovered, P35 has proven to be an important tool due to its ability to inhibit a wide variety of caspases [129]. To date, there are no cellular homologs of this viral protein that directly inhibit caspases. Yet another class of caspase regulators discovered in baculoviruses are the inhibitor of apoptosis proteins (IAPs) [130]. Viral IAPs are related to cellular IAPs and are the only known direct caspase inhibitors in mammals [130]. IAPs are characterized by their baculovirus inhibitory repeat (BIR) domains and by a C-terminal RING finger domain with E3 ubiquitin ligase activity that targets its substrates for proteasomal degradation [127]. Poxviruses encode RING finger proteins that are suggested to have E3 ubiquitin ligase activity, though they lack overall amino sequence similarity to the IAP family [131]. An important poxvirus caspase inhibitor produced by vaccinia and the closely related cowpox virus is CrmA, a member of the serine protease inhibitor

(serpin) superfamily. CrmA inhibits both serine and cysteine proteases, including caspases-1, -8 and -10 [132]. Myxoma virus (Serp-2) can inhibit caspases as well as the related cysteine protease granzyme B [133]. Myxoma virus E13L also acts at the level of caspase activation by binding and inhibiting the apoptosis-associated speck-like protein containing a CARD (ASC) protein, a component of the caspase-1-activating inflammasome complex. Suppression of cell death through the modulation of caspase activity is a widely used strategy by which viruses of all types subvert host cell responses.

Virulence determinants used in this work

Flock House virus B2

Flock House virus (FHV) is a plus-sense single-stranded RNA insect virus of the *Nodaviridae*[134]. The FHV genome is bipartite, consisting of two segments, RNA1 and RNA2. RNA1 encodes the RNA-dependent RNA polymerase (protein A) and RNA2 encodes the capsid protein (protein α). RNA1 also gives rise to RNA3 from a sub-genomic promoter [135]. The single protein made by RNA3 is B2, a non-structural virulence determinant [136]. B2 is a well characterized virus-encoded suppressor of RNAi that is thought to act by sequestering double-stranded RNA in a sequence-independent fashion and preventing its recognition by the host [137–139]. A direct interaction has been shown between B2 and Dicer-2 and infection of *Drosophila* with FHV results in a lethal infection dependant on the presence of the B2 gene [136, 140]. Induction of the *vago* anti-viral effector through *Dcr-2* is suppressed in transgenic flies expressing B2 during an infection with *Drosophila C* virus (DCV) [50]. Phenotypically, heterologous expression of FHV B2 by an alphavirus results in a highly-virulent infection in a broad range of host mosquitoes including all three genera of disease

vectoring mosquitoes: *Aedes*, *Anopheles* and *Culex* [141, 142]. Mutational analysis showed that B2 killing in mosquitoes was completely dependent on its capacity to bind RNA [141].

Drosophila Reaper

The *Drosophila* gene *reaper* was originally discovered in a genetic screen of mutants deficient for embryonic cell death [143]. The amino-terminal consensus sequence [A-(V/T/I)-(P/A)-(F/Y/I/V/S)] shared by Reaper was subsequently shown to be essential for binding the BIR domain of *Drosophila* IAP1 (DIAP) preceding its ubiquitylation, thus promoting its degradation [51, 144, 145]. Uninhibited by IAPs, active caspases are free to engage their polypeptide substrates, resulting in apoptotic cell death [146, 147]. Reaper was also reported to act as a general inhibitor of translation that binds directly to the 40S ribosomal subunit independent of its described role in binding IAPs and promoting the degradation of IAPs [148] and more recently implicated in self-association and mitochondrial permeabilization in response to damage [149, 150].

Bunyavirus NSs

The *Bunyaviridae* are a family of enveloped, single-stranded, negative-sense RNA viruses that include many human pathogens of public health importance. Notable among these are viruses of the *Hantavirus* genus, the etiological agents of hantavirus pulmonary syndrome (HPS) [151] and Crimean-Congo hemorrhagic fever virus of the *Nairovirus* genus, a highly virulent pathogen requiring Biosafety Level-4 (BSL-4) containment that causes mortality in as many as 50% of infected humans [152]. The tripartite genomic structure of the *Bunyaviridae* is conserved between genera and consists of large (L), medium (M) and small (S) RNA segments [7]. The large segment encodes the viral polymerase. The M RNA segment encodes a single ORF

that is cleaved co-translationally into two glycoproteins (Gn and Gc) and a poorly characterized non-structural protein (NSm) [6, 153]. The S RNA segment encodes the nucleocapsid coat protein as well as another poorly understood non-structural protein (NSs) of 97 amino acids encoded in an overlapping reading frame [154, 155]. Recent studies investigating the function of NSs have found it to be an important determinant of virulence *in vivo*, despite being dispensable for virus replication *in vitro* [156]. Bunyavirus NSs was suggested to bear primary sequence similarity to the 65 amino acid *Drosophila* death protein Reaper [157] (see previous section 1). Using purified recombinant or synthetic proteins, Colón-Ramos and colleagues reported that Reaper and NSs were both capable of inhibiting cellular protein translation in transcriptionally inactive *Xenopus* extracts. Reaper's translational inhibition is independent of its ability to bind IAP proteins and residues shared between Reaper and NSs were shown to be critical for global inhibition of cellular translation [148, 157]. Both Reaper and NSs possess the capacity to bind to and modulate the activity of the hsp70 chaperone Scythe [157, 158], further supporting convergent functions for Reaper and NSs.

Questions addressed and hypotheses tested

Although the replication cycle and host immune response to alphavirus infection have been studied extensively, less is known about the determinants of virulence. Functional analysis of the three virulence enhancing factors described in Chapter 1 was performed by heterologous expression in recombinant Sindbis viruses to gain a better understanding of the basic cellular processes involved in a virulent virus infection. My first aim was to determine the effect on survival of a pre-existing virus infection on a subsequent encounter with a lethal strain of Sindbis virus (SV-B2) that is capable of suppressing anti-viral RNAi in the mosquito. My next aim was

to determine the effect of enhanced, virus induced cell death on the virulence of Sindbis virus in mosquitoes by evaluating the efficacy of the *Drosophila* protein Reaper as a potential biopesticide effector molecule. The orally infectious strain of SV, dsMRE16, was evaluated concurrently as a delivery vehicle to determine its suitability for eventual incorporation into a vector control strategy. My third and final aim was to perform mutational analysis on San Angelo virus NSs at residues shared with Reaper to parse the distinct reported functions of NSs, including the inhibition of gene expression and the activation of caspases, to determine which are necessary to enhance virulence of Sindbis virus in mice. Together, these functional analyses shed light on the effect of these virulence determinants on host cell processes in both vertebrate and invertebrate arbovirus hosts.

Chapter 2

Specific acquired resistance to virus infection in the Yellow Fever mosquito *Aedes aegypti*

Introduction

Arboviruses and vector control

Arboviruses cause morbidity and mortality worldwide. Sindbis virus (SV) is an arbovirus and the prototype alphavirus [2, 6, 48]. Mosquitoes are responsible for transmitting numerous human pathogens of public health importance, including dengue, Chikungunya, and yellow fever viruses and the malaria parasite [2]. Understanding the insect response to virus infection will aid in developing novel disease and vector control strategies. In contrast to the disease-vector mosquito eradication strategies of the past, newer strategies aimed to reduce the competence of the vector mosquito to transmit pathogens have been proposed as a potential means of disease control [159–161]. These strategies are proposed to operate by rendering mosquitoes refractory to infection by

a human pathogen such as *Plasmodium* or dengue virus or by shortening the vector life-span so that they do not contribute to the disease transmitting population pool [162–165].

RNAi is an essential component of insect anti-viral immunity

RNA interference (RNAi) is a form of post-transcriptional gene regulation ubiquitous in animals whereby double-stranded RNA precursors are cleaved by the endonuclease Dicer into small interfering RNAs of 21-23nt in length and loaded into a protein complex called the RNA-induced silencing complex (RISC) [166–168]. Small-interfering RNAs in the RISC then direct the cleavage and degradation of single-stranded target RNAs by an argonaute family endonuclease (AGO2) [168]. In flies, RNAi was shown to be an essential component of insect anti-viral defense acting to suppress infection through the elimination of transiently produced double-stranded RNA (dsRNA) virus replication intermediates [50, 136, 169, 170]. The virulence factor B2 from Flock house virus (FHV) is a known suppressor of RNAi that binds the sugar-phosphate backbone of dsRNA in a sequence-independent manner [138, 139]. A direct interaction has been shown between B2 and Dicer-2, and infection of *Drosophila* with FHV results in a lethal infection dependent on the presence of the B2 gene [136, 140]. Furthermore, induction of the *vago* anti-viral effector is inhibited in transgenic flies expressing B2 during an infection with *Drosophila* C virus (DCV), indicating a disruption of signaling through *Dcr-2* [50]. Similarly, heterologous expression of FHV B2 by an alphavirus results in a highly-virulent infection in a broad range of host mosquitoes including all three genera of disease vector mosquitoes: *Aedes*, *Anopheles* and *Culex* [141, 142]. In contrast, however, to these highly virulent strains carrying the RNAi suppressor B2, alphavirus infection in mosquitoes is classically characterized by persistent, life-long virus replication with varying degrees of cellular pathology and little to no mortality

in the host [25, 171].

Homologous interference among alphaviruses

Superinfection exclusion, or homologous interference, is a phenomenon described for numerous virus groups, primarily in cell culture models, whereby cells infected with a given virus rapidly develop resistance to further infection by the same or similar viruses [45]. Although the precise mechanism of homologous interference in alphaviruses is not known, a current model proposes a critical role for the nsP2 protease in processing the superinfecting replication complex such that minus-strand synthesis does not proceed [11]. Developing superinfection exclusion in vertebrate cells requires only the translation of the virus non-structural proteins and is established within one hour of infection [38]. By contrast, homologous interference in mosquito C7-10 cells is not established until 10 hours post-infection, longer than an entire virus replication cycle in vertebrate cells [6]. Together, these observations suggest that an induced, host-encoded mechanism may underlie the phenomenon of homologous interference among alphaviruses in mosquitoes.

The prime-challenge model of infection

I developed a prime-challenge model of infection using combinations of SV and another alphavirus, Venezuelan equine encephalitis virus (VEEV), to determine whether an anti-viral response mounted during a primary infection could affect the outcome of a hyper-virulent secondary infection. The vaccine strain TC-83 of VEEV was chosen because it had previously been cloned and because it shares a similar tropism and genome organization to SV, but a sufficiently diverged nucleic acid sequence from TE12Q SV that siRNAs derived from TC-83 would not be expected to react against TE12Q and *vice versa* [172]. Additionally, VEEV resides in the clade of New World

alphaviruses shared by eastern equine encephalitis virus (EEEV), which has been previously shown not to interfere with the Old World alphavirus SV in mosquito cells [46]. The combined characteristics of sequence divergence and the reported absence of interference between these serogroups enabled us to subtract the effects of sequence identity and superinfection exclusion on the development of protection against challenge with SV-B2 in the prime-challenge model.

Acquired resistance to Sindbis virus infection

In this chapter I demonstrate that mosquitoes primed by infection with avirulent SV were completely protected from a subsequent challenge infection with a hypervirulent SV carrying B2. This acquired, refractory state is rapidly established and persists throughout life. At least some proportion of acquired protection is sequence specific, as introduction of a mutated, non-protein-coding B2 ORF with VEEV in the primary inoculation is sufficient to significantly enhance survival of mosquitoes infected with SV-B2. Inserting additional copies of the non-protein-coding B2 ORF into the recombinant virus used in the primary inoculation further enhances survival. Virus replication is essential to develop protection and naked, infectious genomic SV RNA transcribed *in vitro* is sufficient to elicit the response, suggesting that replication-competent virus RNA is the minimal unit required to elicit protection. The serendipitous observation of spontaneous infections developed *de novo* from injected RNA suggests the presence of a mechanism by which long RNAs can be taken into cells without being degraded and may be important for the systemic spread of the infection signal. A model is proposed in which siRNAs produced from an ongoing, controlled primary infection feedback continuously to suppress the replication of closely related sequences encountered subsequently. These observations shed light on the minimum molecular requirements necessary to develop RNAi-mediated anti-viral protection in

mosquitoes *in vivo*.

Materials and methods

Cell lines

Baby hamster kidney (BHK-21) cells (ATCC, CCL-10) were maintained in Dulbecco's modified Eagle's medium (DMEM) supplemented with 10% FBS and Penicillin/Streptomycin at 37°C with 5% CO₂.

Insect rearing

Eggs from the Rockefeller strain of *Aedes aegypti* were kindly provided by Dr. George Dimopoulos (JHSPH, Baltimore, MD). Dried eggs were hatched in a vacuum chamber under deoxygenated conditions in dH₂O for one hour at room temperature. A 1:2:2 mixture of blended Timmy Rabbit Pellets (American Pet Diner, Code: Pellet_TR), liver powder (MP Biomedicals, Cat. #900396) and TetraMin tropical fish flakes was used as larval food. Freshly hatched first-instar larvae were poured into a 10" x 12" plastic photo developing tray (Photoquip, Cat. #CES1012T) in one liter of dH₂O with 10 mg food. Three days later, larvae were diluted to approximately 200 individuals per tray with 10 mg fresh food per tray on that day and every 2 days thereafter until a majority of larvae had entered the pupal stage. Pupae were strained through a fine metal colander and placed in a cup of dH₂O in a plastic cage (Bioquip, Cat. #1452). Pupae were left overnight to eclose with cotton-balls (Fisherbrand, Cat. #07-886) saturated in an autoclaved 10% sucrose solution in water. Young adult mosquitoes newly emerged from the pupal case were collected the following day, making them at most ~24 hours old and either used immediately or allowed to age according to the needs of the experiment, at which time they were removed and placed in individual

custom-made paper cups kindly provided by Dr. Nirbhay Kumar (JHSPH, Baltimore) or Dr. William Collins (CDC, Atlanta).

Virus constructs

Virus constructs were based on bacterial plasmids with the following full-length viral genomes dsTE12Q [14], dsMRE16 [173], and dsTC83, a variant of TC83/GFP [172]. TC83/GFP was kindly provided by Dr. Scott Weaver (University of Texas Medical Branch, Galveston). To create dsTC83, the existing BstEII site at position 1683 was mutated by changing cytosine 1688 to adenine, thereby eliminating the restriction site and retaining threonine 13 of nsP2. Oligonucleotides with this C1688A change were used to amplify a SalI-EcoRI fragment spanning nucleotides 1621-2136 of the virus genome by overlapping two-step PCR using AccuPrimeTM Pfx DNA Polymerase (Invitrogen, Cat. #12344-024). All oligonucleotides used are shown in Appendix I. The ORF encoding EGFP was replaced with a single BstEII restriction site as an ApaI-AflII fragment. PCR amplicons were cloned into the pCR®-Blunt cloning vector using the Zero Blunt® PCR Cloning Kit (Invitrogen, K2700). The integrity of both mutated fragments of the virus backbone was verified by sequencing at the Johns Hopkins University Core DNA Analysis Facility. The B2 ORF from FHV was generated synthetically using a previously described PCR strategy [174]. Briefly, four long overlapping oligonucleotides (see Appendix I) generate the template in the first reaction and overlapping short oligonucleotides at both ends prime the synthesis of the full-length product in the second reaction. Replication incompetent virus was constructed from pJRC122 (pdsTE12Q-EGFP) by deleting a 1629 bp NheI fragment encompassing residues L44-Q586 from the nsP2 protein, while preserving the original reading frame of the non-structural polyprotein. The *reaper* ORF was amplified from a plasmid template (pPI83). The EGFP ORF was amplified from

pEGFP-N1 (Clontech). Primer sequences (Invitrogen, IDT) are located in Appendix I . BstEII-sites were added to the amplicons for cloning into pdsTE12Q or pdsTC83. Restriction digested PCR amplicons were purified using the QIAquick Gel Extraction Kit (Qiagen, Cat. #28704) and cloned first into pCR®-Blunt where their sequence was verified before being subcloned into the appropriately digested vector using T4 DNA ligase (Invitrogen, Cat. #15224-017). The virus plasmid DNA vector was previously dephosphorylated with calf intestinal phosphatase (CIP, NEB Cat. #M0290S) to prevent the recovery of intra-molecular ligation products. Ligation reactions were transformed into *E. coli* strain DH5 α (Invitrogen, Cat. #18265-017) and selected on LB-Agar plates containing Ampicillin (100 μ g/ml). Clones containing inserts were identified by diagnostic restriction digestion with BstEII and separated on a 1% agarose gel. Positive clones were verified by sequencing. Bacterial glycerol stocks were prepared from overnight cultures and frozen in 15% glycerol at -80°C.

In vitro transcription of infectious virus

The procedure for producing infectious SV genomes was adapted from Hardwick and Levine [14]. Transcription templates were prepared from overnight bacterial cultures containing recombinant plasmids (Qiagen, Cat. #12643). Plasmids were linearized by restriction digest with XhoI and MluI for pdsTE12Q and pdsTC83, respectively. Residual enzyme and contaminating RNases were removed by incubating the digests with proteinase K (100 μ g/ml), Invitrogen, Cat. #25530-015) for one hour at 65°C. Remaining protein was then extracted with phenol. Residual phenol was removed by chloroform extraction and the remaining DNA was precipitated and washed in 70% Ethanol. This purified, linearized dsDNA was resuspended in RNase-Free dH₂O and served as the template in the subsequent transcription reactions. Infectious virus genomes were transcribed using 1 μ g template DNA and

SP6 RNA polymerase for 120 minutes at 37°C with the Ambion mMessage mMachine kit (Cat. #AM1340). To favor the production of large transcripts, additional GTP was added, giving a ratio of 1:1 capped to uncapped transcripts in the final product. After two hours, DNase was added to the reaction to eliminate the template and samples were incubated another 15 minutes at 37°C. These reactions were purified on an Ambion MEGAclear column (Cat. #AM1908) and the eluates were quantified on a Nanodrop 2000 spectrophotometer. Highly purified ssRNA, with a 260:280 absorption ratio of ~2.2, was routinely obtained through the above process [175].

Rescue of recombinant virus

Purified infectious vRNA (4 µg) was transfected into BHK cells (ATCC) with Lipofectamine 2000 (Invitrogen, Cat. #11668-027). After two hours, transfection media was replaced with DMEM containing 1% FBS. Virus was harvested by collecting the supernatant when the cells began to show moderate to heavy CPE, 18-24 hours post-transfection. Supernatants were spun for one minute at 16,000 x g to remove cellular debris and frozen in 10 µl aliquots at -80°C. Titres of collected virus were subsequently determined by plaque assay on BHK cells.

Plaque assays

Plaque assays were performed as previously described [14]. Virus was isolated by homogenizing single mosquitoes with a pellet pestle (Sigma, Cat. #Z359947) in 500 µl DMEM with 1% FBS. BHK cells were plated in 6-well plates and 10-fold dilutions of virus aliquots in DMEM containing 1% FBS were adsorbed in 200 µl over the monolayer. MEM (without phenol red) in 0.6% Bacto-Agar was added to immobilize viruses. Focal plaques of infection were stained after 48 hours with neutral red (1%) in MEM. Plaques were counted and corrected for dilution factor. Titre is expressed

as plaque forming units per milliliter (PFU/ml). Results are plotted from three independent experiments. Error bars represent standard deviation.

SV infection of BHK cells

BHK cells were infected with SV at an MOI of five for one hour at 37°C. Aliquots were taken and replaced at 0, 6, 12, 18 and 24 hours post-adsorption. Virus titres from collected supernatants were measured by plaque assay on BHK cells.

Microscopy

Images of live mosquitoes were acquired using Spot 4.0.1 software on a Nikon Eclipse TE200 inverted microscope. Whole body images were acquired at 20X total magnification with Nikon Plan UW 2X/0.06 objective. Images of the eye and head were taken at 100X total magnification with a Modulation Optics, Inc HML ELWD Plan Fluor 10X/0.30 objective. Fluorescent images were acquired using a Nikon B-2E/C filter. Image black levels were optimized using Adobe Photoshop CS. The same transformations were applied across each image to avoid bias.

The prime-challenge model and virus infections

Adult, female *Ae. aegypti* mosquitoes were separated into custom-made soup cups kindly provided by Dr. Nirbhay Kumar (JHSPH, Baltimore) and Dr. William E. Collins (CDC-Malaria Branch, Atlanta). Mosquitoes were knocked down (anesthetized) on ice for five minutes. Needles for virus microinjection (Drummond Scientific, Cat. #3-000-210-G) were pulled on a Sutter P-2000 microcapillary puller using the following program: Heat=350, Filament=4, Velocity=50, Delay=225, Pull=150. Pulled microcapillaries were backfilled with mineral oil (Sigma, M5904) and fitted to

onto a Nanoject II microinjector (Drummond Scientific). Needles were then used to draw up thawed virus supernatant diluted to 1000 PFU per 69 nl injection volume ($1.45 \cdot 10^7$ PFU/ml) and filled from the tip. At the time of injection, mosquitoes were knocked down on ice, then aligned and injected on an EchoTherm chilling plate (Torrey Pines Scientific) set to 0°C with a piece of wet, white filter paper (Fisher Scientific, Cat. #09-790-12C) on top to enhance contrast. Injected mosquitoes were returned to their cages and allowed to recover at insectary conditions (28°C, 80% RH). For prime-challenge experiments, the injection procedure was repeated five days later except for the experiments where the length of time between prime and challenge was varied explicitly (Figure 2-2D) at 1d, 2d, 5d and 15d post-prime. After challenge, mosquitoes were returned to insectary conditions and monitored for mortality daily thereafter. Cotton balls saturated with 10% sucrose were changed every two days to prevent the buildup of pathogenic bacteria and fungi. Univariate survival analysis was performed according to the methods of Kaplan and Meier [176] and Cox [177]. P-values are derived from the log-rank test statistic for pairwise comparisons and from the Z-score in the case of multiple comparisons.

Quantitative RT-PCR

Total RNA was prepared from individual mosquitoes. Infected mosquitoes were homogenized with a pellet pestle (Sigma, Cat. #Z359947) in 350 µl Qiagen buffer RLT. Homogenates were purified using the RNeasy Mini Kit according to the manufacturer's protocol for animal cells (Qiagen, Cat. #74104). Five microliters of purified RNA, representing 0.1 mosquito equivalents, were loaded into the qRT-PCR reaction to maximize the detection of low-abundance RNAs. PCR reactions were setup using the TaqMan® One-Step RT-PCR Master Mix Reagents Kit (Applied Biosystems, Cat. #4310299 D) according to the manufacturer's recommendations on an ABI 7500

Real-Time PCR System with the following program: 48°C for 30 minutes for the reverse transcription step, 95°C for 10 minutes to inactivate the RT and 40 cycles of 95°C for 15 seconds followed by 60°C for 60 seconds. Primers and FAM-labeled Taqman probes were designed using Primer Express software (ABI). Primer and probe sequences are located in Appendix I. SV RNAs transcribed *in vitro* served as highly purified, spectrophotometer-quantified standards for absolute quantification of RNA copy number. Plotted data are from three independent experiments. Error bars represent standard deviation.

Results

Replication of hypervirulent SV in *Aedes aegypti*

Recombinant Sindbis viruses were based on the virus clone dsTE12Q, whose subgenomic promoter has been duplicated near the 3'-end of the viral genome to drive the expression of a transgene at high levels in infected cells. By contrast, the duplicated subgenomic promoter of Venezuelan equine encephalitis virus (VEEV) clone dsTC83 resides internal to the structural genes adjacent to the natural promoter (Figure 2-1A) [14]. To determine the effect of B2 expression in dsTE12Q, adult female *Aedes aegypti* mosquitoes were inoculated intrathoracically with 10³ PFU SV five days after eclosion. Mosquitoes infected by injection with Sindbis virus (SV) containing no insert display little mortality following infection, whereas mosquitoes inoculated with recombinant Sindbis virus expressing B2 (SV-B2) develop a fatal infection characterized by enhanced virus replication and death of the animal 7-10 days post-inoculation (Figure 2-1B) [141, 142]. Moreover, disruption of the dsRNA binding activity of B2 by rational mutagenesis of an RNA contact point (C44Y) nullifies both the dsRNA binding activity and killing capacity of B2 in SV [139, 141]. Thus, the hyper-virulent phenotype is

thought to be dependent on the ability of B2 to bind dsRNA. To determine whether enhanced killing was accompanied by enhanced virus replication, both functional and molecular measurements of virus replication in mosquitoes were made over time (Figure 2-1C and 2-1D). Readouts of virus RNA copy number by quantitative RT-PCR correlate highly with the functional readout of the plaque assay (Figure 2-1D and 2-7) thereby validating RNA copy number as a surrogate measurement for functional virus growth in this system and making it possible to monitor the infection kinetics of multiple virus strains or species simultaneously in a single infected mosquito. At early time points, there was no significant difference between the replication of the two viruses, suggesting that differences in replication rates do not likely account for the observed differences in maximal titres (Figure 2-1C and 2-1D). By two days post-infection, hypervirulent Sindbis virus (SV-B2) replicates to significantly higher titres ($p = 0.048$) and RNA copies ($p = 0.075$) than control virus (SV-GFP). Differences between the two groups at four and 8 days post-infection were highly significant for both RNA levels and infectious virus produced per mosquito ($p < 0.001$ for each). Control virus titres peaked between two and four days post-inoculation, after which time they begin to decrease (Figure 2-1C). This observation is consistent with previous reports and suggests that avirulent SV-GFP replication is suppressed by the insect anti-viral response [1, 32]. In contrast, SV-B2 titres and RNA levels did not stabilize and continued to rise, as if running unchecked by the host anti-viral surveillance machinery until the death of the hapless mosquito. SV-B2 replication in vertebrate BHK cells, however, was not significantly enhanced (Figure 2-6). Despite this, SV-B2 inoculated into four-day old CD1 mice intracranially causes significant mortality relative to insert-size matched controls that do not encode a protein (Figure 2-15, $p = 0.001$). These results suggest that the difference in replication between the two viruses in insect cells, combined with the difference in the magnitude of their virulence between vertebrate and invertebrate infection models, highlights a fundamental difference in the

mechanism by which invertebrates respond to virus infection relative to vertebrates.

Priming with avirulent SV protects against subsequent hyper-virulent challenge

It was reported in *Drosophila* that a specific antiviral response to Sindbis virus appears in the head as early as two days post inoculation, although the virus itself remained undetectable in the head until five days after inoculation [178]. The authors suggest that a cell non-autonomous, systemic immune response is generated against Sindbis virus [178]. If a rapidly disseminated systemic anti-viral response were indeed at work in flies, one would expect to see protection against a hyper-virulent challenge to arise rapidly in the presence of an appropriate stimulus. To determine the effect of an existing infection on a subsequent hyper-virulent infection, mosquitoes were infected with an innocuous virus strain (SV-GFP) within 24 hours of eclosion and challenged five days later with hyper-virulent virus (SV-B2) (Figure 2-2A). Five days post-injection roughly corresponds to the peak of the acute infection, when virus titres begin to drop as they are brought under control by the host (Figure 2-1C and 2-1D). At this time in *Drosophila*, host responses are actively engaged in defending against the initial inoculation [178]. GFP expression was readily detectable in live mosquitoes examined five days post-inoculation with SV-GFP, with the most intense focus of fluorescence in the brain (Figure 2-2E). This observation is reminiscent of the tropism of SV in vertebrate hosts, suggesting that the virus uses common strategies for replication and amplification by SV in both the vertebrate and invertebrate systems. Given the enhanced replication capacity of SV-B2 relative to control virus, it was anticipated that infected mosquitoes would succumb to the lethal strain regardless of their infection status at the time of challenge. However, mosquitoes given a priming inoculation with SV-GFP were protected against hyper-virulent SV-B2 challenge five

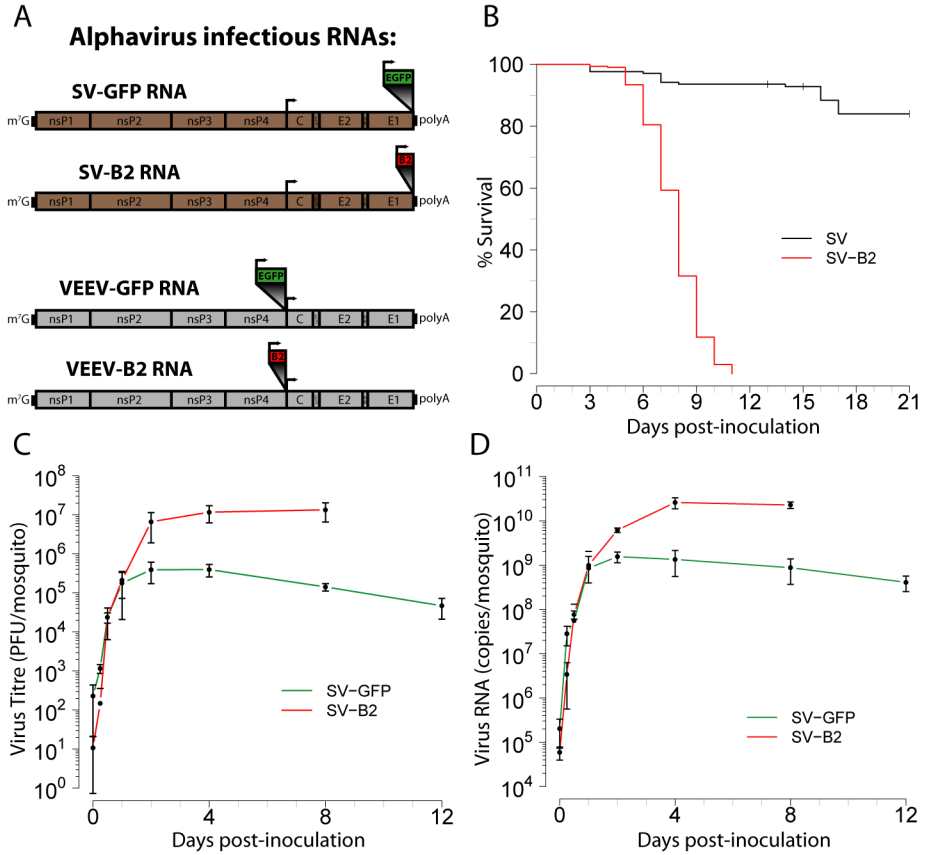


Figure 2-1. Hypervirulent Sindbis Virus kills adult *Aedes aegypti* mosquitoes. **(A)** Recombinant alphaviruses used in this study were based on dsTE12Q (SV) and dsTC83 (VEEV). Sub-genomic promoters were duplicated downstream (SV) or upstream (VEEV) of the structural genes to drive transgene expression. **(B)** Adult female mosquitoes inoculated with hypervirulent SV-B2 ($N = 318$) die within 11 days of inoculation. Greater than 80% of mosquitoes infected with control SV ($N = 172$) remain alive at 21 days post-infection ($p < 0.0001$, log-rank test). **(C-D)** Replication of SV *in vivo*. **(C)** SV-B2 replicates to significantly higher titres than SV-GFP at two days ($p = 0.0484$), four days ($p = 0.000826$) and 8 days ($p = 0.000137$) post-inoculation. (2-way ANOVA, factoring on time and virus) **(D)** SV-B2 replicates to a significantly higher RNA copy number than SV-GFP at two days ($p = 0.0751$), four days ($p = 7.41 \cdot 10^{-11}$) and 8 days ($p = 9.75 \cdot 10^{-10}$) post-inoculation. (2-way ANOVA, with time and virus as factors). The results from at least three independent experiments are plotted for each panel and error bars represent SD.

days later (Figure 2-2B). The same experiment performed with the *Drosophila* death gene *reaper*, which is also capable of killing mosquitoes when expressed in SV (see Chapter 3), yielded a similar outcome (Figure 2-8). This is consistent with the notion that acquired protection is not dependent on the B2 transgene *per se*. Therefore, inoculation with avirulent SV gives rise to a state in which otherwise susceptible mosquitoes gain protection against lethal challenge by a homologous virus. Probe-based, quantitative RT-PCR was performed to determine the relative replication rates of both viruses in individual mosquitoes beginning on the day of challenge (Figure 2-2C). The priming virus SV-GFP, which had already been present for five days, established a disseminated infection and replicated to a steady state neither increasing nor decreasing rapidly in copy number. Importantly however, replication of SV-B2 was suppressed more than 10,000-fold compared to its replication in naïve animals (Figure 2-2C and 2-3C). The presence of the primary infection, therefore, limits the replication of a spontaneously introduced hyper-virulent mutant.

Protection develops rapidly and persists throughout life

We next asked about the kinetics of the protective phenotype induced by infection with avirulent SV to determine the amount of time necessary for the mosquito to develop protection and for how long this protection is maintained, as this information may provide clues about the nature of the protective response. To address this, the length of time between the prime and challenge was varied. While mosquitoes given only SV-B2 exhibited the expected death kinetics, mosquitoes challenged with killer virus as soon as 24 hours after prime were immune to the otherwise lethal effects of SV-B2. The survival of mosquito groups challenged at two, five and 15 days was indistinguishable from control groups challenged with SV-GFP at the same time points (Figure 2-2D). That is, protection from superinfection develops rapidly and is

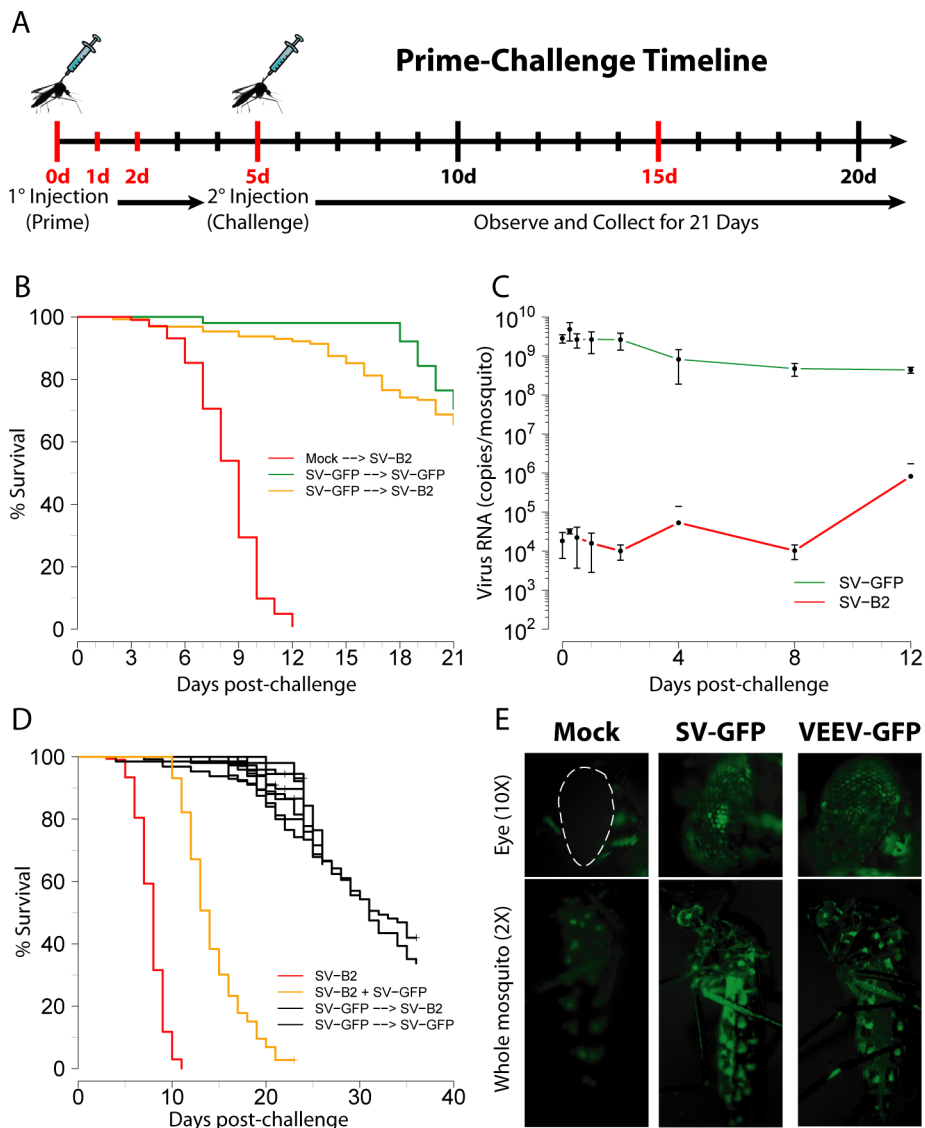


Figure 2-2. Primary infection with avirulent SV induces sequence-specific protection against subsequent hypervirulent challenge. **(A)** The prime-challenge timeline. The standard incubation between prime and challenge was five days. **(B)** Priming with SV-GFP protects mosquitoes from challenge with SV-B2 ($N = 128$). **(C)** Quantitation of virus RNA copy number in mosquitoes exposed to SV-GFP then SV-B2 shows a greater than 4-Log suppression of SV-B2 replication. **(D)** Varying the length of time between prime and challenge. Challenges were performed at day 0 (mixture of both viruses, $N = 73$), 1d, 2d, 5d and 15d (black lines, total $N = 638$) post-priming. Protection develops within 24 hours of priming and is retained for at least 15 days. Results from three independent experiments are plotted in each panel. Error bars in panel B represent SD. **(E)** Live adult mosquitoes were screened for EGFP fluorescence five days post-inoculation show most prominent EGFP expression in the eye and brain.

sustained for at least 15 days and thus for the practical life of the insect. Even when both viruses were mixed into the priming inoculation (500 PFU per virus at time = 0), killing was significantly attenuated, resulting in a five day shift in the median day of death (Figure 2-2D). As measured by the survival phenotype, interference established by SV-GFP is ultimately completely overcome by the more virulent and better replicating virus SV-B2 when they are co-administered. Alternatively, if the two Sindbis viruses did not interact with each other, one might speculate that the lower dose of SV-B2 given (1,000 versus 500 PFU) must account for the difference in killing. However, a two-fold difference in a virus inoculum giving rise to a five day average life span extension seems unlikely, given the logarithmic nature of virus replication. Therefore, avirulent SV-GFP interferes with the capacity of SV-B2 to replicate and kill *in vivo*, resulting in an infected animal that is refractory to infection by a closely related, hyper-virulent strain of the same virus.

Acquired protection is sequence specific

Superinfection exclusion among homologous alphaviruses has been observed in both vertebrate and invertebrate cells [38, 46]. Therefore, we asked whether the protective phenotype observed was due to this phenomenon [46]. To test this, it was necessary to use a virus that would neither be excluded by SV nor share substantial windows of sequence identity with TE12Q in the primary inoculation. We sought a virus for which there was no block of sequence identity 21 nucleotides or greater, such that siRNAs derived from one virus could act directly and immediately on the other. Pre-aligned sequences were compared for windows of sequence identity and only one such (23 nt) window exists, near the 5'-end of the genome comprising nucleotides 168-190 in nsP1 of the VEEV and SV genomes (Figure 2-9). As VEEV and EEEV belong to the same phylogenetic clade and are thus more closely related to each other than to SV,

and since EEEV is not excluded by SV [46], it was anticipated that SV would not exclude the cloned vaccine strain TC-83 of VEEV [48, 179]. Therefore, a variant of pTC83/GFP was constructed that replaced the EGFP ORF with a BstEII restriction site for cloning genes downstream of the subgenomic promoter (Figure 2-1A) [172]. Recombinant VEEV expressing B2 or EGFP were capable of establishing infections *in vivo* when injected intrathoracically into adult *Aedes* mosquitoes, but replicated to lower titres and correspondingly lower RNA copy numbers per mosquito than SV, showing no significant difference in replication between viruses expressing EGFP or B2 (Figure 2-10 and 2-11). Consistent with this observation, but unexpectedly, VEEV-B2 did not kill mosquitoes (Figure 2-12). The most likely explanation for this is that although gross EGFP expression patterns and intensities in VEEV-infected mosquitoes appeared similar to those of Sindbis virus, VEEV does not infect the cell type necessary to kill the animal. Indeed, the reported tropism for SV in mosquitoes is wider than that reported for VEEV, which is confined mostly to the insect CNS [6]. Alternatively, the lack of killing by VEEV-B2 could be explained if B2 does not provide the necessary gain of virulence for VEEV to kill the cells necessary for the animal to die. When mosquitoes were inoculated with recombinant VEEV-GFP in place of SV-GFP as the priming virus, mosquitoes were unprotected against challenge with SV-B2 and killing was restored (Figure 2-3A). This result indicates that protection against SV-B2 is not due to a general effect or “anti-viral state” induced by the primary infection. Furthermore, the unfettered replication of SV-B2 in the VEEV-infected background, indistinguishable from naïve controls, indicates an absence of competition between these two viruses (Figure 2-3C). Yet another cloned strain of SV, MRE16, is a low passage invertebrate-adapted strain that was originally selected for its enhanced infectivity to mosquitoes in bloodmeals taken per *os* [173].

If acquired protection arose entirely from homologous interference, TE12Q-SV-B2 would not be expected to kill in an MRE16-SV-GFP-infected background, since both

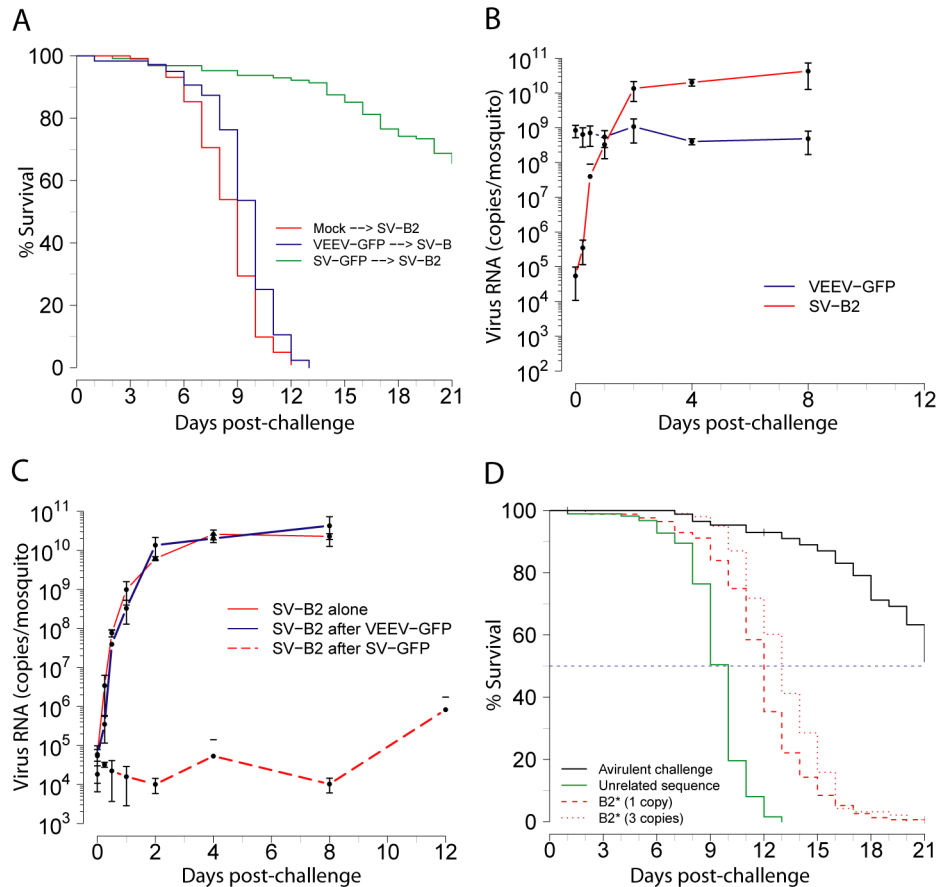


Figure 2-3. Acquired protection to hypervirulent SV is sequence-dependent. **(A)** Priming with VEEV-GFP does not protect against challenge with SV-B2 ($N = 182$) relative to SV-B2 alone ($N = 102$). **(B)** Replication of SV-B2 in a VEEV-infected background. **(C)** Replication of SV-B2 by infection background type. The data plotted are from three independent experiments. Error bars represent SD. **(D)** Priming with VEEV-B2* (1 copy, $N = 169$) delays killing by 2 days relative to priming with VEEV-GFP ($N = 272$; $p < 0.0001$, log-rank test). Priming with VEEV-B2* (3 copies, $N = 96$) delays killing by 4 days relative to priming with VEEV-GFP ($p < 0.0001$, log-rank test). Survival data are plotted from at least three independent experiments.

of these viruses are strains of Sindbis virus which are thus quite closely related and would be expected to exclude each other. But mosquitoes infected with MRE16-GFP are not protected from killing by SV-B2 relative to controls challenged with avirulent SV (Figure 2-13), which would be the expected result in the absence of interference. I next asked whether a non-viral nucleotide sequence provided in the priming virus would be sufficient to produce protection in *trans*. To address this, the first codon in the B2 sequence was mutated from methionine to a stop codon to abolish protein expression while retaining the maximum possible length of RNA sequence identity between the two viruses. Mosquitoes primed with VEEV-B2^{1M*} survived an average of two days longer (12d) than controls primed with VEEV-GFP (10d), indicating that homologous sequence provided in *trans* is sufficient to delay, if not prevent, killing by hyper-virulent SV-B2 ($p < 0.001$) (Figure 2-3D). Since VEEV-B2 does not kill mosquitoes, it was possible to use it in the primary inoculation to assess its ability to protect against challenge from SV-B2. In contrast to priming with VEEV-B2^{1M*}, priming with VEEV-B2 (encoding a functional protein) gives rise to no protection at all and mosquitoes die at the same rate as immunologically naïve animals or those inoculated with a virus containing unrelated sequence (VEEV-GFP) (Figure 2-14). This is likely due to the immunosuppressive effect of B2 expression, which is thought to protect transient dsRNA intermediates from recognition by the insect non-self surveillance machinery, effectively masking the VEEV-B2 infection.

Infection with recombinant VEEV possessing three copies of the B2 sequence, with stop codons introduced at multiple positions and in multiple reading frames, B2***, gave rise to even greater protection compared to viruses containing only one copy (Figure 2-3D, $p = 0.000168$). Curiously, significant enhanced survival was not observed in clones containing two copies of B2^{1M*} or B2***, nor in the clone containing three copies of B2^{1M*} (Figure 2-14). Additionally, B2*** does not enhance protection relative to B2^{1M*} unless it is present in three copies. Together, these data indicate

that adding additional copies of the same sequence in the primary infection, while sufficient to significantly augment protection, has at best a modest effect. This raises the question of what defines the “quantity” versus the “quality” of the immunizing template, as the precise molecular mechanism governing the efficacy virus derived siRNAs is not well understood.

Priming virus replication is necessary for acquired protection

To determine the minimum requirements for acquiring protection against SV-B2, we asked if replication of the priming virus was required to establish a protective response. Intrathoracic priming with purified infectious genomic viral RNA transcribed *in vitro* is sufficient to produce protection in a 90% of surviving mosquitoes by 21 days (Figure 2-4A). The increased death in mosquitoes injected with SV-GFP RNA compared to those injected with SV-GFP virus at earlier time points may be due to the failure of the infectious RNA to establish an infection in all animals, but may also be indicative of immunogenic properties of virion components. To address this, aliquots of SV-GFP were UV-inactivated to render the RNA non-infectious and tested for their ability to induce protection against SV-B2 when given as a prime. Inactivated SV-GFP (1,000 inactivated PFU) was unable to elicit protection against SV-B2, indicating a requirement for replication of the priming virus in producing the protective phenotype and highlighting the dispensability of virion protein components in eliciting protection (Figure 2-4B). Remarkably, mosquitoes injected with purified RNA developed SV infections *de novo*, as determined by the expression of EGFP in the eye and brain of infected individuals (Figure 2-4C). This suggested that injected RNA was taken up by cells in the mosquito, and because the naked RNA of this virus is infectious, was sufficient to initiate an infection cycle. To determine whether the initiation of an SV infection was required to develop protection against SV-B2, a replication-incompetent

SV-GFP RNA was constructed. Residues 44–586 of nsP2 were deleted by digest of dsTE12Q with NheI and subsequent intramolecular ligation of the plasmid backbone, thus preserving the reading frame of the SV polyprotein. If protection observed by injecting virus RNA alone was the result of a *bona fide* SV infection, then a replication incompetent RNA would not be expected to produce protection. Indeed, dsTE12Q^{ΔNheI} RNA produces no protection when injected as a prime, confirming that replication-competent SV RNA is both necessary and sufficient to elicit protection against hypervirulent SV-B2, presumably through the development of a persistent infection disseminated throughout the susceptible tissues of the animal (Figure 2-4B). These data show that the minimal unit required to elicit the protective phenotype is a replication competent, homologous virus RNA.

Discussion

The present study illustrates the specificity and functional capacity of the insect anti-viral immune response. When an adult mosquito is injected with Sindbis virus, a disseminated, systemic infection immediately ensues. SV encoding the B2 suppressor of RNAi from Flock House virus exhibit a lethal gain-of-function that correlates with massive virus overgrowth compared to controls infected with SV-GFP (Figure 2-1). Production of B2 by SV probably results in reduced recognition of virus dsRNA replication intermediates and siRNAs by the host RNA surveillance machinery in addition to inhibition of *Dcr2*-mediated anti-viral immune signaling. Suppression of the host anti-viral response allows the virus to replicate to levels causing cellular pathogenesis and ultimately, cell death. However, if anti-viral effectors are already in place at the time of challenge, incoming virus replication is attenuated. The primary virus inoculation results in a persistent infection that rapidly suppresses homologous sequences *in vivo*. If mediated by specific effector siRNAs, this response is

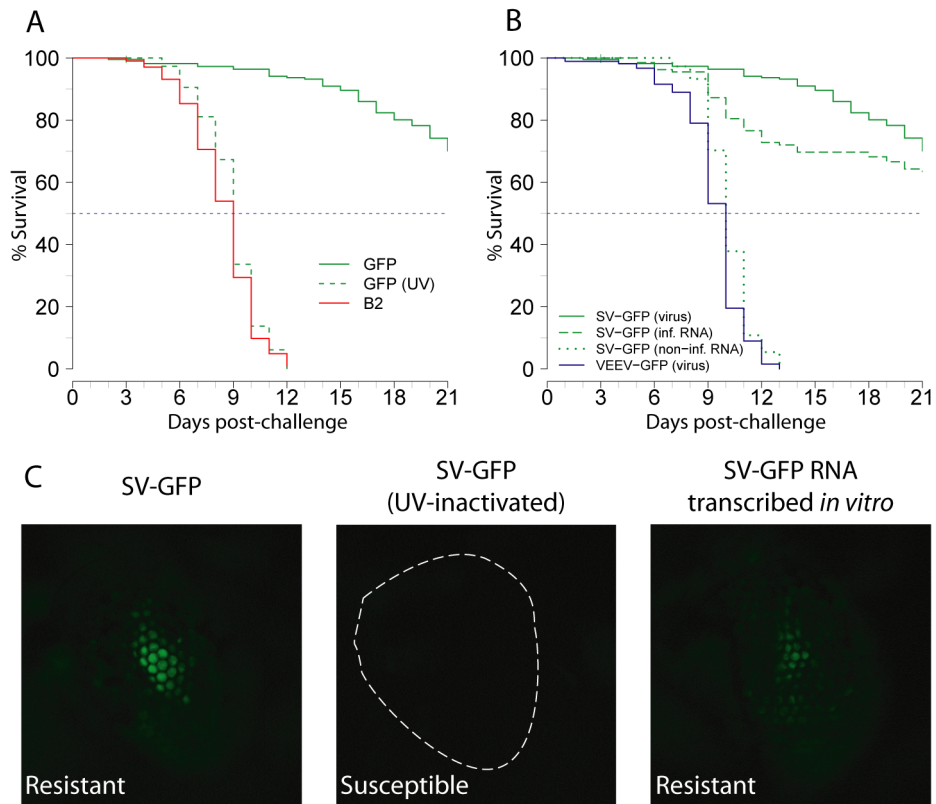


Figure 2-4. Determining the minimum molecular requirements for protection. **(A)** Priming with UV-inactivated SV-GFP ($N = 74$) abolishes protection against SV-B2. **(B)** Priming with *in vitro* transcribed infectious SV-GFP RNA ($N = 133$) is sufficient to confer protection against challenge by SV-B2. Conversely, injection with a replication incompetent RNA ($N = 78$) confers no protection from SV-B2 infection. Results are plotted from at least three independent experiments. **(C)** EGFP expression in the eye is a definitive marker for SV infection. Mosquitoes injected with UV-inactivated SV-GFP show no detectable fluorescence in the eye. Unexpectedly, mosquitoes injected with naked SV-GFP vRNA develop SV infections *de novo*.

analogous to the antibody-mediated humoral response of vertebrates. Virulent Sindbis virus infections are accompanied by significant increases in virus production in both vertebrate [21] and invertebrate models of infection [141]. Acquisition of immunity or enhanced resistance to virulent SV-B2 through a controlled, persistent infection by VEEV-B2^{1M*} may bring to light a mechanism of protection against spontaneously arising virulent strains during the course of infection, as even a single coding change in SV is sufficient to kill mice [19]. Indeed, Coffey and colleagues reported that serial passage of VEEV through live mosquitoes did not affect virus titre [180] and acquired zero mutations after serial passage in live mosquitoes, as would be expected if there was a constraint to mutation and (by extension) replication *in vivo*. Furthermore, alphavirus evolution is reported to be an order of magnitude slower than that of other RNA viruses, although the error rate of their polymerase is comparable to that of other RNA viruses, suggesting that the necessity of arboviruses to replicate in disparate hosts imposes greater constraints on sequence evolution [6]. A higher mutation rate amongst virus-derived RNAs isolated from infected *Dcr2*^{-/-} flies compared to wild type flies would be expected if RNAi-mediated anti-viral immunity is indeed responsible for the strong purifying selection giving rise to homogeneous arbovirus populations within individual mosquitoes. Since mosquitoes cannot cure a systemic Sindbis virus infection, equilibrium is established between virus replication and the host response to suppress it. Meanwhile, the controlled infection protects the animal from homologous viruses encountered subsequently.

I propose a model (Figure 2-5) in which siRNAs produced from an ongoing, systemic primary infection provide continuous feedback to suppress the replication of closely related sequences, even if they vary at a distal site outside the boundaries of the siRNA sequence. If 350 bp of homologous, immunogenic sequence is sufficient to delay killing by SV-B2 for 2 days, it is reasonable to expect that the response derived from the entire 12.5 kilobase genomic complement of SV-GFP would be even more

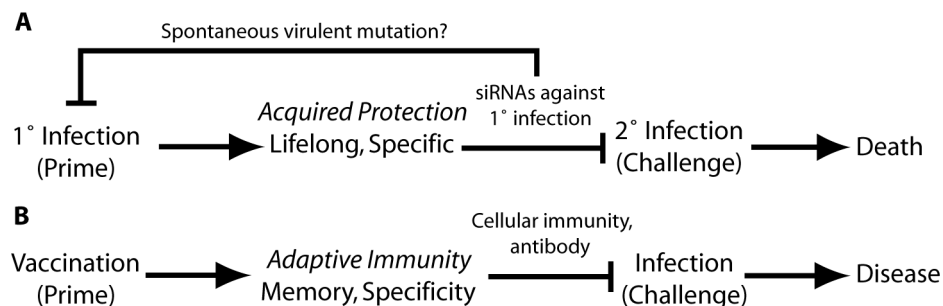


Figure 2-5. A model for sequence-specific anti-viral immunity in insects. **(A)** siRNAs produced during the primary infection are continuously produced in the persistently infected animal and act to degrade the superinfecting virus. Acquired protection is a result of siRNA effectors produced continuously from the prime. **(B)** Vaccination in vertebrates.

effective against SV-B2, owing to the greater length of homologous sequence from which to draw effector siRNAs. On the other hand, adding additional copies of the same homologous sequence did not largely alter the degree of protection, suggesting that a mere increase in the quantity of derived siRNA effectors is insufficient to provide additional protection. This model does not preclude virus-mediated interference based on the protease activity of nsP2. Rather, the two phenomena may operate in parallel. Additionally, the distinct “acute” and “persistent” phases of infection may, in fact, be due to inherent limitations of the cell culture system. In vertebrate cells, replication proceeds until the cells die and then, with no host cells remaining to parasitize, virus titres crash. In insect cells, there is also an early phase of exponential virus growth, but the cells generally do not die, having brought the virus under control by the endogenous anti-viral machinery. At later times post-infection *in vitro*, a persistent infection is established in which virus replication drops more than 100-fold relative to peak titres [171, 181]. In live mosquitoes, however, virus replication at later time points during the persistent phase of infection is similar to the maximum virus titre during the acute phase of replication at early times post-inoculation, with virus titres dropping less than one order of magnitude by 12 days post-infection (Figs. 2-1, 2-10 and 2-11).

The observation that adding additional copies of the homologous sequence in the primary infection results in slightly greater protection from SV-B2 addresses the question of template quantity in the RNAi-mediated insect anti-viral response, but it does not address the relative immunogenic capacity or “quality” of other homologous sequences (e.g. the 5-prime and 3-prime untranslated leaders of the SV genome). Would a fragment from the 5-prime UTR of SV of same length as B2 have similar protective properties if given in VEEV as a prime? What are the sequence determinants of effective virus-derived siRNAs? Are the most abundant siRNAs also the most effective? Untranslated regions of the virus genome contribute disproportionately to the production of anti-viral siRNAs, but it is not known if the greater number siRNAs derived from regions of secondary structure in the virus genome are functionally important [141]. Furthermore, the finding that live mosquitoes were able to take up and express a large (12.5 kb) single-stranded RNA without degrading it was unexpected. The mechanism by which such large RNAs could be taken into cells is currently unknown and deserves further investigation, as they could themselves facilitate the systemic spread of RNAi during virus infection. The identification of sequence-specific, acquired protection to virus infection in *Aedes aegypti* advances our understanding of the molecular requirements for engineering anti-viral immunity in insects of medical and agricultural importance.

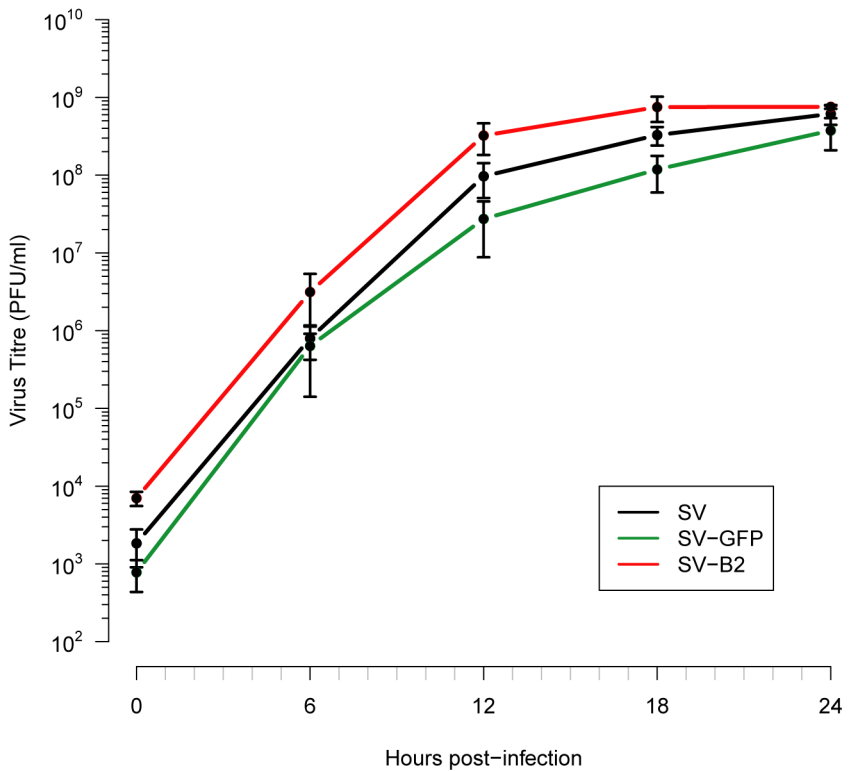


Figure 2-6. Replication of SV constructs in BHK cells. Plotted results are from three independent experiments. Error bars represent SD. Differences between groups are not significant. Monolayers were infected with five infectious units per cell and supernatants were collected at 6, 12, 18 and 24 hours after adsorption at 37°C.

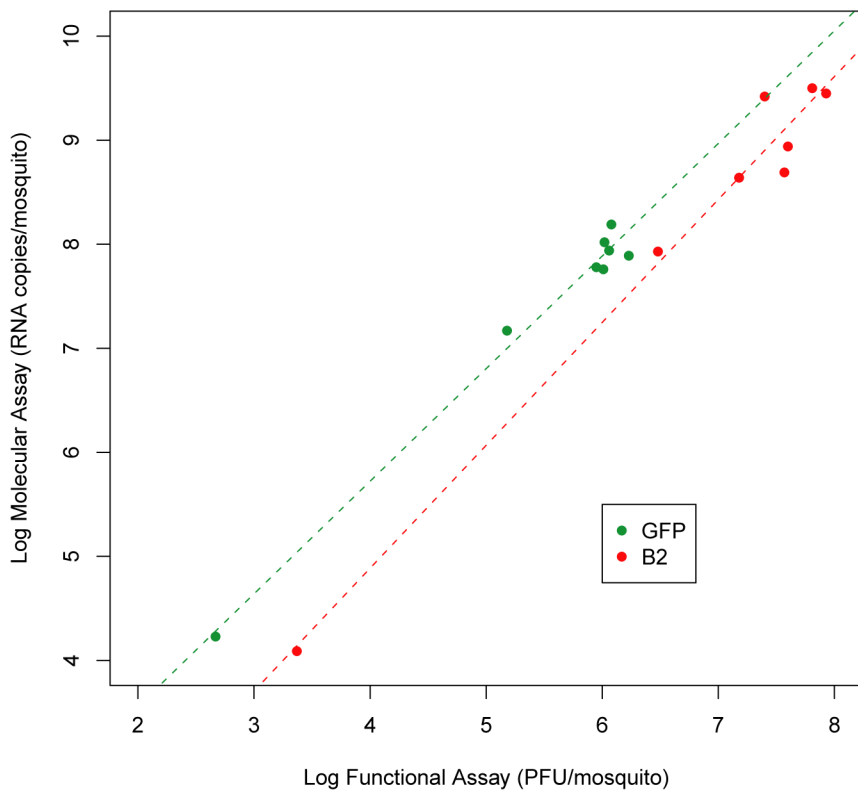


Figure 2-7. Correlation of molecular and functional readouts of virus replication. Each data point represents a single mosquito measured twice; by plaque assay and quantitative RT-PCR. A linear regression for measurements made with each Taqman probe (GFP and B2) show that the two different readouts are highly correlated in both cases. $R^2 = 0.983$; $R^2 = 0.974$.

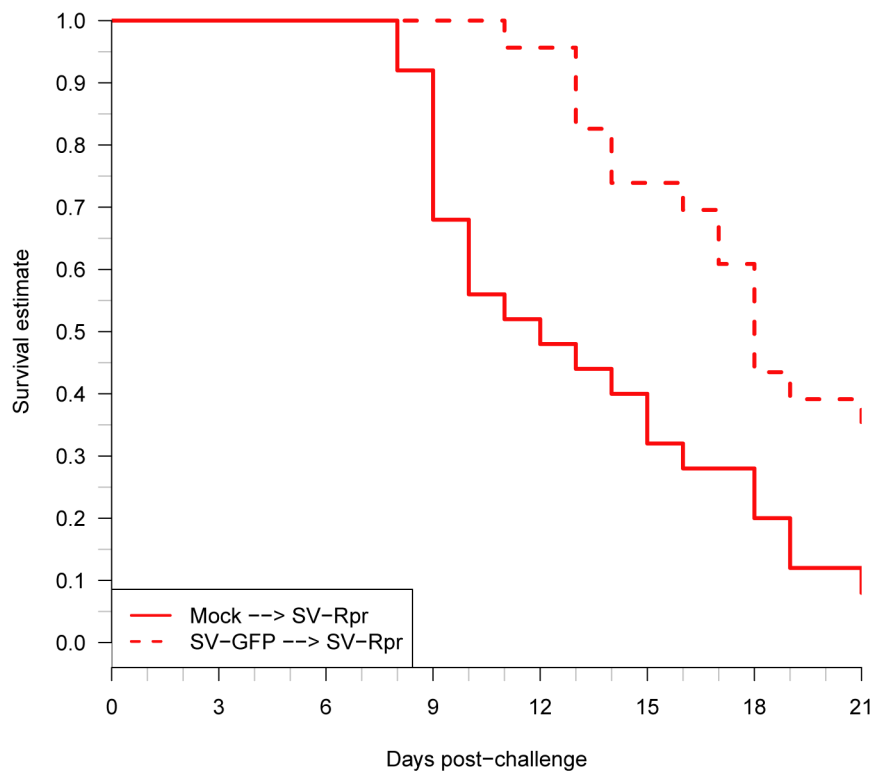


Figure 2-8. Priming with SV-GFP protects against challenge with SV-rpr ($N = 23$). This suggests that the protective phenotype is not peculiar to the B2 virulence factor. (Mock \rightarrow SV-rpr, $N = 25$).

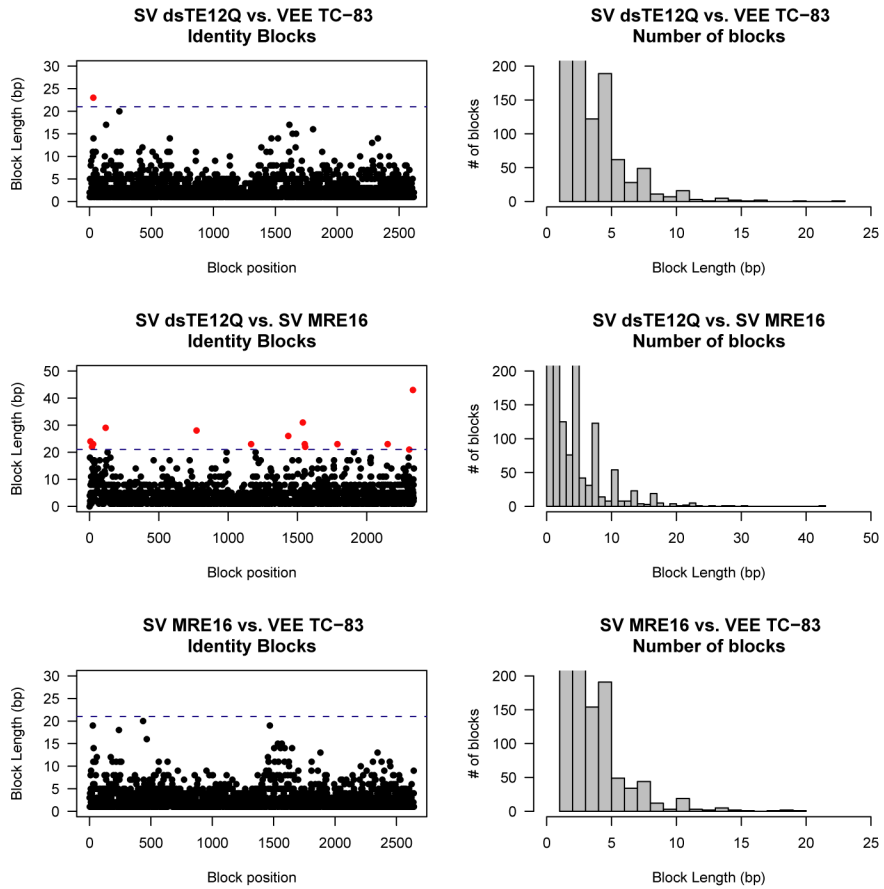


Figure 2-9. Comparison of nucleotide identity blocks between alphaviruses. Block lengths are plotted in the left panels as a function of genomic position. Histograms of block distributions are plotted on the right panels. Virus RNA sequences were aligned with ClustalW. A perl script was written to compare pairwise alignments for blocks of identity. Data were plotted in R. One 23 nt block (red) exists between dsTE12Q and dsTC83. SV strains dsTE12Q and dsMRE16 share 14 identity blocks 21 nt or greater in length. There are no identity blocks greater than 20 bp shared between dsMRE16 and dsTC83.

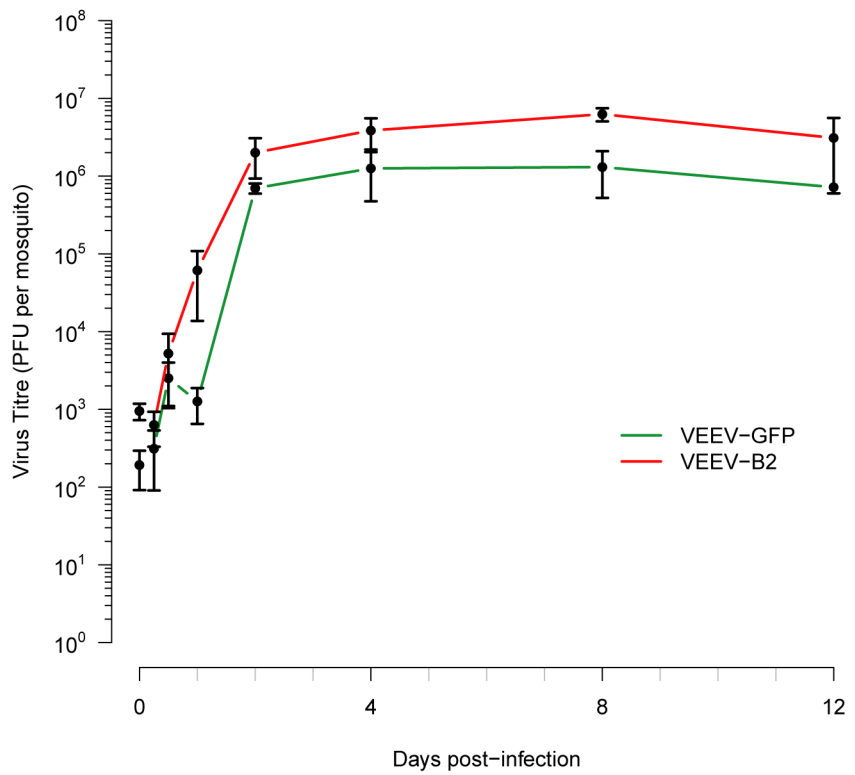


Figure 2-10. Replication of dsTC83 constructs (PFU/mosquito). There was no significant difference between VEEV-GFP and VEEV-B2 replication *in vivo*. This is consistent with the observation that VEEV-B2 does not kill mosquitoes. Data are plotted from three independent experiments. Error bars represent SD.

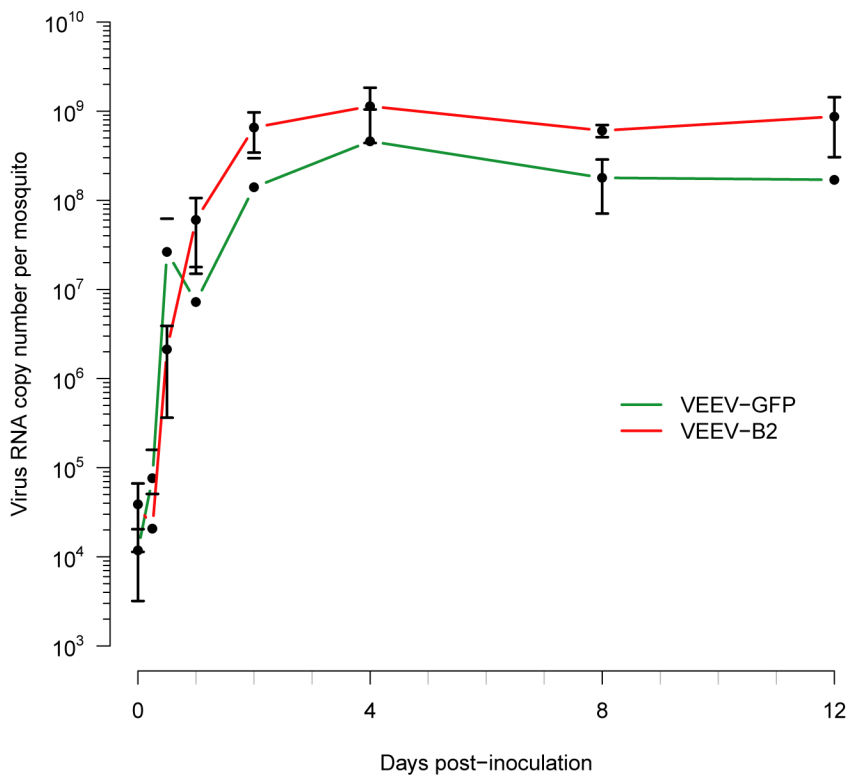


Figure 2-11. Replication of dsTC83 constructs (RNA copies/mosquito). There was no significant difference between VEEV-GFP and VEEV-B2 replication *in vivo*. This is consistent with the observation that VEEV-B2 does not kill mosquitoes. Data are plotted from three independent experiments. Error bars represent SD.

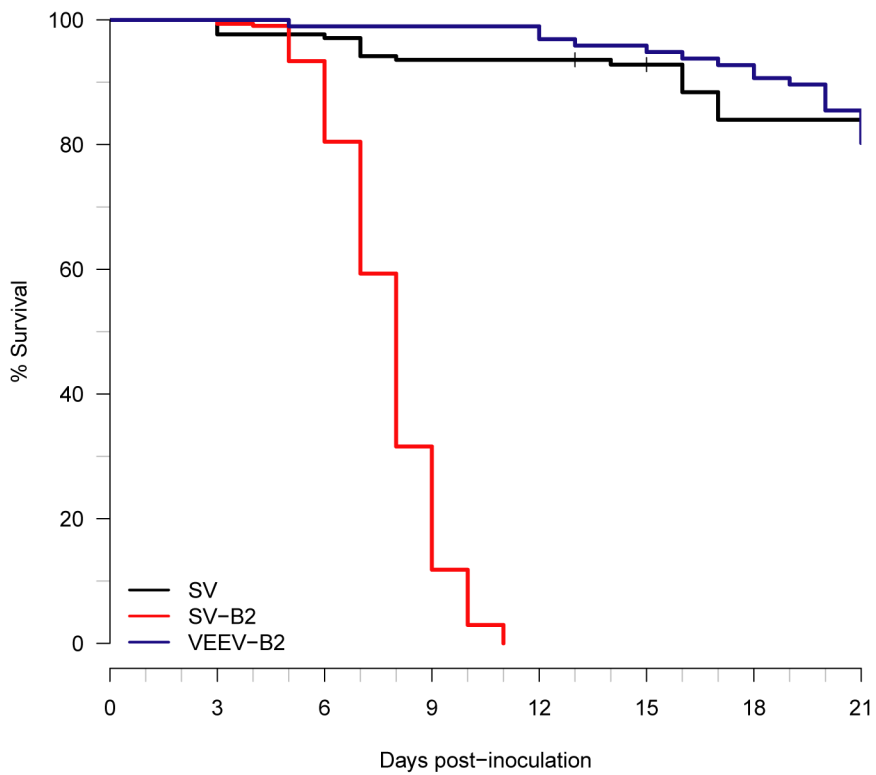


Figure 2-12. VEEV-B2 does not kill mosquitoes. Adult female mosquitoes were inoculated with 1000 PFU virus within 24 hours of eclosion and observed daily for mortality for 21 days thereafter. There was no significant difference between SV and VEEV-B2-infected groups. SV (N = 172); SV-B2 (N = 318); VEEV-B2 (N = 98). Data are combined from at least three different experiments.

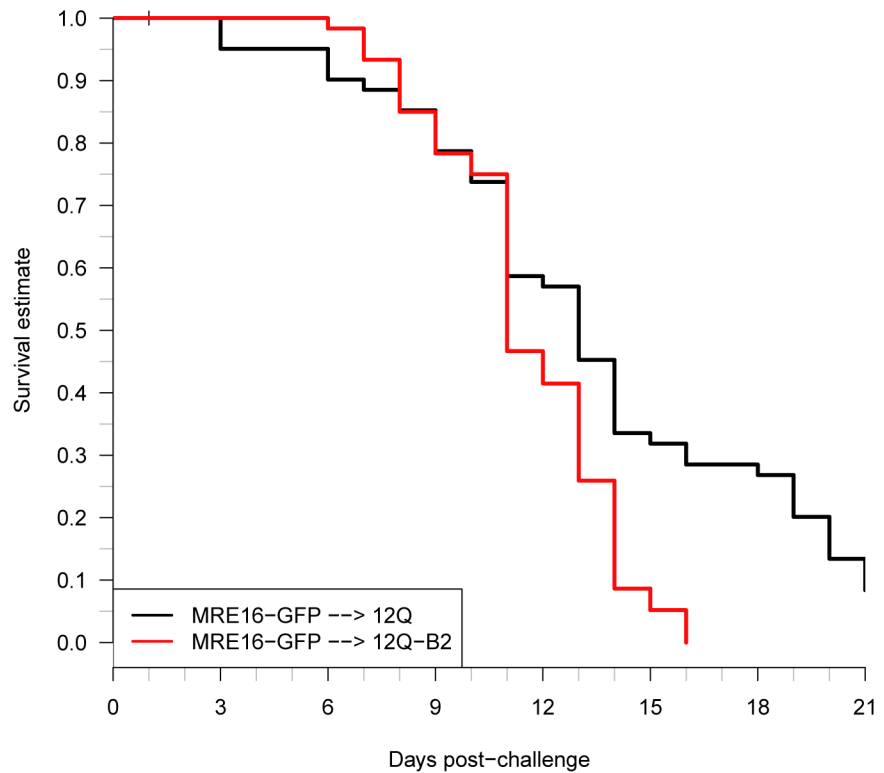


Figure 2-13. Killing by dsTE12Q-B2 in animals inoculated with MRE16 SV. The two strains of SV appear to synergize during coinfection. Nevertheless, mosquitoes challenged with dsTE12Q-B2 show significantly greater mortality than controls infected with both strains but not B2. MRE16-GFP→12Q (N = 62); MRE16-GFP→12Q-B2 (N = 60). P < 0.001.

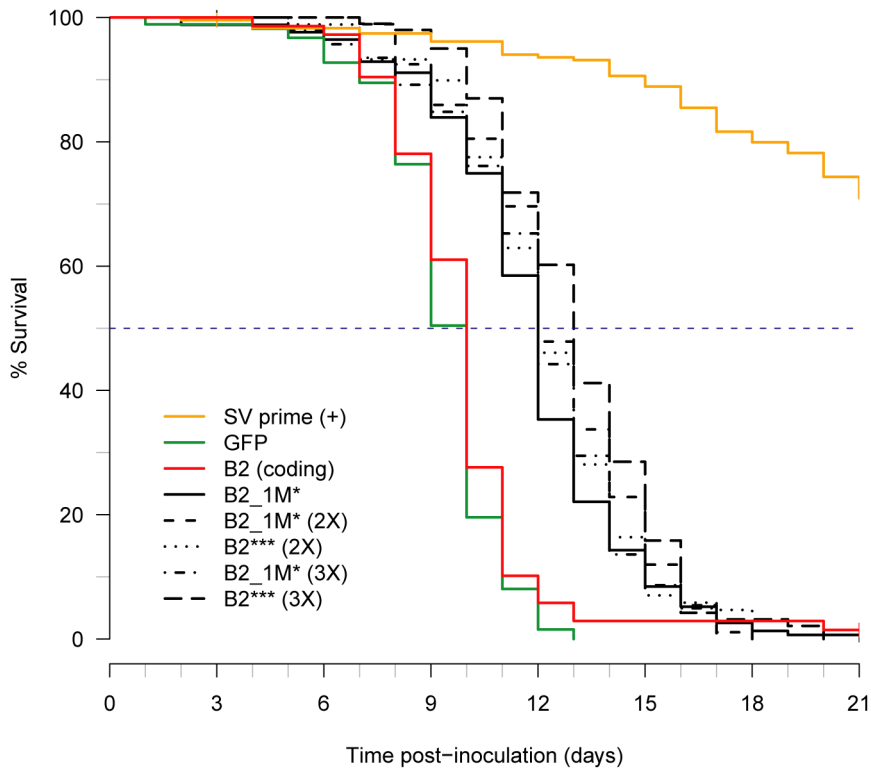


Figure 2-14. Killing by SV-B2 in VEEV-infected mosquitoes. Although several forms of non-protein-coding B2 were used in the study, all produced similar degrees of protection statistically indistinguishable from each other. The only priming virus to produce significantly greater protection compared to VEEV-B2_1M* was VEEV- B2*** (3X), ($N = 96$; $p = 0.000137$, Cox proportional hazards model). Differences between other groups with various copies of B2 sequence was not significant ($N = 414$). However, mosquitoes primed with VEEV encoding a functional B2 protein (red) are no more protected from hypervirulent SV-B2 than mosquitoes primed with VEEV-GFP. Mosquitoes primed with SV (orange) are shown as a control for survival. Data are plotted from at least three independent experiments.

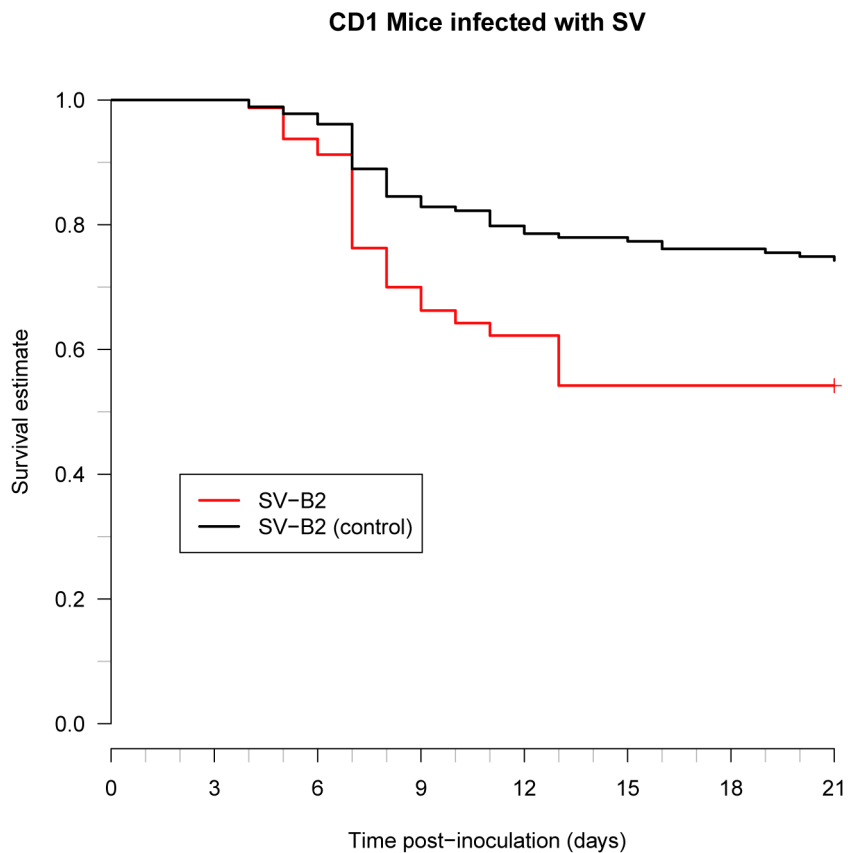


Figure 2-15. SV-B2 enhances virulence in four day old CD1 mice ($N = 80$), resulting in 20% greater mortality compared to control viruses of similar insert sizes ($N = 181$; $p = 0.001$, log-rank test). Data are plotted from 10 independent experiments.

Chapter 3

Evaluating recombinant Sindbis virus expressing *reaper* for use as a biopesticide

Introduction

Mosquitoes as disease vectors

Mosquitoes are obligate hosts for a variety of pathogens of human health importance. Examples include the malaria parasite *Plasmodium*, nematode filarial worms such as *Brugia* and *Onchocerca*, and viruses of several families including the etiological agents of yellow fever and dengue fever (*Flaviviridae*), California encephalitis (*Bunyaviridae*) and numerous alphaviruses from the *Togaviridae* including Venezuelan equine encephalitis virus (VEE), Eastern equine encephalitis virus (EEE), Western equine encephalitis (WEE) and Chikungunya virus (CHIK) [182]. Over the second half of the twentieth century numerous efforts were made to control insect vectors of human disease, perhaps most notably with the introduction of dichlorodiphenyltrichloroethane (DDT) in the

1950s through the end of the 1960s during the World Health Organization's (WHO) ambitious campaign to eradicate malaria [183, 184]. The goals of the program were ultimately changed to focus on control rather than eradication due to the appearance of resistance to DDT and permethrin among vector insects and a lack of cost-effective alternatives [159, 183].

Biopesticides for insect control

Recent years, however, have seen renewed interest in the development of a variety of infectious biological insecticides, or biopesticides, based on existing microbial pathogens for the purpose of insect control. Examples of biopesticides include the naturally occurring and engineered baculoviruses used commercially to kill a wide variety of agricultural pests [185] and the proposed use of fungal pathogens against disease-vector mosquitoes [162, 186]. As yet, no commercial virus-based biopesticides have been developed against mosquitoes, although a number of research labs have tested potential prospects [187, 188]. It has been speculated that since most vector-borne pathogens require substantial time (as long as two weeks) to develop in their arthropod host, specific targeting and elimination of the older, transmission-competent individuals in the population need be accomplished to effectively reduce disease burden. These transmission-competent insects represent only a small proportion of the total pest population and contribute little to the effective population size, prompting some investigators to speculate on the development of “evolution-proof” virus-based biopesticides that act relatively late in the adult animal’s life [163, 188, 189].

Drosophila Reaper as a biopesticide effector

The *Drosophila* gene *reaper* (*rpr*) is a potent regulator of cell death originally discovered in a genetic screen of mutants deficient for embryonic cell death [143]. The amino-

terminal consensus sequence [A-(V/T/I)-(P/A)-(F/Y/I/V/S)] shared by Reaper was subsequently shown to be essential for binding the BIR2 domain of DIAP1 preceding its ubiquitylation, thus promoting its degradation [51, 144, 145]. Uninhibited by IAPs, active caspases are free to engage their polypeptide substrates, resulting in apoptotic cell death [146, 147]. Reaper was also reported to act as a general inhibitor of translation that binds directly to the 40S ribosomal subunit independently of its described role binding IAPs and promoting the degradation of IAPs [148] and more recently implicated in self-association and mitochondrial permeabilization in response to damage [149, 150]. The potent and multi-functional killing capacity of Reaper combined with its small size (65 amino acids) and its conserved N-terminal IAP-binding motif (IBM) made it an attractive candidate virus-based biopesticide effector molecule [190, 191].

Alphaviruses as gene expression vectors

Sindbis virus (SV) is a single-stranded, enveloped RNA virus of plus-sense polarity and the type-species of the *Alphavirus* [7] genus. SV was first isolated from mosquitoes in Egypt in 1953 [192, 193]. Shortly thereafter it was found that although the virus could cause a lethal infection of newborn mice, mice became completely resistant to cell death by one week of age [194, 195]. A major technical advance was the development of infectious clones of full-length virus, which allowed mutations to be introduced for the purpose of studying mechanisms of virulence [13, 196]. Two strains of cloned alphaviruses were used in the study. The first, dsTE12Q, is a cloned virus derived from a virulent, vertebrate-adapted strain of Sindbis virus [14, 19]. The virus encodes two promoters, one at the 5' end to drive expression of the non-structural genes, and a strong sub-genomic promoter that drives expression of the structural genes at the 3' end of the genome. This dsTE12Q strain contains a duplicated copy of the strong sub-genomic (double subgenomic, or ds) promoter that is inserted downstream of the

coding sequences (Figure 3-1A). Genes of interest inserted downstream of this second sub-genomic promoter can then be expressed in tissues capable of supporting SV replication [14]. As a control for the known effects of insert size on the replication and packaging efficiency of recombinant viruses [197], the Reaper transgene was cloned into the virus cDNA in both the forward (protein-coding) and reverse orientations (Figure 3-1A). A Reaper mutant allele ($Rpr^{\Delta IBM}$) lacking amino acid residues two through five (Ala-Val-Ala-Phe), critical for binding IAPs, was constructed to investigate the involvement of IAP-binding in cell death phenotypes (Figure 3-1B). The SV strain MRE16 was isolated from cells derived from the mosquito *Aedes pseudoscutellaris* [197]. MRE16 was passaged exclusively in arthropod cells before its genome was cloned into a bacterial plasmid as a cDNA [198]. In contrast to dsTE12Q, the sub-genomic promoter of MRE16 was placed upstream of the structural genes for the purpose of adding stability to the insert-containing virus genomic RNA [173].

Materials and methods

Cell lines

Baby Hamster Kidney (BHK-21) cells (ATCC, CCL-10) were maintained in Dulbecco's Modified Eagle's Medium (DMEM) supplemented with 10% FBS and penicillin/streptomycin at 37°C with 5% CO₂. *Aedes albopictus* C7-10 cells were a gift kindly provided by Dr. Raquel Hernandez (North Carolina State University). C7-10 cells were maintained in minimum essential medium (MEM) supplemented with 10% FBS and penicillin/streptomycin at 28°C with 5% CO₂.

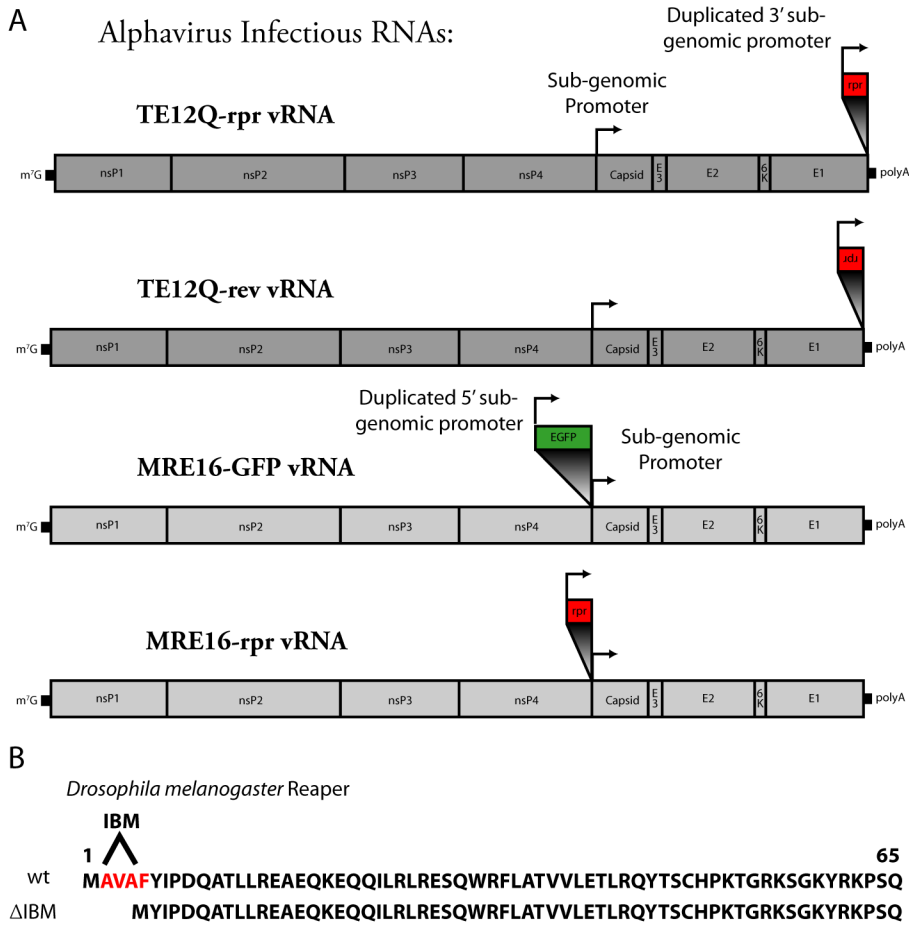


Figure 3-1. Alphavirus expression constructs used in the study. **(A)** Recombinant alphaviruses used in this study were based on TE12Q (SV) and MRE16 (SV). Subgenomic promoters were duplicated upstream (dsMRE16) and downstream (dsTE12Q) of the structural genes to drive transgene expression. **(B)** Amino acid sequence of Reaper from *Drosophila melanogaster*. The IAP-Binding motif (Ala-Val-Ala-Phe) is deleted in the Δ IBM mutant.

Insect rearing

Eggs from the Rockefeller strain of *Aedes aegypti* were kindly provided by Dr. George Dimopoulos (JHSPH). Dried eggs were hatched in a vacuum chamber under deoxygenated conditions in dH₂O for one hour at room temperature to stimulate egg-hatching. A 1:2:2 mixture of blended Timmy Rabbit Pellets (American Pet Diner, Code: Pellet_TR), liver powder (MP Biomedicals, Cat. #900396) and TetraMin tropical fish flakes was used as larval food. Freshly hatched first-instar larvae were poured into a

10" x 12" plastic photo developing tray (Photoquip, Cat. #CES1012T) in one liter of dH₂O with 10 mg food added. Three days later, larvae were diluted to 200 individuals per tray with 10 mg food per tray on that day and every 2 days thereafter until a majority of larvae had entered the pupal stage. Pupae were strained through a fine metal colander and placed in a cup of dH₂O in a plastic cage (Bioquip, Cat. #1452). Pupae were left overnight to eclose with cotton-balls (Fisherbrand, Cat. #07-886) saturated in an autoclaved 10% sucrose solution in water. Young adult mosquitoes newly emerged from the pupal case were either used immediately or allowed to age according to the needs of the experiment, at which time they were removed and placed in individual paper cups.

Virus constructs

Virus constructs were based on either pdsTE12Q [14] or pdsMRE16 [173]. The *reaper* ORF and the N-terminal deletion mutant were amplified from a plasmid template (pPI83) kindly provided by Dr. Pablo Irusta. The GFP ORF was amplified from pEGFP-N1 (Clontech). The dsTE12Q-Rpr clone (pMVM3) was provided by Dr. Mary Vander Maten. Control constructs shown in Figure 3-8 were provided by Dr. Bing Qi (pBQ8) and Dr. Emily Cheng (pHYC86). For expression in mammalian cells, *reaper* was cloned into plasmid pSG5 (Stratagene) as a BglII fragment. Primer sequences (Invitrogen, IDT) are located in Appendix I. BstEII or NotI-sites were added to the amplicons for cloning into pdsTE12Q or pdsMRE16, respectively. Restriction digested PCR Fragments were purified using the QIAquick Gel Extraction Kit (Qiagen, Cat. #28704) and cloned directly into the appropriate digested vector using T4 DNA ligase (Invitrogen, Cat. #15224-017). The virus vector had previously been dephosphorylated with calf intestinal phosphatase (CIP, NEB Cat. #M0290S) to prevent the recovery of intra-molecular ligation products. Ligation reactions were transformed into *E. coli* strain DH5 α (Invitrogen, Cat. #18265-017) and selected on

LB-Agar plates containing ampicillin (100 µg/ml). Clones containing inserts were identified by a diagnostic digest on a 1% agarose gel with either BstEII (pdsTE12Q) or NotI (pdsMRE16). Positive clones were verified by sequencing at The Core DNA Analysis Facility at Johns Hopkins University. Bacterial stocks were prepared from overnight cultures and frozen in 15% glycerol at -80°C.

Cell counts and viability stains

C7-10 cells were plated in a 6-well plate (10^5 cells per well) and infected at a multiplicity of infection (MOI) of five in the case of dsTE12Q-based viruses and an MOI of 0.1 in the case of MRE16-based viruses, which did not grow to sufficiently high titres to infect at a higher MOI. At the indicated times post-infection, supernatant media was aspirated into a 15-ml conical Falcon tube. Cells were washed twice with 1 ml PBS and each wash was added to the conical tube. Finally, remaining adherent cells were trypsinized and added to the conical tube, along with an additional wash of the well surface with PBS. The entire volume was then spun at 3000 x g for 30 minutes to pellet the small mosquito cells, which were resuspended in PBS. An equal volume of trypan blue was added to an aliquot of cells which were then counted on a hemocytometer and corrected for the dilution.

In vitro transcription of infectious virus

Transcription templates were prepared from overnight bacterial cultures containing recombinant plasmids (Qiagen, Cat. #12643). Plasmids were linearized by restriction digest with XhoI and AscI for pdsTE12Q and pdsMRE16, respectively. Residual enzyme was removed by incubating the digests with proteinase K (100 µg/ml) (Invitrogen, Cat. #25530-015) for one hour at 65°C. Remaining protein was then extracted with phenol. Residual phenol was removed with chloroform and the remaining DNA

was precipitated and washed in 70% ethanol. This purified, linearized dsDNA was resuspended in RNase-free dH₂O and served as the template in the subsequent transcription reaction. Infectious virus genomes were transcribed using 1 μ g template DNA and SP6 RNA polymerase for 120 minutes at 37°C with the Ambion mMessage mMachine kit (Cat. #AM1340). To favor the production of large transcripts, additional GTP was added, giving a ratio of 1:1 capped to uncapped transcripts in the final product. After two hours, DNase was added to the reaction to eliminate the template and samples were incubated another 15 minutes at 37°C. These reactions were purified on an Ambion MEGAclear column (Cat. #AM1908) and the eluates were quantified on a Nanodrop 2000 spectrophotometer. Highly purified ssRNA, with a 260:280 absorption ratio of ~2.2 [175] was routinely obtained through the above process.

Rescue of recombinant virus

Purified infectious vRNA (4 μ g) was transfected into BHK cells (ATCC) with Lipofectamine 2000 according to the manufacturer's protocol (Invitrogen, Cat. #11668-027). After two hours, transfection media was replaced with DMEM containing 1% FBS. Virus was harvested 18-24 hours post-transfection, when the cells began to show moderate to heavy CPE. Supernatants were spun for one minute at 16,000 x g to remove cellular debris and frozen in aliquots at -80°C. Titres of collected virus were subsequently determined by plaque assay on BHK cells.

Plaque assays

Plaque assays were performed essentially as described [14]. BHK cells were plated in 6-well plates and 10-fold dilutions of virus aliquots in DMEM containing 1% FBS were adsorbed for one hour at 37°C in 200 μ l over the cell monolayer. MEM (without

phenol red) in 0.6% Bacto-Agar was added to immobilize viruses. Focal plaques of infection were stained after 48 hours with neutral red (1%) in MEM. Plaques were counted and corrected for dilution factor. Titre is expressed as plaque forming units per milliliter (PFU/ml).

Western blotting

Cultured cells were lysed in RIPA Buffer with protease inhibitor cocktail (Sigma, P2714). Samples were sonicated and their concentrations were measured using the BCA Protein Assay Kit (Thermo Scientific, Cat. #23225). Each sample was boiled for five minutes at 95°C in Laemmli's buffer [175, 199]. Proteins were separated by sodium-dodecyl-sulfate-polyacrylamide gel electrophoresis (SDS-PAGE) in a discontinuous Tris · tricine buffer system essentially as described [200]. Gels were run overnight and transferred to an Immobilon-P_{SQ} Membrane (Millipore, Cat. #ISEQ 101 00). The membrane was washed and blocked against non-specific binding with 5% non-fat dried milk (Lab Scientific, Cat. #M0841). The primary antibody was directed against the well characterized HA-epitope of influenza hemagglutinin (α -HA clone 12CA5, Roche Cat. #11 666 606 001) which was engineered into the expression constructs via PCR. Primary antibody was diluted 1:1000 in 3% non-fat milk and TBS · T. The HRP-conjugated secondary antibody (GE Healthcare, Cat. #NA931V) was diluted 1:10,000 in 3% milk. Labeled proteins were detected on auto-radiographic film (GE Healthcare, Cat. #28906839) using the SuperSignal® West Pico Chemiluminescent Substrate Assay (Pierce, Cat. #34078).

Microscopy

Images of mosquito C7-10 cells and dissected mosquito midguts were acquired using Spot 4.0.1 software and camera on a Nikon Eclipse E800 microscope equipped with

a high pressure mercury halogen lamp using differential interference contrast (DIC) optics and a Nikon Plan Fluor 20X/0.50 DIC M objective at 200X total magnification. Epi-fluorescence was acquired using a Nikon B-2E/C filter. Images of live mosquitoes were acquired using Spot 4.0.1 software on a Nikon Eclipse TE200 inverted microscope with a Modulation Optics, Inc HML ELWD Plan Fluor 20X/0.60 objective. Whole body images were acquired at 20X total magnification with a Nikon Plan UW 2X/0.06 objective. Images of the eye and head were taken at 100X total magnification with a Modulation Optics, Inc HML ELWD Plan Fluor 10X/0.30 objective. White light images were taken with bright field optics. Fluorescent images were acquired using a Nikon B-2E/C filter. Dissected midguts were fixed with 4% para-formaldehyde in PBS for 15 minutes. Guts were washed twice for 15 minutes and mounted with Mowiol 4-88 (Calbiochem, Cat #475904). Slides were allowed to dry overnight at 4°C and examined the following day. Image black levels were optimized using Adobe Photoshop CS. The same transformations were applied across each image to avoid bias.

Virus injections

Adult, female *Ae. aegypti* mosquitoes were separated into small cups kindly provided by Dr. Nirbhay Kumar (JHSPH) and Dr. William E. Collins (CDC-Malaria Branch). Mosquitoes were knocked down on ice for five minutes. Needles for virus microinjection (Drummond Scientific, Cat. #3-000-210-G) were pulled on a Sutter P-2000 microcapillary puller using the following program: Heat=350, Filament=4, Velocity=50, Delay=225, Pull=150. Pulled microcapillaries were backfilled with mineral oil (Sigma, M5904) and fitted to onto a Nanoject II microinjector (Drummond Scientific). Needles were then submerged in thawed virus supernatant diluted to 1000 PFU per 69 nl injection ($1.45 \cdot 10^7$ PFU/ml) and filled from the tip. Mosquitoes were injected on an EchoTherm chilling plate (Torrey Pines Scientific) set to 0°C with a

piece of wet, white filter paper (Fisher Scientific, Cat. #09-790-12C) on top to enhance contrast. Injected mosquitoes were returned to their cages and allowed to recover at insectary conditions (28°C, 80% RH) and monitored for mortality daily thereafter. Cotton balls saturated with 10% sucrose were changed every two days to prevent the buildup of pathogenic bacteria and fungi.

Feeding *per os*

Recombinant MRE16 virus was concentrated by ultracentrifugation at 100,000g for 120 minutes. Concentrated virus was resuspended from the pellet and quantified via plaque assay. Viruses were diluted to 10^9 PFU/ml and stored in 100 μ l aliquots at -80°C until further use. Aliquots were diluted in 900 μ l whole human blood consisting of 50% erythrocytes and 50% human inactivated plasma at a final titre of 10^8 PFU/ml. Experiments using 10^5 or 10^6 PFU/ml virus are indicated where relevant. Virus-spiked bloodmeals were contained in a water-jacketed glass membrane feeder warmed to 37°C and wrapped in parafilm. Mosquitoes starved the night before were allowed to feed on blood for 30 minutes. After feeding, mosquitoes were knocked down on ice and fed animals were separated from unfed individuals immediately after feeding (thereby ensuring the accuracy of selection). Mosquitoes were allowed to recover in the insectary and monitored at 24 hour intervals for survival assays.

Virus decay assay

To determine the stability of MRE16-SV in a variety of media vehicles, 10^5 PFU was diluted and incubated at 37°C for one or two hours, after which it was immediately quantified with a plaque assay on BHK cells. Plotted data represent two independent experiments.

Results

Vertebrate-adapted SV expressing reaper enhances mosquito cell death in a manner dependent on the IAP-binding motif

Recombinant viruses based on dsTE12Q were used to infect C7-10 cells, which were derived from the mosquito *Aedes albopictus* [201] and monitored at 12, 24 and 96 hours post-infection. Cytopathology was not detectable through 12 hours post-infection (Figure 3-2C) although functional, new progeny virus was readily detectable at this time (Figure 3-2B). All viruses displayed similar replication kinetics through 24 hours post-infection. Differences between treatment groups was significant ($p = 0.0296$) at 96 hours post-infection, but can be explained by the absence of cells in which to replicate in the case of SV-Rpr, which was present at the lowest titre of the three viruses at that time point. By 24 hours post-infection, cytopathic effects (CPE) were observed in all virus infected groups, although this pathology was distinct between viruses. Cells infected with SV-Rpr displayed the morphologically characteristic membrane blebbing of insect apoptosis [128] consistent with the described role of Reaper in caspase activation, whereas mosquito cells infected with SV-Rpr $^{\Delta IBM}$ clumped into web-like masses of live cells (Figure 3-2C). The Reaper-associated phenotype was clear by 24 hours post-infection. By 96 hours post-infection, the cell population was annihilated in the SV-Rpr-infected cells. The dependence of the phenotype on the presence of the N-terminal IBM of Reaper was indicated by a significant difference between the total cell counts of SV-Rpr and SV-Rpr $^{\Delta IBM}$ infected cells at 96 hours post-infection ($p < 0.0001$). Measurements of cell viability by Trypan blue exclusion indicated a significant difference in viability between cells infected with SV-Rpr relative to cells infected with SV- Rpr $^{\Delta IBM}$ by 24 hours that remained through 96 hours post-infection ($p < 0.01$ and 0.025, respectively) (Figure 3-7). These data show that infection of insect cells

with SV-Rpr results in enhanced killing of insect cells relative to control viruses *in vitro*. Cytopathology was also observed in cells infected with the control virus, SV-rev, as well as the virus carrying the deletion mutant, SV-Rpr^{ΔIBM}. However, the degree of CPE in these two groups was far less than with SV-Rpr. While mock-infected cells continued to grow to confluence over the four day experiment, virus-infected cells showed little proliferation at early time points compared to mock-infected cells, but largely recovered by 96 hours post-infection (Figure 3-2C). This may represent a stall in the cell cycle during the acute phase of infection. Alternatively, the absence of cell proliferation may be a result of a subset of cells dying during the acute infection, only to be replaced by those persistently-infected cells capable of supporting SV replication over time. These results indicate that vertebrate-adapted SV expressing *reaper* is able to induce apoptotic death in C7-10 *Aedes albopictus* cells within 24 hours of infection. Furthermore, this cell death phenotype is dependent on the N-terminal IBM of Reaper, implying that inhibition of IAP-like proteins may be important for the cell death. Thus, the efficacy of Reaper as an effector molecule for use in a mosquito control strategy would be dependent on both the presence and retention of this sequence during the infection.

An orally infectious clone of Sindbis virus expressing *reaper* enhances cell death in an IBM-dependent manner

The killing phenotype associated with Reaper expression in the dsTE12Q strain of SV prompted us to recreate the strains described above in the genetic background of the MRE16 strain of SV, which has been shown to disseminate in a majority of infected mosquitoes [173]. Systemic spread of the virus from a bloodmeal in the mosquito midgut is essential for infection of the salivary glands and thus transmission of virus to a new vertebrate host. Virus dissemination beyond the gut is also critical for the

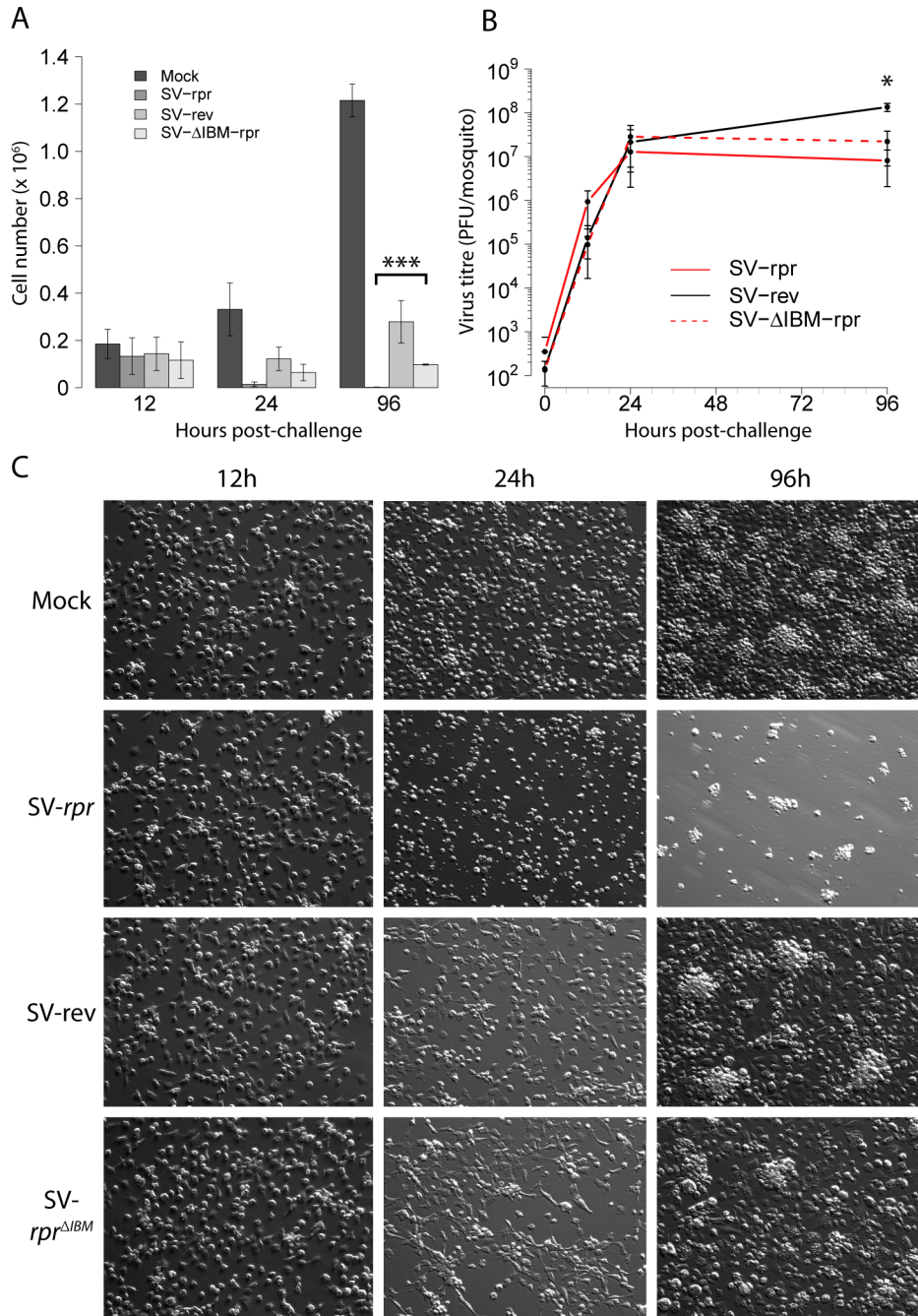


Figure 3-2. Recombinant, vertebrate-adapted Sindbis viruses (dsTE12Q) expressing Reaper enhance mosquito cell death in an IAP-binding motif (IBM)-dependent manner. **(A)** C7-10 cells were infected with recombinant Sindbis viruses as indicated and total cell numbers were counted at 12, 24 and 96 hours post-infection ($p < 0.0001$, t-test). **(B)** Replication of SV in C7-10 cells over time was determined by plaque assay on BHK cells ($p = 0.0297$, t-test). **(C)** C7-10 cells were either mock infected or infected with the indicated virus (MOI = 5). Representative images were captured at the indicated time points post-infection (200X, HMC).

infection of susceptible nervous tissues that may be associated with killing *in vivo*, reminiscent of vertebrate models of viral encephalomyelitis with SV [13, 194]. Infection of C7-10 cells with MRE16-based expression vectors produced similar phenotypes to those associated with dsTE12Q SV *in vitro*. Virus titres peaked earlier (48 hours post-infection) in cells infected with MRE16-Rpr than in cells infected with either MRE16-rev or MRE16-Rpr^{ΔIBM} (72 hours post-infection). Recombinant MRE16 SV expressing *reaper* replicated to a significantly higher titre at this time point when compared to either the insert size control virus MRE16-rev ($p = 0.0281$) or the IAP-binding deficient mutant virus MRE16-Rpr^{ΔIBM} ($p = 0.0319$) (Figure 3-3A). By 48 hours post-infection, C7-10 cells infected with MRE16-Rpr were annihilated similarly to those infected with dsTE12Q-*Rpr* (Figure 3-3C and 3-2C). In the latter case, however, it took only 24 hours for prominent apoptotic CPE to appear, whereas MRE16-infected cells showed no CPE until 48 hours post-infection. Nevertheless, both the Reaper-associated cell death and the virus-associated CPE were similar in C7-10 cells infected with either vertebrate-adapted dsTE12Q or mosquito-adapted MRE16. Construction of a GFP-expressing strain of MRE16 confirmed the nearly complete cellular prevalence of MRE16 infection and high per cell expression levels of the viral transgene *in vitro* (Figure 3-3B).

Imaging mosquitoes infected by MRE16-GFP *in vivo*

To examine the tissue distribution and relative intensity of transgene expression of MRE16 in mosquitoes, adult female *Aedes aegypti* were infected *per os* with MRE16-GFP in a virus-spiked human bloodmeal. Three days after blood-feeding, mosquito guts were dissected and examined for fluorescence as an indication of virus replication. Fluorescence at this time was restricted to the tissues of the midgut, where it emanated from multiple distinct foci of virus replication (Figure 3-4H and 3-4J). Mock-infected midguts showed no observable auto-fluorescence (Figure 3-4F). By 7 days post-infection

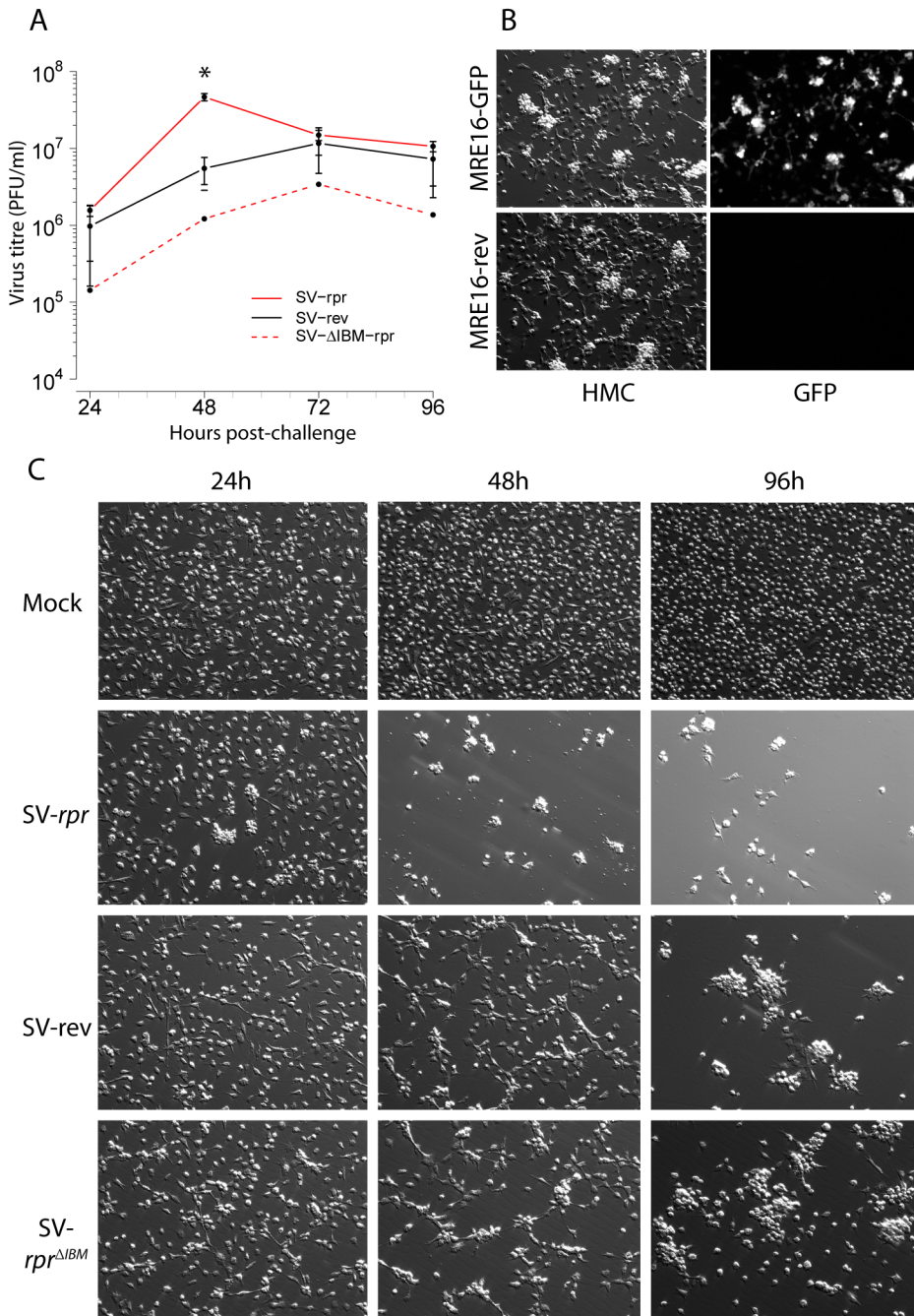


Figure 3-3. An orally infectious, low-passage clone of Sindbis virus (dsMRE16) expressing Reaper enhances mosquito cell death in an IAP-binding motif (IBM)-dependent manner. **(A)** Replication of recombinant MRE16 SVs in C7-10 cells over time was determined by plaque assay on BHK cells (MOI = 0.1). Significant differences in replication are apparent at 48 hpi between SV-Rpr and SV-Rpr $^{\Delta IBM}$ ($p = 0.0319$) and between SV-Rpr and SV-rev ($p = 0.0281$). Error bars represent SD. **(B-E)** Cells infected with recombinant MRE16-GFP at 72h post-infection show intense GFP fluorescence relative to control virus. **(F)** C7-10 cells were either mock infected or infected with the indicated virus (MOI = 0.1). Representative images were captured at the indicated time points post-infection (200X, HMC).

per os, disseminated infections were indicated by GFP expression in tissues throughout the insect, including the whole of the gut and nervous tissues including the neural ganglia in the flagella of the antennae and the brain (Figure 3-4B and 3-4D). The tissue tropism of MRE16-SV and its dissemination pattern in *Aedes aegypti* in our hands is consistent with that reported previously, with the greatest intensity of GFP expression in the eye and brain [173].

Disseminated infection with SV-Rpr kills mosquitoes in an age dependent manner when injected

To determine the killing capacity of SV-Rpr under the idealized conditions of an assured disseminated infection, we injected 1,000 PFU SV intrathoracically into the hemocoel of adult *Aedes aegypti* female mosquitoes within the first 24 after eclosion or at 3 or 10 days post-eclosion (Figure 3-5). A significant decrease in survival was observed for animals infected with dsTE12Q-*Rpr* regardless of their age at the time of infection relative to age-matched controls infected with dsTE12Q-rev ($p < 0.0001$ for Figure 3-5A, 3-5B and 3-5C). Additionally, mosquitoes inoculated within their first day of life displayed enhanced mortality relative to either 3 or 10 day old animals (Figure 3-5D, $p < 0.0001$). There was no significant difference in mortality between 3 and 10 day old mosquitoes infected with dsTE12Q-*Rpr*. Parallel experiments tested the killing capacity of Reaper in the insect-adapted MRE16 virus background, but no significant differences between groups were observed over 15 days (Figure 3-9). Therefore, intrathoracic inoculation of the vertebrate-adapted dsTE12Q clone of SV expressing Reaper caused substantial killing of adult mosquitoes in an age-dependent fashion analogous to vertebrate models of SV infection [18, 202]. However, injection with MRE16-Rpr and the accompanying disseminated infection produced no significant effect on survival *in vivo* over the course of the experiment, suggesting that Reaper

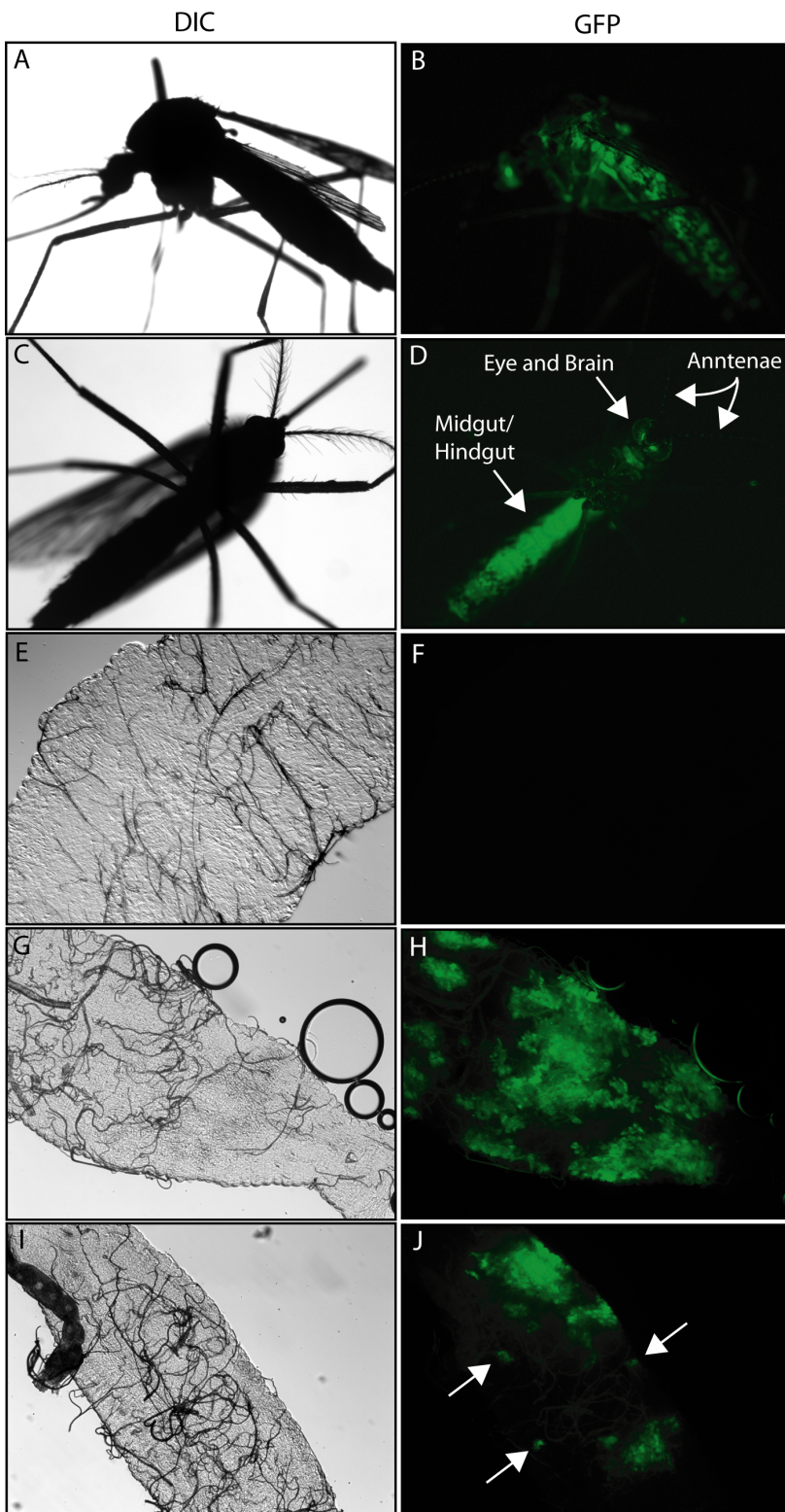


Figure 3-4. Infection *per os* of *Aedes aegypti* by MRE16-SV gives rise to a systemic infection disseminated throughout the animal. (A-D) MRE16-GFP expression patterns in whole, live mosquitoes 7 days after infectious bloodmeal (20X total magnification). (E-J) Midguts show widespread GFP expression 72 hours after taking an infectious bloodmeal, small foci of infection (white arrows) are indicated (200X total magnification).

would be unsuitable for use as a biopesticide effector in MRE16.

Infection of adult *Aedes aegypti* *per os* with MRE16-SV in sucrose or a bloodmeal

Given the low passage history since retrieval from mosquitoes of MRE16 and its described capacity to produce a disseminated, systemic infection in *Aedes aegypti* when administered *per os*, we fed the virus to adult female mosquitoes either as a bloodmeal or diluted in an osmotically balanced sucrose solution. To verify the stability of the virus under the conditions of blood-feeding, aliquots of virus were heated for one or two hours at 37°C and subsequently plaque titrated on BHK cells (Figure 3-10). When delivered in blood, MRE16-SV retains 40-50% infectivity after one hour and 30-50% infectivity after two hours. When delivered in a 10% sucrose solution, MRE16-SV retained over 50% infectivity after one hour and about 30% infectivity after two hours. These observations show that less than one Log of virus is lost during the feeding process in either vehicle at 37°C for up to two hours. All preparations used had preserved virus infectivity to a much greater extent than a previously described synthetic bloodmeal [203]. The blood feeding solution contained 10^8 PFU/ml. Conservative estimation of a mosquito bloodmeal at one microliter yields a dose per animal of 10^5 PFU. If 10% (1 Log less) of those remain after two hours of feeding each mosquito should be exposed to over 10,000 infectious units of virus. *Aedes aegypti* do not desire to take blood immediately after eclosion. Thus, it was not practical to feed adults during this window of enhanced susceptibility. No significant effect was observed when giving a dose (10^5 PFU/ml) of virus in a 10% sucrose solution compared to a virus-free 10% sucrose solution (Figure 3-6A). Similarly, feeding a relatively low dose in blood (10^6 PFU/ml) had no significant effect on survival between groups of 3 day old mosquitoes (Figure 3-6B). Feeding a higher

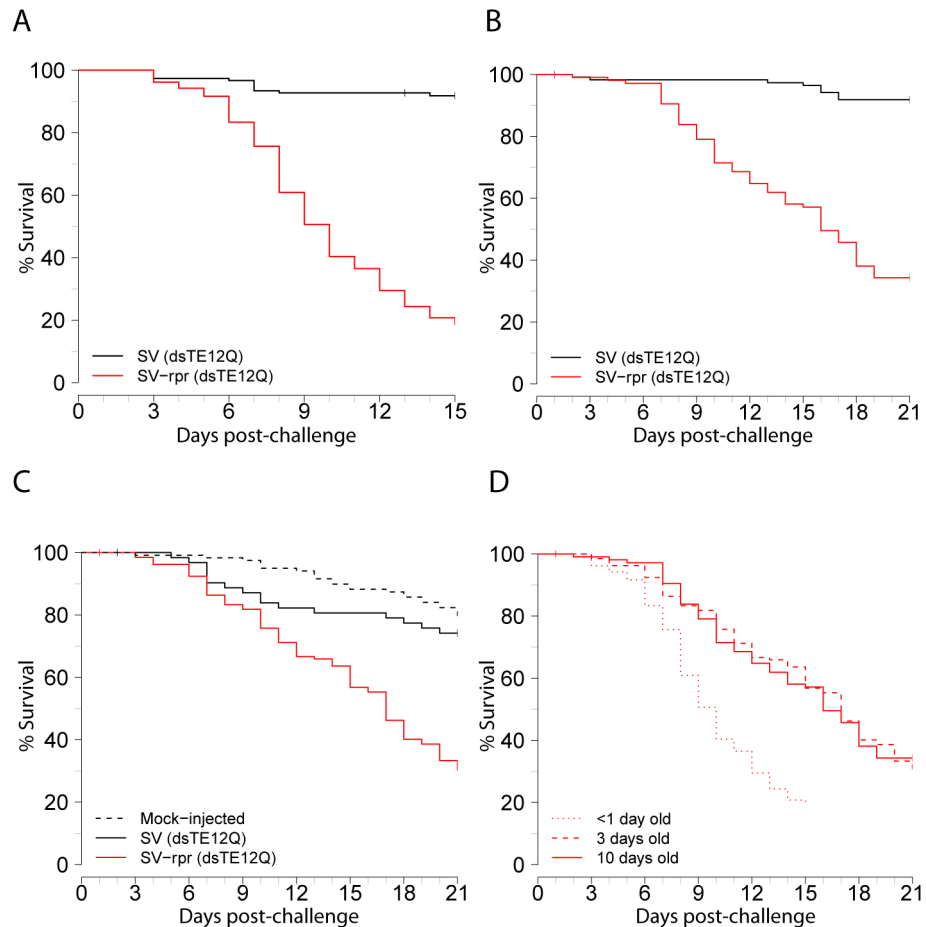


Figure 3-5. Disseminated infection with SV-Rpr kills mosquitoes in an age dependent manner when injected *in vivo*. Adult female *Aedes aegypti* were injected with 1000 PFU recombinant SV and monitored for survival. Survival of adults less than 1 day (N = 120 and 124) (**A**), 3 days (N = 126 and 113) (**B**) or 10 days (N = 122, 70 and 135) (**C**) old at the time of injection were inoculated with dsTE12Q-based viruses. (**D**) SV-Rpr killing as a function of mosquito age at the time of inoculation. Results plotted represent three independent experiments.

dose, however, produced a significant effect. Feeding 10^8 PFU/ml MRE16 resulted in significant death in individuals infected with recombinant virus expressing *reaper* relative to infected controls (Figure 3-6C, $p = 0.0104$). During this set of experiments, mortality was generally high even in the mock infected group, probably due to the accumulation of pathogenic bacteria and fungi on the sucrose-saturated cotton ball food source, with an estimated survival of only 29.7% at 21 days post-infection. To correct for this high general mortality, values plotted in Figure 3-6C were taken as a fraction of the mock survival estimate for each time point (Figure 3-6D). Nevertheless, by 21 days post-infection, only 3.25% of the animals infected with SV-Rpr survived. This represents an 80% reduction in survival relative to infected controls by 21 days, indicating that infection with SV-Rpr enhances the death of infected mosquitoes *in vivo*.

Discussion

Expression of the *Drosophila* death gene *reaper* in Sindbis virus kills mosquitoes and mosquito-derived cells. The killing capacity of the vertebrate-adapted, dsTE12Q strain of SV was greater both in time to and extent of killing than that observed in the insect-derived, orally infectious SV strain MRE16. In the absence of *reaper*, Sindbis virus infection of C7-10 cells proceeds through a characteristic acute phase of logarithmic viral replication followed by an indefinite persistent phase in which virus titres stabilize. This stabilization is probably not due to the death of a sub-population of highly susceptible cells, as comparable numbers of cells were present at early and late time points post-infection. By 96 hours post-infection, titres of control virus reached over 10^8 PFU/ml, which corresponds to between 10^2 and 10^3 infectious viruses per cell. Conversely, cells infected with SV-Rpr are obliterated within 24 hours post-infection, illustrating the remarkable cell-killing potential of *reaper* in invertebrate cells and highlighting its

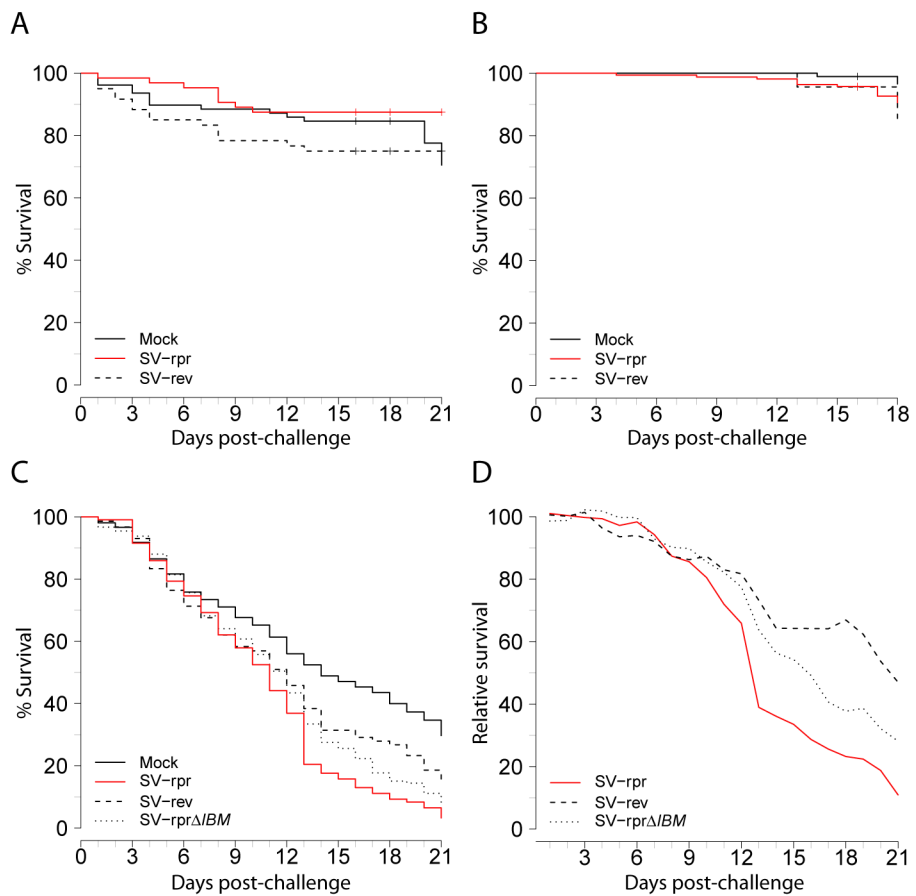


Figure 3-6. Infection *per os* of adult *Aedes aegypti* with MRE16-SV in sucrose (A) or in a bloodmeal (B, C). (A) There was no significant difference in mortality between group fed on a virus-spiked (10^5 PFU/ml) sugar solution ($N = 78, 64$ and 60). Data plotted are from three independent experiments. (B) There was no significant difference between groups fed on virus-spiked blood (10^6 PFU/ml) ($N = 94, 164$ and 91). Data plotted are from three independent experiments. (C) When fed in a virus- spiked bloodmeal, SV-MRE16 (10^8 PFU/ml) expressing reaper significantly enhances mosquito mortality relative to infected controls ($p = 0.0104$). There was no significant difference in mortality between viruses expressing reverse controls and those expressing a reaper IAP-Binding Motif deletion mutant (Reaper Δ IBM) ($N = 207, 213, 216$ and 242). Data plotted are from 8 independent experiments. (D) Survival estimates of (B) normalized to mock survival at each time point highlight relative differences in mortality between virus-infected groups.

functional conservation in mosquitoes, despite the absence of an orthologous gene [204]. Infection of C7-10 cells with MRE16 proceeds in much the same way as infection with dsTE12Q, but death occurred later than with dsTE12Q. The delay in CPE and killing is likely due to the differences in multiplicity of infection (MOI) between the two experiments. Alternatively, the delay could be due to the lower replication capacity or altered tropism of the insect-adapted MRE16 relative to the vertebrate-adapted dsTE12Q in mosquitoes. However, SV-GFP-infected mosquitoes appeared to have similar distributions of fluorescence with either strain (see Chapter 2 for dsTE12Q whole mosquito fluorescence) including the brain and antennae. Feeding MRE16 SV-Rpr in a reconstituted bloodmeal did produce a significant effect, but not to the degree seen with dsTE12Q delivered by way of injection. Indeed, when MRE16-Rpr was injected into adult mosquitoes, rather than per *os*, thereby immediately initiating a systemic infection, they did not die. As the experiment ran for only 15 days, it is not known whether there may have been a “life-shortening” (i.e. pathogenic) effect in the longer term. The small but significant enhanced mortality seen when feeding greater (10^8 PFU/ml in blood) amounts of virus may have been due to massive cell death in the *reaper* over-expressing infected gut. Alternatively, greater mortality observed in the SV-Rpr infections when substantial death was observed in the mock-infected group is consistent with the previously proposed role of *reaper* in lowering the threshold for cell death in times of stress [148, 205]. The observation that MRE16-Rpr does not kill when injected suggests that it does not share at least a component of the virulence of dsTE12Q-Rpr. This is surprising in light of their shared tropism for the insect brain and warrants further investigation. Namely, which cells must die and how many of them must die for the animal to succumb to infection? The relative inefficiency with which TE/3'2J-based viruses to invade mosquito midgut epithelia [206] and subsequently disseminate to the salivary glands suggests that TE-based viruses (such as dsTE12Q) would be poor candidate biopesticide strains for delivery per

os, especially if disseminated infection is required for its virulence. Although MRE16 SV efficiently replicates and disseminates *in vivo* when administered in blood per *os*, its inability to kill mosquitoes when expressing *reaper* makes Reaper an unsuitable candidate effector molecule for this system. However, the intriguing observation that killing by dsTE12Q-*Rpr*, in the context of an assured disseminated infection was enhanced in mosquitoes less than one day old when injected is reminiscent of the enhanced susceptibility to infection observed in weanling mice, whose neurons become resistant to SV-induced death with age [18, 207]. Identifying the tissues critical for SV pathogenesis could be daunting, given the wide variety of tissues susceptible to infection by SV [6]. However, a clue may be found in the VEEV infection model (see Chapter 2), since VEEV-B2 does not kill mosquitoes. The absence of killing may be explained by differences in tropism between these two viruses. If the above phenotypes are readily reproduced in *Drosophila*, transgenic flies could be created to express fragments of the SV genome in specific tissues (e.g. the fat body) or developmental stages. If transgenic flies ectopically expressing fragments of the SV genome in a specific tissue became refractory to SV-B2 induced death, it would be evidence for the involvement of that tissue in SV pathogenesis in insects. Results from *Drosophila* could then be verified in the less tractable mosquito infection model. Should Sindbis virus induced death in insects *in vivo* prove to be dependent on the death of specific cell types, it will aid not only in the study of cell death pathways and viral pathogenesis in general, but also in the discovery of conserved virus-host interactions.

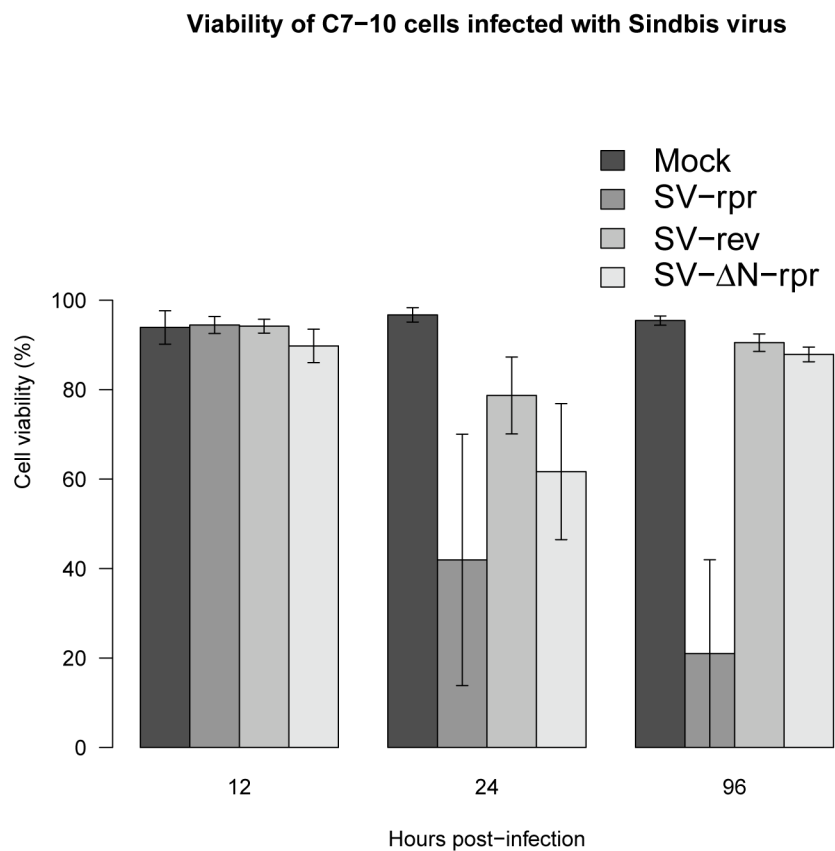


Figure 3-7. Reduction in viability measured by Trypan blue exclusion of C7-10 cells infected with SV-Rpr (MOI = 0.1). Data are plotted from three independent experiments. Error bars represent SEM.

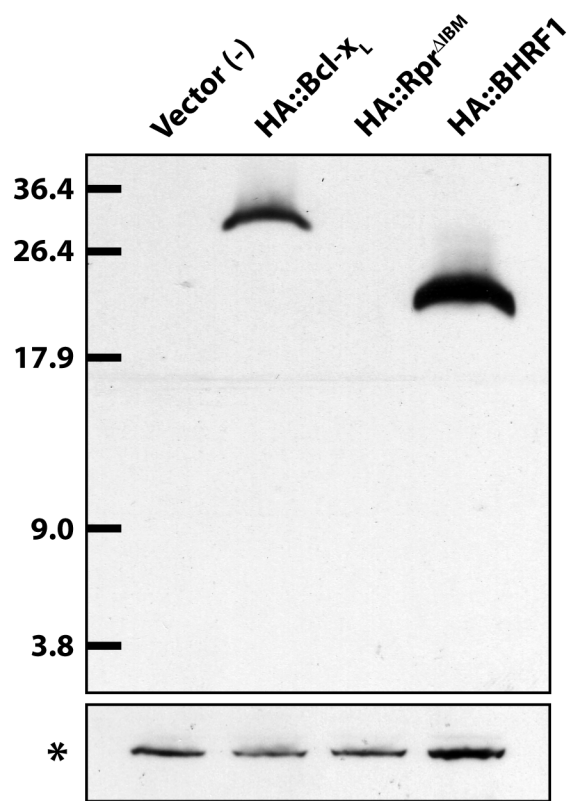


Figure 3-8. Tricine-SDS-PAGE western blot from HeLa lysates with α -HA antibody. While both Bcl-xL and BHRF1 are both readily detectable, Reaper $^{\Delta IBM}$ is absent, consistent with its described role as a general translational inhibitor. The characteristic background band seen in this cell type (*) is shown as a control for loading.

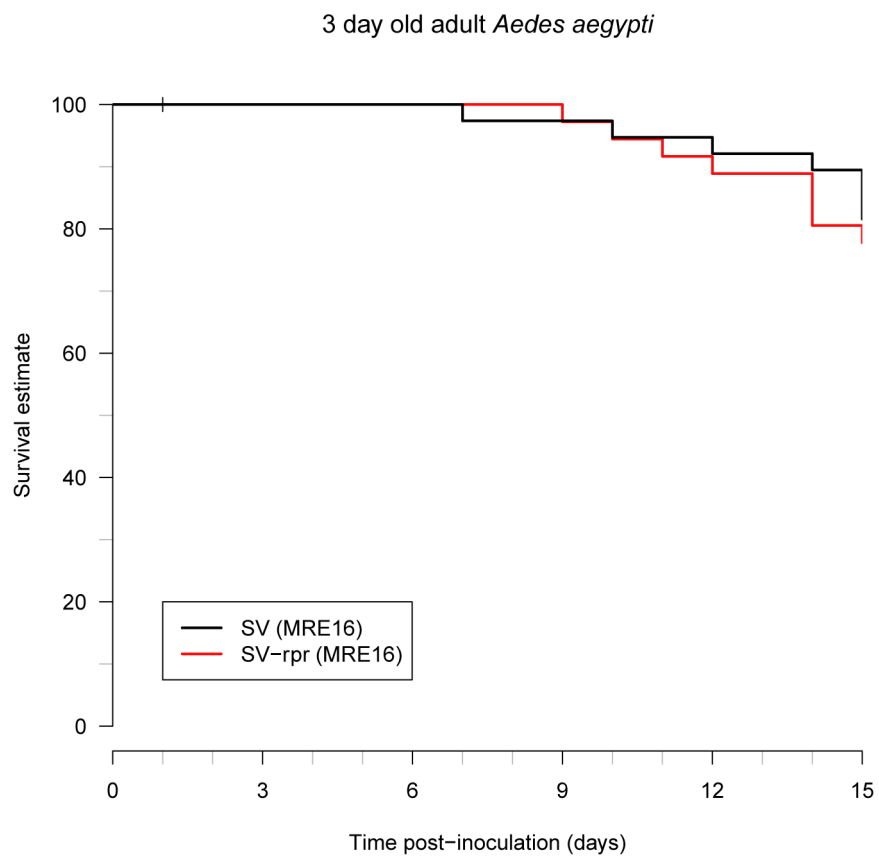


Figure 3-9. The MRE16-Rpr does not kill 3-day old mosquitoes by 15 days when injected ($N = 39, 40$). The results from a single experiment are plotted.

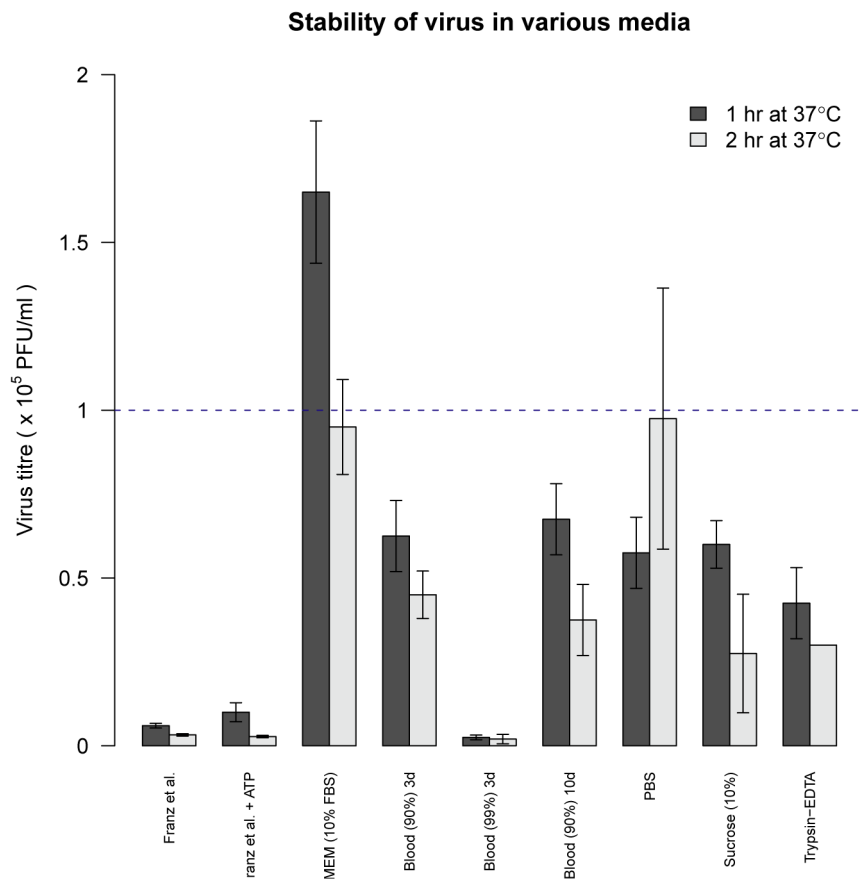


Figure 3-10. Stability of MRE16-Rpr after incubation at one or two hours at 37°C. Duplicate measurements were plotted for both time points in each group. Error bars represent SD.

Chapter 4

Functional analysis of San Angelo virus NSs in the Sindbis virus neurovirulence model

Introduction

Bunyavirus NSs

The *Bunyaviridae* are a family of enveloped, single-stranded, negative-sense RNA viruses that include many human pathogens of public health importance. Notable among these are viruses of the *Hantavirus* genus, the etiological agents of hantavirus pulmonary syndrome (HPS) [151] and Crimean-Congo hemorrhagic fever virus of the *Nairovirus* genus, a highly virulent pathogen requiring Biosafety Level-4 (BSL-4) containment that causes mortality in as many as 50% of infected humans [152]. Pathogenic bunyaviruses of the genus *Orthobunyavirus* include viruses of the California encephalitis serogroup, which contains La Crosse virus and San Angelo virus, among others [208]. The tripartite genomic structure of the *Bunyaviridae* is conserved between

genera and consists of large (L), medium (M) and small (S) RNA segments [7]. The large segment encodes the viral polymerase. The M RNA segment encodes a single ORF that is cleaved co-translationally into two glycoproteins (Gn and Gc) and a poorly characterized non-structural protein (NSm) [6, 153]. The S RNA segment encodes the nucleocapsid coat protein as well as another poorly understood non-structural protein (NSs) of 97 amino acids encoded in an overlapping reading frame [154, 155]. Recent studies investigating the function of NSs have found it to be an important determinant of virulence *in vivo*, despite being dispensable for virus replication *in vitro* [156]. Another group reported a role for Bunyavirus NSs in transcription regulation, wherein NSs interacts with a component of the RNA polymerase II (RNAPII) complex, MED8, in addition to affecting the phosphorylation status and the activity of the C-terminal repeat domain (CTD) of RNAPII itself [209, 210]. Because bunyaviruses lacking NSs potently induce type-I interferon, it was speculated that general host transcriptional shut-off is the mechanism by which NSs suppresses the early interferon response to virus infection, specifically by blocking the induction of response genes by the interferon regulatory factor-3 (IRF-3) transcription factor [211, 212]. A recent study has shown that a mutant lacking the N-terminal 22 residues of NSs is unable to inhibit RNAPII, even though it retains the described MED8 interaction domain. Although the authors suggest that this implies a critical role for the NSs N-terminus in transcription inhibition, a more conservative interpretation of the data is that binding MED8 is not sufficient to inhibit transcription.

Similarities between NSs and Reaper

Bunyavirus NSs was suggested to bear primary sequence similarity to the 65 amino acid *Drosophila* death protein Reaper [157]. The N-terminus of Reaper contains a 16-amino acid motif shared with two other death-inducing cellular proteins, Grim and Hid, and deletion of all three of these genes blocks programmed cell death in the

developing embryo [213]. Using purified recombinant or synthetic proteins, Colón-Ramos and colleagues reported that Reaper and NSs were both capable of inhibiting cellular protein translation in transcriptionally inactive *Xenopus* extracts. Reaper's translational inhibition is independent of its ability to bind IAP proteins. Indeed, residues shared between Reaper and NSs were shown to be critical for global inhibition of cellular translation [148, 157]. A later study by the same group confirmed the direct role of Reaper in translational regulation by specifically binding to the 40S ribosomal subunit [205]. Moreover, both Reaper and NSs possess the capacity to bind to and modulate the activity of the hsp70 chaperone Scythe [157, 158], further supporting a convergent role for Reaper and NSs. The disparate observations of NSs function as outlined above are not necessarily irreconcilable given the economy of coding and function often exhibited by viruses.

Functional analysis of NSs by heterologous expression in SV

Sindbis virus is a single-stranded, enveloped 11.7 kb RNA virus of plus-sense polarity and the prototype of the genus *Alphavirus* [7]. The strain used in this study, TE12Q, is a cloned virus of a vertebrate-adapted strain of Sindbis virus (SV) [14, 19]. This virus, like the wild virus from which it was derived, is avirulent in juvenile and adult mice, but can cause a lethal infection of newborn mice [19, 123]. This virus was engineered to serve as an infectious expression vector, dsTE12Q, with a duplicated subgenomic (ds) promoter to drive the expression of genes of interest [14, 214]. This strong subgenomic promoter normally drives expression of the structural genes at the 3' end of the viral genome (Figure 4-1A). *Bunyavirus* NSs and *Drosophila* Reaper were cloned downstream of the duplicated copy of this promoter in the viral genome for expression in tissues capable of supporting SV replication [14]. To control for the known effects of insert size on the replication and packaging of recombinant viruses [215], the NSs transgene was cloned into the dsTE12Q cDNA in both forward (protein-coding) and

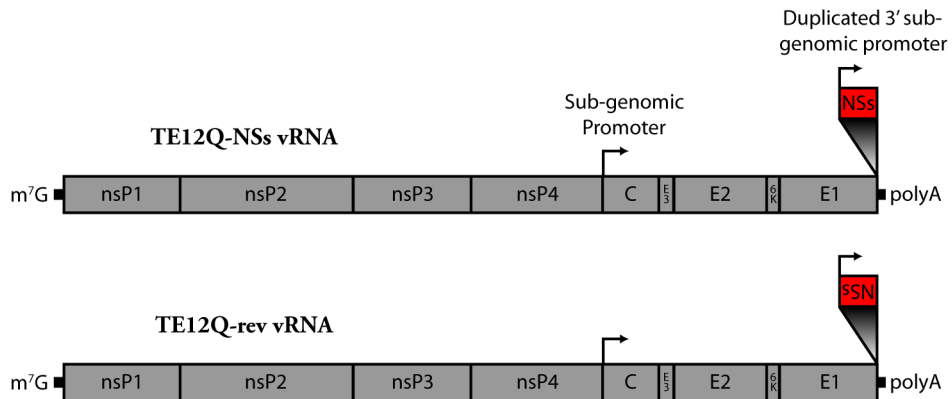
reverse orientations (Figure 4-1A). In addition, a panel of mutants was constructed to examine the effect of individual residues on NSs virulence and function (Figure 4-1B). The mutants were designed rationally based on published results [157]. Namely, an N-terminal truncation of the 33 residues not similar to Reaper was synthesized to examine the role of this region during infection. Leucine to arginine mutations at residues 57 and 59 were shown to abolish caspase activation measured with the peptide substrate Ac-DEVD pNa [157]. Glutamine to alanine mutations at positions 51 and 55 and an arginine to alanine mutation at position 52 were implicated in the translation inhibition function of NSs [157]. The predicted lipid association domain known as GH3 (Grim Helix-3, after the *Drosophila* gene of the same name) was deleted in yet another mutant. The GH3 domain of Reaper is critical for association with lipids on the mitochondrial membrane, where it promotes IAP degradation and hence caspase activation and cell death in both flies and *Xenopus* extracts [214, 216, 217]. NSs mutants deficient for specific NSs functions could be used as tools to examine the contribution of distinct biochemical activities to virulence *in vivo*.

Materials and methods

Cell lines

Baby Hamster Kidney (BHK-21) cells (ATCC, CCL-10), Vero cells (ATCC, CCL-81) and HeLa cells (ATCC, CCL-2) were all maintained in Dulbecco's Modified Eagle's Medium (DMEM) supplemented with 10% FBS, penicillin and streptomycin at 37°C with 5% CO₂.

A Alphavirus Infectious RNAs:



B

Orthobunyavirus NSs



Figure 4-1. Alphavirus expression constructs used. **(A)** Recombinant alphaviruses used in this study were based on dsTE12Q (SV), whose sub-genomic promoter was duplicated downstream of the structural genes to drive transgene expression. **(B)** Amino acid sequence of NSs from the Orthobunyavirus San Angelo virus with emphasis on similarity to *Drosophila* Reaper. Mutated residues are shown in red and numbered according to their position in NSs.

In vitro transcription of NSs mRNAs

NSs and derived mutants were cloned into the pSG5 variant pDB59 [218] as BglII fragments, thereby generating N-terminally HA-tagged fusion proteins. Plasmids were linearized with AflIII. Residual enzyme was eliminated with proteinase K (Invitrogen, Cat. #25530-015) and phenol:chloroform extraction. Samples were concentrated via precipitation with 42% isopropanol and washed with 70% ethanol. Dried pellets were resuspended in RNase-free dH₂O. One microgram of purified linear pDNA was loaded into a transcription reaction using the mMESSAGE mMACHINE® T7 Kit (Ambion, Cat. #AM1344) for one hour at 37°C. Reaction products were purified on an Ambion MEGAclear column (Cat. #AM1908) and quantified on a Nanodrop-2000

spectrophotometer.

Transfection of NSs RNAs

NSs mRNAs were transfected into HeLa and Vero cells with Lipofectamine 2000 (Invitrogen, Cat. #11668-027) according to the manufacturer's protocol. For experiments in which the amount of RNA transfected was a variable, the deficit mass was filled with uncut pSG5 to 4 μ g such that the nucleic acid mass to lipid ratio remained constant between groups.

NSs co-transfection assay

Four micrograms of plasmid DNA encoding wild-type NSs or an NSs mutant were co-transfected with 100 ng pEGFP-N1 into HeLa cells as a reporter for inhibition of gene (EGFP) expression. At 24 hours post-transfection, images of fluorescent cells were acquired under constant exposure time. ImageJ [219] was used to quantify the fluorescence intensity levels for each image.

Cell counts and viability stains

HeLa and Vero cells were plated in a 6-well plate ($5 \cdot 10^5$ cells per well) and transfected with NSs mRNAs. At 21 hours post-transfection, supernatant media was aspirated into a 15-ml conical Falcon tube. Cells were washed twice with 1 ml PBS and each wash was added to the conical tube. Finally, remaining adherent cells were trypsinized and added to the conical tube, along with an additional wash of the well surface with PBS. The entire volume was then spun at $3000 \times g$ for 10 minutes to pellet the cells, which were resuspended in PBS. An equal volume of 0.4% trypan blue solution (Gibco, Cat. #15250-061) was added to an aliquot of cells, which were then counted on a hemocytometer and corrected for the dilution to determine viability.

Immunofluorescence imaging

HeLa cells were grown on coverslips and fixed in 4% paraformaldehyde in PBS for 15 minutes at RT and washed twice in cold (0°C) PBS for five minutes at RT. Cells were permeabilized for 10 minutes with 100 μ M digitonin in PBS and washed three times for five minutes at RT. Non-specific binding to cellular antigens was blocked by incubating fixed, permeabilized cells in 1% BSA in TBS · T for 30 minutes at RT. Cells were incubated with primary antibody (α -HA clone 12CA5, 1:500) for one hour on an oscillating platform at RT. Samples were then washed and incubated with the 1:500 anti-mouse AlexaFluor® 594 (Invitrogen, Cat. # A-11037) for one hour at room temperature in 1% BSA in TBS · T on an oscillating platform in the dark. Samples were washed and nuclei were stained with Hoechst 33258 (Invitrogen, Cat. # H3569) before mounting coverslips on glass slides using Mowiol 4-88 (Calbiochem, Cat # 475904). Slides mounted with Mowiol were allowed to polymerize overnight at 4°C and examined the following day. Images were acquired using Spot 4.0.1 software and camera on a Nikon Eclipse E800 microscope equipped with a high pressure mercury halogen lamp using differential interference contrast (DIC) optics with a Nikon Plan Apo 100X/1.4 Ph3 DM Oil immersion objective at 1000X total magnification. Epi-fluorescence was acquired using a Nikon G2-E/C filter set and constant exposure time between images. Image black levels were optimized using Adobe Photoshop CS. The same transformations were applied across each image to avoid bias.

Live cell imaging

Live images of HeLa and BHK cells were acquired using Spot 4.0.1 software on a Nikon Eclipse TE200 inverted microscope with a Modulation Optics, Inc HML ELWD Plan Fluor 10X/0.30 objective at 100X total magnification. White light images were acquired using Hoffman Modulation Contrast (HMC) optics. GFP fluorescence was acquired using a Nikon B2-E/C filter. Image black levels were optimized using Adobe

Photoshop CS and all transformations were applied to each image to avoid bias.

Protein blotting

Cultured cells were lysed in RIPA buffer with protease inhibitor cocktail (Sigma, P2714). Samples were sonicated using two duty cycles at 75% on a Branson Sonifier 250 and their concentrations were measured using the BCA Protein Assay Kit (Thermo Scientific, Cat. #23225). Each sample was boiled for five minutes at 95°C in Laemmli's buffer [175, 199]. Proteins were separated by sodium-dodecyl-sulfate-polyacrylamide gel electrophoresis (SDS-PAGE) in a discontinuous Tris · tricine buffer system essentially as described [200]. Gels were run overnight and transferred to an Immobilon-P_{SQ} Membrane (Millipore, Cat. #ISEQ 101 00) to enhance the detection of low molecular weight proteins. The membrane was washed and blocked against non-specific binding with 5% non-fat dried milk (Lab Scientific, Cat. #M0841). The primary antibody was directed against the well characterized HA-epitope of influenza hemagglutinin (α -HA clone 12CA5, Roche Cat#11 666 606 001). Monoclonal HA-antibody was diluted 1:1000 in 3% non-fat milk and TBS · T. Polyclonal GFP-antibody (Invitrogen, Cat. # A6455) was diluted 1:3000 in 3% non-fat milk and TBS · T. The monoclonal actin antibody (clone C4, MP Biomedicals, Cat. # 691001) was diluted 1:5000 in 3% non-fat milk in TBS · T. The HRP-conjugated secondary antibody (GE Healthcare, Cat. #NA931V) was diluted 1:10,000 in 3% milk. Labeled proteins were detected on auto-radiographic film (GE Healthcare, Cat. #28906839) using the SuperSignal® West Pico Chemiluminescent Substrate Assay (Pierce, Cat. #34078).

Virus constructs

Virus constructs were based on pdsTE12Q [14]. The *NSs* ORF was amplified from a plasmid template (pdsTE12H-*NSs*) kindly provided by Dr. Pablo Irusta. The GFP ORF was amplified from pEGFP-N1 (Clontech). The control construct shown in

Figure 4-4 was provided by Dr. Emily Cheng (pHYC86). For expression in mammalian cells, NSs and its constructed variants were cloned into pSG5 (Stratagene) as a BglII fragment. NSs and mutants were cloned into a variant of pSG5 provided by Dr. David Bellows (pDB59) containing an HA-epitope tag upstream and in frame with BglII restriction sites. HA-tagged constructs were cloned into pdsTE12Q using flanking BstEII sites engineered into pDB59. BstEII sites were added to the amplicons for cloning into pdsTE12Q. Primer sequences (Invitrogen, IDT) are located in Appendix I. Restriction digested PCR fragments were purified using the QIAquick Gel Extraction Kit (Qiagen, Cat. #28704) and cloned into the pCR-Blunt cloning vector using the Zero Blunt® PCR Cloning Kit (Invitrogen, Cat. #K2700). BstEII-digested fragments were then sub-cloned into the appropriate restriction-digested vector using T4 DNA ligase (Invitrogen, Cat. #15224-017). The virus vector had previously been dephosphorylated with calf intestinal phosphatase (CIP, NEB Cat. #M0290S) to prevent the recovery of intra-molecular ligation products. Ligation reactions were transformed into *E. coli* strain DH5 α (Invitrogen, Cat. #18265-017) and selected on LB-Agar plates containing Ampicillin (100 μ g/ml). Clones containing inserts were identified by a diagnostic digest on a 1% agarose gel with BstEII. Positive clones were verified by sequencing at The Core DNA Analysis Facility at Johns Hopkins University. Bacterial stocks were prepared from overnight cultures and frozen in 15% glycerol at -80°C.

In vitro transcription of infectious virus

Transcription templates were prepared from overnight bacterial cultures containing recombinant plasmids (Qiagen, Cat. #12643). Plasmids were linearized by restriction digest with XhoI. Residual enzyme was removed by incubating the digests with proteinase K (100 μ g/ml) (Invitrogen, Cat. #25530-015) for one hour at 65°C. Remaining protein was then extracted with phenol. Residual phenol was removed with chloroform and the remaining DNA was precipitated and washed in 70% ethanol. This purified,

linearized dsDNA was resuspended in RNase-free dH₂O and served as the template in the subsequent transcription reaction. Infectious virus genomes were transcribed using 1 μ g template DNA and SP6 RNA polymerase for 120 minutes at 37°C with the Ambion mMessage mMachine kit (Cat. #AM1340). To favor the production of large transcripts, additional GTP was added, giving a ratio of 1:1 capped to uncapped transcripts in the final product. After two hours, DNase was added to the reaction to eliminate the template and samples were incubated another 15 minutes at 37°C. These reactions were purified on an Ambion MEGAclear column (Cat. #AM1908) and the eluates were quantified on a Nanodrop 2000 spectrophotometer. Highly purified ssRNA, with a 260:280 absorption ratio of ~2.2 was routinely obtained through the above process [175].

Rescue of recombinant virus

Purified infectious vRNA (4 μ g) was transfected into BHK cells (ATCC) with Lipofectamine 2000 according to the manufacturer's protocol (Invitrogen, Cat. #11668-027). After two hours, transfection media was replaced with DMEM containing 1% FBS. Virus was harvested 18-24 hours post-transfection, when the cells began to show moderate to heavy CPE. Supernatants were spun for one minute at 16,000 \times g to remove cellular debris and frozen in aliquots at -80°C. Titres of collected virus were subsequently determined by plaque assay on BHK cells.

Plaque assays

Plaque assays were performed essentially as described [14]. BHK cells were plated in 6-well plates and 10-fold dilutions of virus aliquots in DMEM containing 1% FBS were adsorbed for one hour at 37°C in 200 μ l over the cell monolayer. MEM (without phenol red) in 0.6% Bacto-Agar was added to immobilize viruses. Focal plaques of infection were stained after 48 hours with 1% neutral red in MEM. Plaques were

counted and corrected for dilution factor. Titre is expressed as plaque forming units per milliliter (PFU/ml).

Virus injections

Outbred CD1 mice (Charles River Laboratories) were injected with $5 \cdot 10^3$ PFU recombinant SV in 30 μl Hanks Buffered Salt Solution (HBSS) at four days of age and monitored daily for mortality for 21 days thereafter. Univariate survival analysis was performed according to the methods of Kaplan and Meier [176] and Cox [177]. P-values are derived from the Log-rank test statistic in the case of pairwise comparisons and from the Z-score in the case of multiple comparisons.

Results

NSs toxicity in vertebrate cells

To examine the effects of the NSs virulence factor on mammalian cell death, *in vitro* transcribed mRNAs encoding either wild-type NSs or the reverse mRNA sequence were transfected into HeLa and Vero cells. RNA was used to circumvent the NSs-mediated suppression of its own messenger RNA. Viability was determined 24 hours later by Trypan blue exclusion. No effect on viability was observed in either group receiving 80 ng mRNA as both groups retained viability greater than 95% (Figure 4-2A, 4-2B and 4-2G). However, a five-fold increase in the mass of NSs mRNA transfected resulted in a 20% decrease in viability at 21 hours-post infection with no discernable effect on control cells, which remained ~95% viable (Figure 4-2C, 4-2D and 4-2G). Increasing the dosage given to 2 μg or 4 μg resulted in even greater cell death of NSs-transfected cells (Figure 4-2F and 4-2G), but also caused death in the control groups given the reverse mRNA (Figure 4-2E and 4-2G). The cell death observed when transfecting

large quantities of mRNA suggests a non-specific, toxic effect of RNA *per se* in addition to the specific toxicity of NSs mRNA in HeLa cells. In contrast, Vero cells transfected with 2 μ g mRNA show no reduction in viability even after 45 hours, suggesting that susceptibility to the effects of NSs is variable between cell types (Figure 4-2G). These data rely on the presumption that both HeLa and Vero cells are similarly transfectable, since transfection efficiency was not measured in these experiments. Nevertheless, expression of NSs is sufficient to cause cell death in HeLa cells but not in Vero cells, assuming similar transfection efficiencies between cell types.

NSs protein suppresses GFP expression in *trans*

We devised a co-transfection assay to determine the effect of NSs and its derived mutants on the expression of a reporter construct *in trans*. The pEGFP plasmid drives expression of EGFP under control of the strong cytomegalovirus immediate-early promoter [220]. The intensity of EGFP expression is used as an indicator of inhibitory function when co-transfected as plasmids with NSs or one of its constructed mutant alleles (Figure 4-3). The expression of tagged mutants themselves can be verified via protein blots (Figure 4-4). When transfected into BHK cells, wild-type NSs almost completely abolishes EGFP expression (Figure 4-3C) compared to cells transfected with the wild-type NSs sequence cloned in the reverse orientation (Figure 4-3A). The fluorescent signal in NSs-transfected cells was only slightly above the background fluorescence intensity of cells receiving no reporter (Figure 4-3B and 4-3G). All three compound mutants tested showed substantial increases in reporter expression, the intensity of which was indistinguishable from negative controls in both the NSs^{L5759} and NSs^{QRQ}-transfected cells (Figure 4-3D, 4-3E and 4-3G). NSs ^{Δ GH3} still appeared to retain some inhibitory capacity, indicating an independence of this domain from the inhibitory activity of wild-type NSs (Figure 4-3F and 4-3G). The same reduction of suppression was observed for individual point mutants tested (NSs^{L57} and NSs^{L59}),

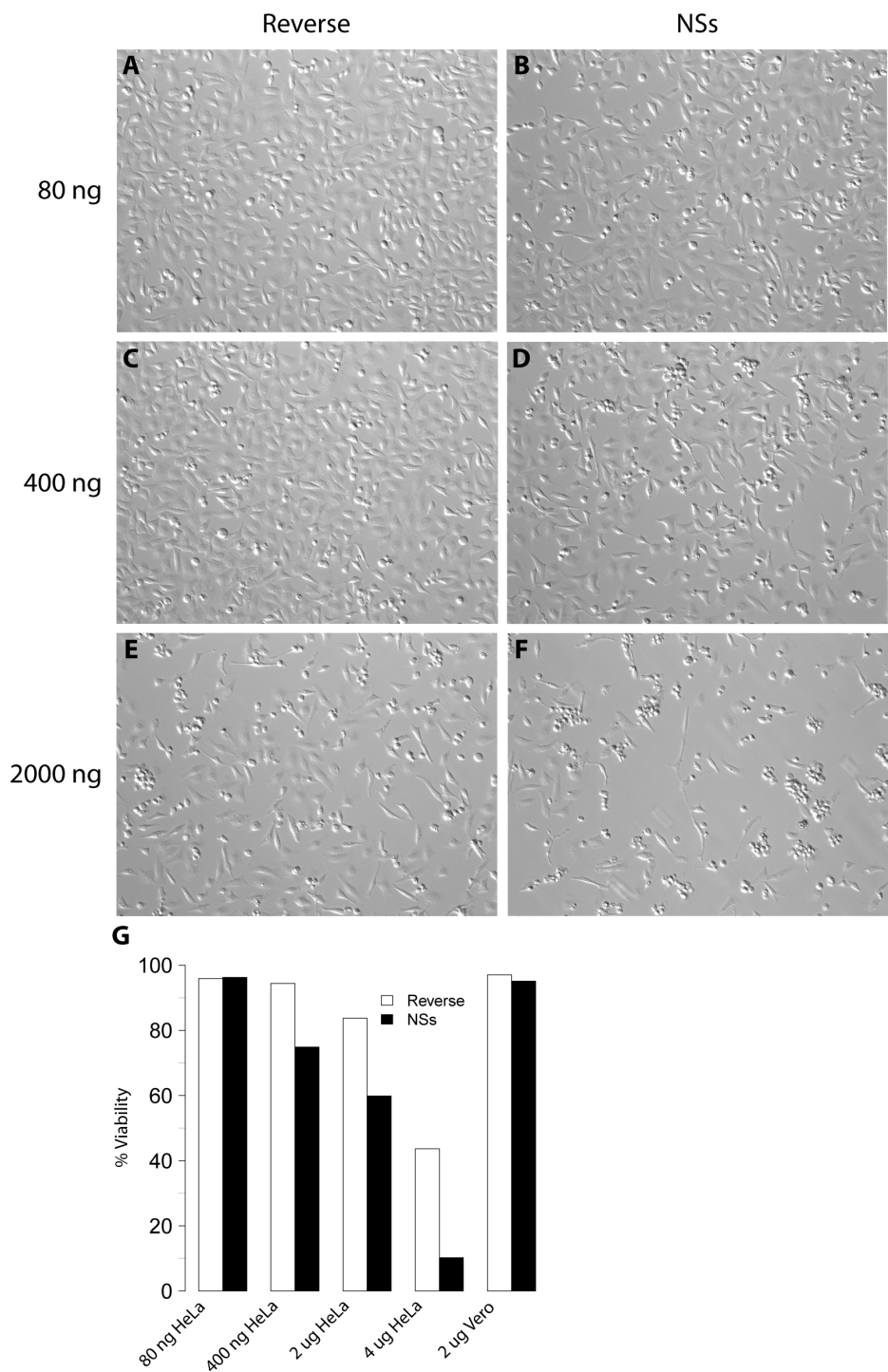


Figure 4-2. NSs RNA is toxic to HeLa cells. NSs mRNA was transcribed *in vitro* and transfected into HeLa cells at various concentrations. The balance of the total transfected mass ($4 \mu\text{g}$) was filled with pSG5 DNA (**A**, **B**) 80 ng mRNA. (**C**, **D**) 400 ng mRNA and (**E**, **F**) 2 μg mRNA. Images were acquired 21 hours post-transfection at 100X total magnification using HMC optics. Viability assessed by Trypan blue exclusion is plotted for each series. In contrast to the toxicity observed in HeLa cells, Vero cells transfected with 2 μg mRNA show no reduction in viability. That is, the phenotype is cell-type specific. Data are plotted from a single experiment.

suggesting that NSs possesses a highly immutable amino-acid sequence in this region, even a small perturbation of which strongly affects its function (Figure 4-7F and 4-7G). Curiously, neither the NSs^{QR} mutant nor the NSs^{Q55} mutant were sufficient to recapitulate the nullifying effect of the triple mutant, NSs^{QRQ} (Figure 4-7D, 4-7E and 4-7H). Therefore, the capacity of NSs to inhibit GFP expression is not dependent on any one of these three residues in BHK cells. The NSs^{ΔN33} allele also retains some inhibitory function, indicating that the 33 N-terminal residues of NSs, which have no counterpart in the translation-inhibiting cellular protein Reaper, do not appear to be essential for the ability of NSs to suppress gene expression (Figure 4-7C and 4-7H).

The difficulty that arises from measuring the expression levels of a protein that globally inhibits gene expression is apparent when attempting to detect functional NSs on a protein blot. EGFP is nearly undetectable when co-transfected with wild-type NSs, indicating the presence of its functional activity, despite wild-type NSs itself being completely undetectable in both BHK and HeLa cells (Figure 4-4A lane 3 and 4-4B lane 2). As expected, the EGFP expression readout in BHK cells closely matches the observed fluorescence of Figure 4-3 and 4-7, with NSs^{L5759} and NSs^{QRQ} showing greater than control levels of EGFP expression (Figure 4-4A lanes 9 and 12 compared to lane 3). Although several NSs mutants are not directly detectable with the HA-antibody, this is only the case when the protein retains at least some inhibitory function. While it cannot be ruled out that some of these mutant alleles are undetectable due to instability, it must also be true that they are present in sufficient (although undetectable) quantities to exert an effect. Interestingly, the NSs^{L5759} mutant and to a lesser extent the NSs^{QRQ} allele induces the appearance of a higher molecular weight band of roughly 26 kDa, which corresponds to the predicted size of an NSs dimer. Several differences in the expression profile of NSs and EGFP in HeLa cells are apparent when compared to BHK cells. Nearly every mutation restores EGFP expression to levels comparable to controls (Figure 4-4B). The only exceptions

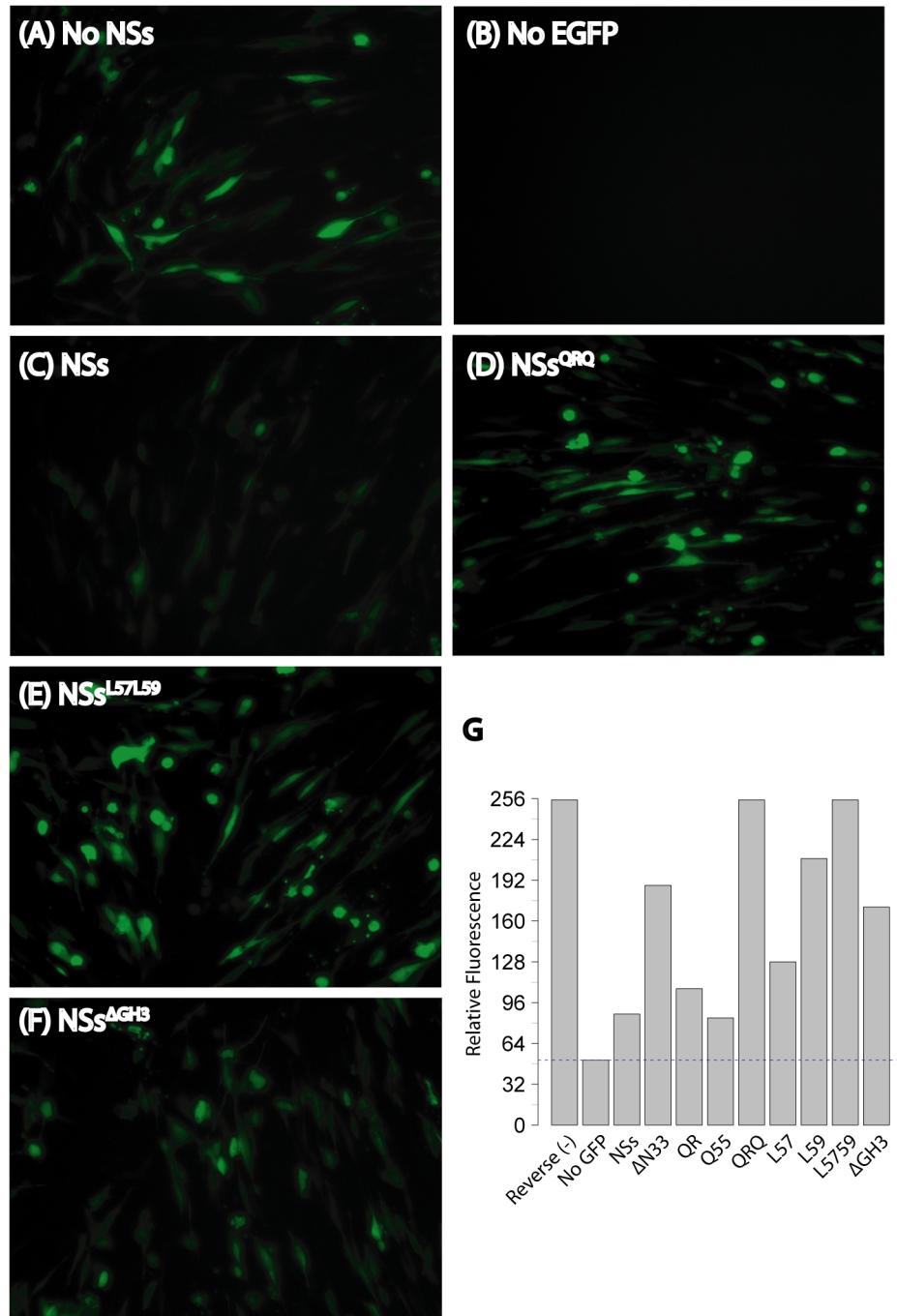


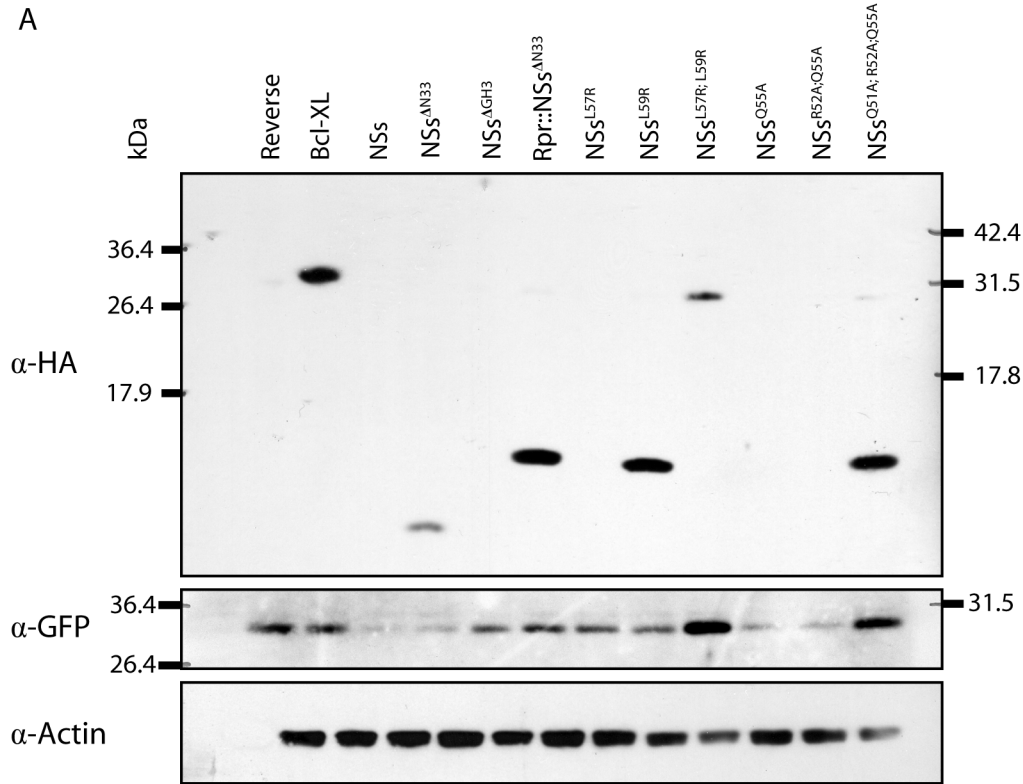
Figure 4-3. Functional NSs protein inhibits EGFP expression in *trans*. BHK cells were co-transfected with pEGFP and wt NSs or an NSs mutant. The ability of NSs to suppress its own expression (**C**) is abolished in the compound mutants QRQ (**D**) and L57L59 (**E**). Deletion of the lipid interaction domain gives rise to an intermediate suppression phenotype (Δ GH3, **F**). Fluorescence intensity for all NSs mutants was quantified using ImageJ. The maximum intensity of GFP expression in the Reverse control was used as a standard. Images from point mutants are included in Figure 4-7. Images were acquired 24 hours post-transfection at 100X total magnification.

to this are NSs^{L57} (lane 7), NSs^{QR} (lane 11) and NSs^{QRQ} (lane 12). Not only does NSs^{QRQ} retain its inhibitory function of EGFP in HeLa cells, it is also undetectable. Another mutant allele, NSs^{Q55}, appears to be functional in BHK cells, but not in HeLa cells (compare Figure 4-4A lane 10 to 4-4B lane 10). Additionally, the higher molecular weight bands observed in BHK cells are absent from HeLa. The capacity of NSs to suppress EGFP expression is influenced by the cell type in which it is expressed. As such, *in vitro* mammalian cell culture models may be of limited use in deciphering NSs function *in vivo*.

Localization of NSs mutants

Determining the sub-cellular localization of NSs may yield insight into its function and mechanism of action. Since wild-type NSs protein is undetectable, we turned our attention to two detectable forms of NSs, one of which retained some inhibitory activity (NSs^{ΔN33}) in BHK cells and the other of which (NSs^{L57S9}) did not (Figure 4-4A). Our aim was to determine if any differences in localization were apparent between these two mutants and whether the sub-cellular localization of wild-type NSs was detectable. HeLa cells were transfected with HA-tagged versions of each protein and fixed for microscopy 48 hours later. DNA was stained with Hoechst 33258. A reticular, peri-nuclear staining pattern was observed in both mutants (Figure 4-5A and 4-5B). In contrast, cells stained for wild-type NSs protein showed no detectable fluorescence above background (Figure 4-5C). The absence of NSs staining serves as a negative control in this case. The shared localization between these two distinct NSs alleles suggests that the introduced mutations did not cause the redistribution of NSs from diffuse cytoplasmic to reticular perinuclear. Furthermore, the specific pattern of staining suggests that this localization is independent of the gene expression inhibiting activity of NSs.

A



B

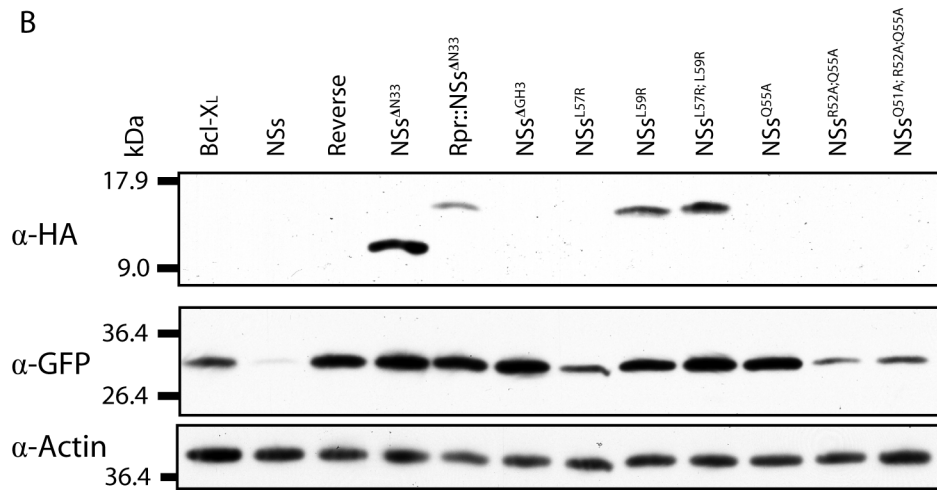


Figure 4-4. Expression of NSs and mutants in BHK (**A**) and HeLa cells (**B**). N-terminally HA-tagged mutants of NSs were co-transfected into mammalian cells with pEGFP. Lysates were prepared 24 hours after transfection. EGFP expression intensity serves as a readout for NSs capacity to inhibit gene expression in *trans*. EGFP expression is nearly undetectable when co-transfected with wild-type NSs protein in both cell types. All mutants show an increase in EGFP expression relative to wt NSs, regardless of whether the NSs variant itself is detectable. While readily detectable in BHK cells, the QRQ mutant of NSs is not detectable in HeLa cells. Blots are representative of three independent experiments for each cell type.

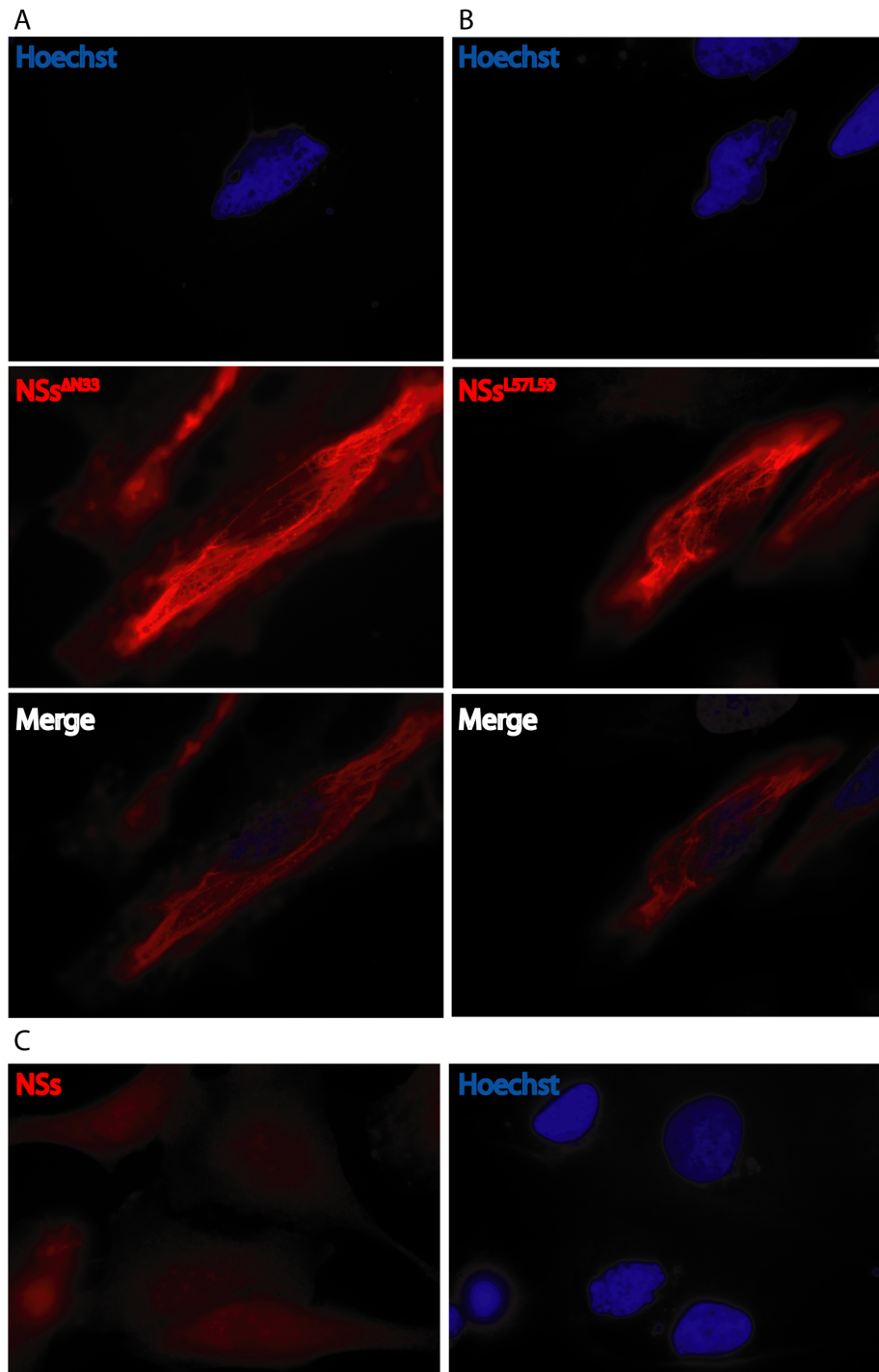


Figure 4-5. Sub-cellular localization of NSs in HeLa cells. HA-tagged $\text{NSs}^{\Delta\text{N}33}$ (**A**) and $\text{NSs}^{\text{L}57\text{L}59}$ (**B**) were transfected into HeLa cells and fixed 48 hours later. Nuclei were stained with DAPI (blue). In both mutants tested, NSs exhibits a reticular, peri-nuclear staining pattern. The specific localization pattern of these mutants suggests that localization is independent of their ability to suppress gene expression. (**C**) As expected, specific staining of NSs-transfected cells was undetectable. Images were acquired at 1000X total magnification.

Survival Analysis

NSs mutants were expressed in recombinant Sindbis virus to determine the relationship between gene expression inhibitory capacity and virulence *in vivo*. Outbred CD1 weanling mouse pups were injected at four days of age with 5,000 PFU recombinant SV and monitored daily for mortality for three weeks (Figure 4-6 and 4-8). Expressing the orthobunyavirus virulence factor NSs in an SV infection enhances mortality in weanling mice (Figure 4-6A, $p < 0.0001$). The ability of NSs to enhance the virulence of SV is retained in the caspase-activating [157] triple mutant NSs^{QRQ} ($p < 0.0004$), but not in the double mutant, NSs^{L57/59} (Figure 4-6B and 4-6C). Enhanced mortality is also ablated by NSs alleles carrying only one of these mutations at Q51, R52, L57 or L59 (Figure 4-8B, 4-8C, 4-8E and 4-8F). Of the five point mutants tested, only NSs^{Q55} retained killing activity ($p = 0.0321$), indicating dispensability of this residue (Figure 4-8D). Mutants deficient for the hydrophobic lipid interaction domain GH3 also retain a small degree of killing that is marginally significant ($p = 0.0670$), suggesting that this domain may contribute to but is not essential for the killing phenotype (Figure 4-6D). Two additional mutants were constructed to determine whether expression of NSs protein is required for killing or whether NSs RNA *per se* is toxic. The NSs^{fs} mutant contains four insertions at ORF positions 7, 44, 75 and 76 to destroy the NSs reading frame. The other non-coding mutant, NSs^{STOP} contains nucleotide transversions G27T and T32A that introduce stop codons into the two overlapping ORFs of the RNA. Mice infected with these two viruses exhibit significantly enhanced mortality relative to controls (Figure 4-6E, $p = 0.0152$). The data suggest that L57 and L59 are essential for the killing phenotype, but that Q51, R52 and Q55 are not. This is consistent with the observation in HeLa cells (Figure 4-4B) that NSs^{QRQ} retains some inhibition of EGFP expression in addition to remaining undetectable similar to functional, wild-type NSs.

Discussion

The small non-structural protein of the orthobunyaviruses, NSs, causes enhanced cell death *in vitro* and confers enhanced virulence to Sindbis virus *in vivo*. Direct transfection of NSs mRNA results in approximately 20% fewer viable cells than controls (Figure 4-2D and 4-2G). When transfected in a plasmid, NSs potently suppresses reporter expression *in trans*, confirming a general inhibition of gene expression by undetectable amounts of protein. The NSs^{QRQ} mutant can enhance mortality despite its apparent loss of inhibitory function in BHK cells. The residues most likely to be involved in this phenotype include Q51 and R52, both of which abolish virulence as single point mutants. This was unexpected, given that the triple mutant (QRQ) retains its killing function *in vivo*. It is possible that the addition of the third mutation at position 55 rescues the nullifying effects of the mutations at positions 51 and 52. It is intriguing to speculate that the inhibition of cellular gene expression and caspase activation activity are indeed separate functions of NSs [157]. Viruses use a variety of strategies to shut-off host gene expression and promote the synthesis of their own macromolecules using cellular nutrients and Sindbis virus is among these [221]. The inhibitory activity of NSs on host cell protein production, therefore, may not greatly benefit SV, which independently performs this task during infection [221, 222]. The implication of these observations is that it is not the inhibition of gene expression, be it at the transcriptional or translational level, which causes enhanced virulence. Rather, virulence conferred by NSs is independent of both its gene expression inhibition activity as well as its lipid interactions, as the GH3 deletion mutant also retained its killing function to some degree. Whether the sub-cellular localization of NSs to reticular, peri-nuclear structures throughout the cytoplasm is dependent on the GH3 domain, which has been shown to be essential for mitochondrial localization of Reaper, could be determined by further studies with colocalization markers for the prominent reticular cytoplasmic structures of the eukaryotic cell including the

endoplasmic reticulum, Golgi apparatus and mitochondria. The observation that both constructs engineered to encode N-terminally truncated forms of NSs retain the ability to kill could mean that the orthobunyavirus small subunit RNA itself is sufficient to enhance mortality. Alternatively, the phenotype may arise from translational initiation from internal methionines in the ORF, in particular the methionine at position 39, would produce a peptide very similar to $\text{NSs}^{\Delta N33}$, which partially retains its inhibitory function as well as its localization *in vitro*. It is also conceivable that co-expression of the truncated nucleocapsid protein in the overlapping reading frame contributes to the killing phenotype [223]. Whether the putative NSs dimer shown in Figure 4-4A represents a physiologically relevant form of NSs or is simply a peculiarity of overexpression in BHK cells remains to be resolved. A recent report indicates that self-association (dimerization) of Reaper is essential for its killing activity, thus supporting a functional role for NSs multimers in the induction of cell death [150]. Together, these observations address an important issue in determining virulence mechanisms in general: the relevance and extensibility of phenotypes observed almost exclusively *in vitro* on the complex environment of susceptible and refractory host tissues *in vivo*.

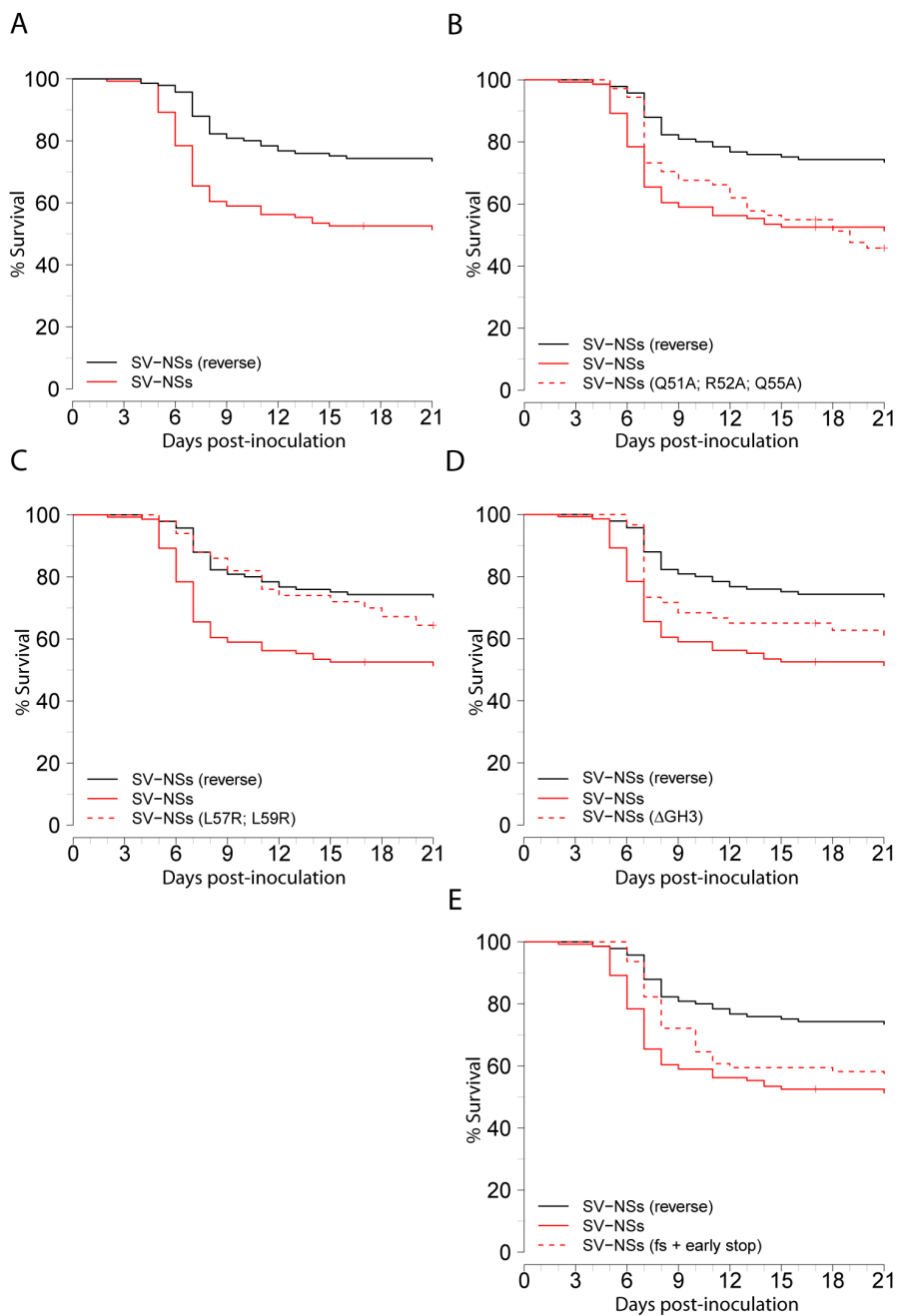


Figure 4-6. Survival of CD1 mice infected with NSs point mutants. Four day old mice were inoculated intracranially with 5×10^3 PFU recombinant SV. **(A)** Mortality is significantly enhanced in mice inoculated with wild-type NSs ($p < 0.0001$, $N = 139$ and 141). **(B)** The triple mutant allele of NSs at residues Q51, R52 and Q55 retains enhanced killing compared to reverse controls ($N = 71$, $p < 0.0004$). **(C)** The double mutant allele of NSs at residues L57 and L59 does not enhance killing relative to controls ($N = 50$). **(D)** Removal of the lipid-interacting GH3 domain of NSs is nearly sufficient to reduce killing significantly ($p = 0.0669$, $N = 60$). **(E)** Non-protein coding mutants, one frameshifted and the other with an introduced stop codon, retain the capacity to kill mice ($N = 79$, $p = 0.0152$). Data plotted are from at least three independent experiments.

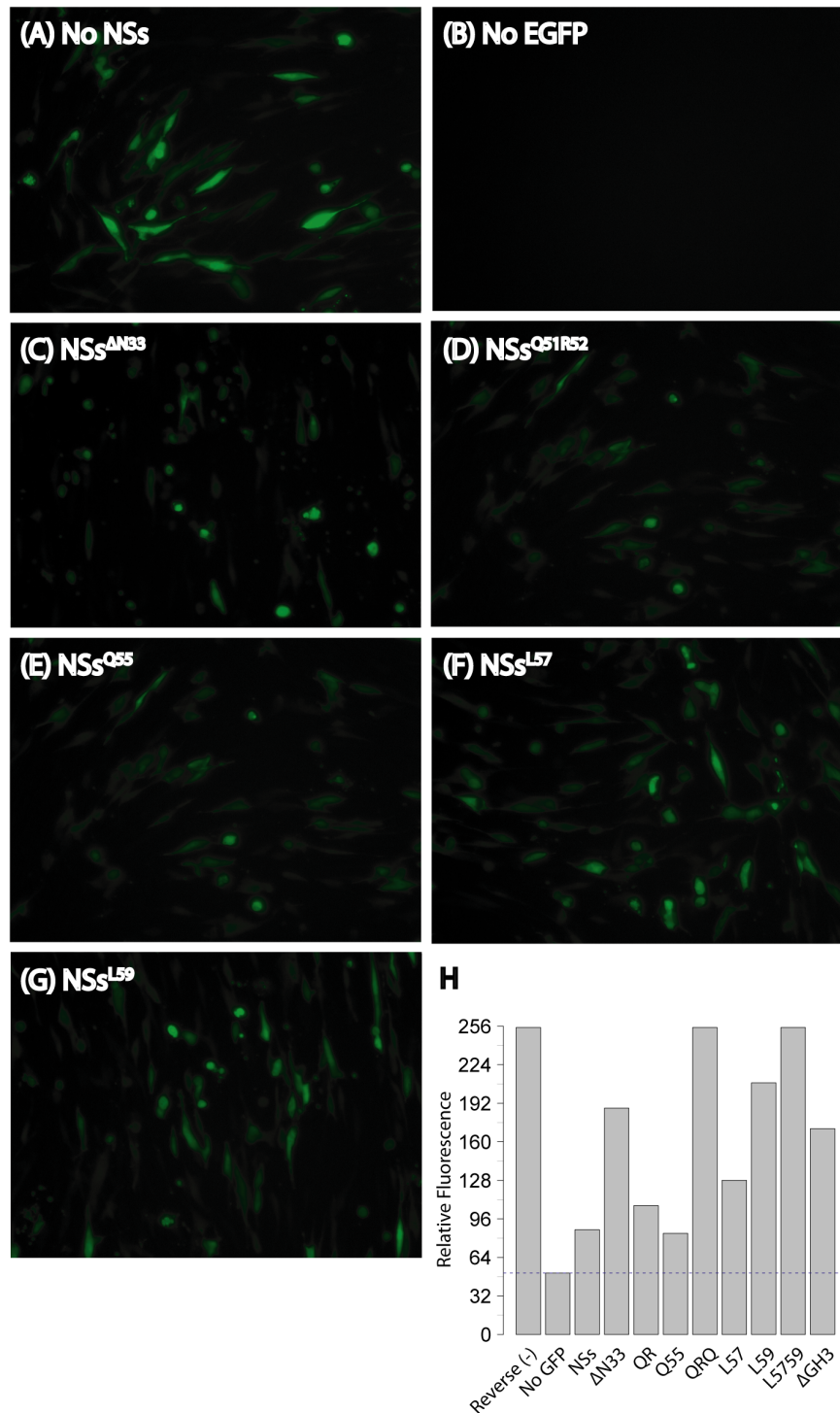


Figure 4-7. Functional NSs protein inhibits EGFP expression in *trans*. BHK cells were co-transfected with pEGFP and wt NSs or an NSs mutant. The ability of NSs to suppress its own expression is partially abolished in the point mutants $\Delta N33$ (C), Q51R52 (D), Q55 (E), L57 (F) and L59 (G). Fluorescence intensity for all NSs mutants was quantified using ImageJ (H). The maximum intensity of GFP expression in the Reverse control was used as a standard. Images were acquired 24 hours post-transfection at 100X total magnification.

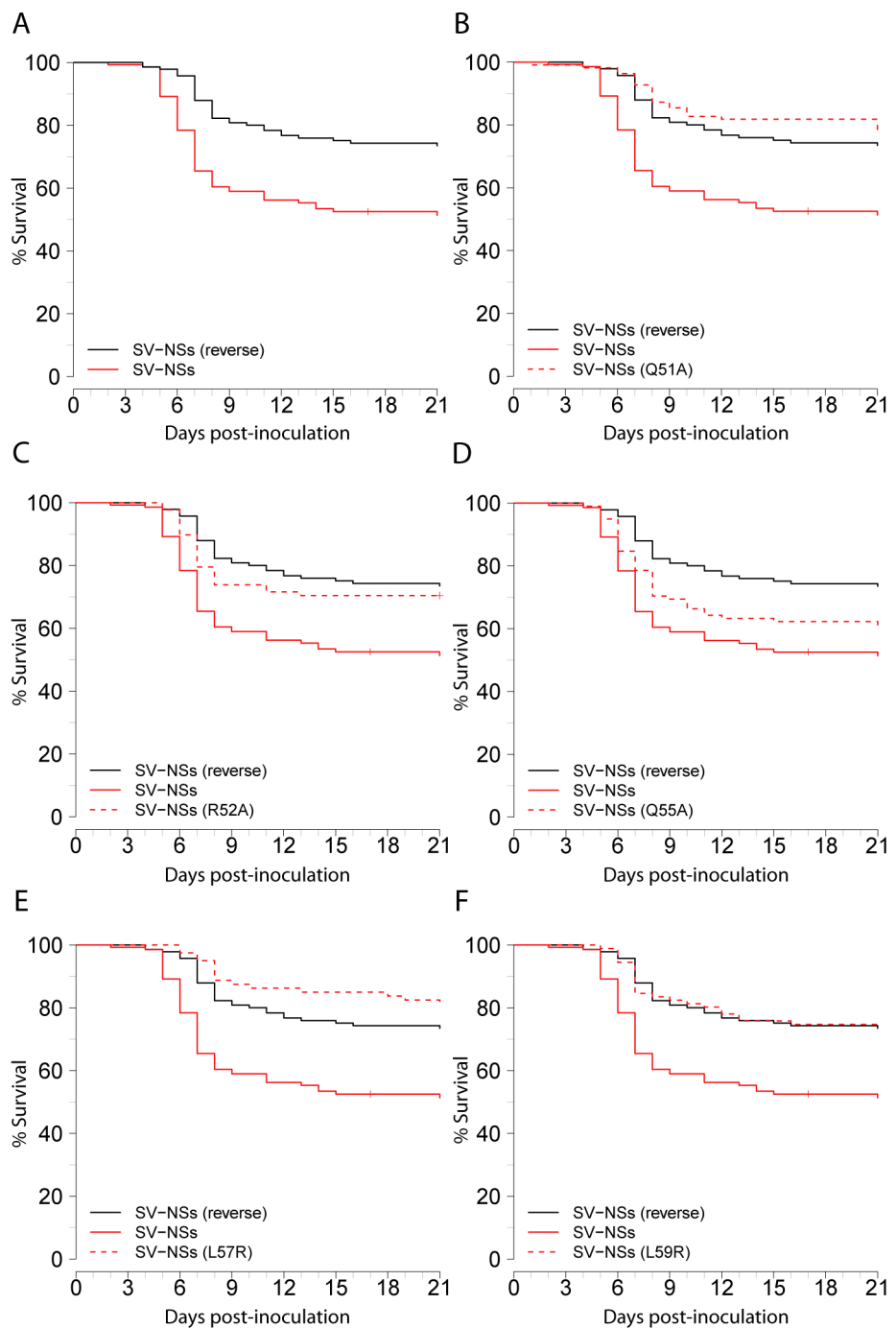


Figure 4-8. Survival of CD1 mice infected with NSs point mutants. Four day old mice were inoculated intracranially with 5×10^3 PFU recombinant SV. **(A)** Mortality is significantly enhanced in mice inoculated with wild-type NSs ($p < 0.0001$, $N = 139$ and 141). **(B-C)** Mutations at Q51 ($N = 110$) and R52 ($N = 88$) abolish killing by NSs. **(D)** The Q55A point mutant retains a marginally significant killing function ($N = 98$, $p = 0.0322$). **(E-F)** Mutation of either L57 ($N = 80$) or L59 ($N = 91$) is sufficient to nullify killing by NSs. Data plotted are from at least three independent experiments.

Conclusions and general discussion

In the present work, we have performed functional analysis on three distinct virulence determinants using two strains of Sindbis virus and one strain of Venezuelan equine encephalitis virus in mosquitoes and mice *in vitro* and *in vivo*. In the first study, it was discovered that homologous sequence introduced in a primary infection can attenuate, if not abolish, killing by a hyper-virulent strain of SV. The existence of acquired resistance to virus infection in a non-chordate animal is novel. It was also shown that the minimum requirement for the establishment of protection is the infection established by a replication-competent virus RNA. The observation that the copy number of homologous sequence contributes little to the protective phenotype is important when considering the requirements for engineering immunity in insects to make them refractory to infection by and transmission of pathogens important for public health, such as dengue and West Nile viruses.

However, numerous questions remain. Providing B2 sequence in the primary inoculation led to an attenuation of killing, but the penetrance of killing remained complete. Would priming with a region of comparable size from the SV genome generate a comparable degree of protection? In other words, are all homologous sequences equally immunogenic? This is easily addressed by inserting the region of interest into recombinant SV. If the capacity of acquired resistance to SV infection is indeed limited, to what end would such a system evolve? How plausible is the evolution of acquired immunity to an animal with a lifespan as short as a mosquito?

How likely is it that an insect would encounter multiple variants of the same pathogen in its lifetime? If one considers that spontaneous mutants continuously arise during the course of a single virus infection, it seems quite plausible that a system could be selected to keep such potentially harmful variants in check, since the siRNA effectors are already in place. Put more succinctly, “That which does not kill me, makes me stronger” [224]. This hypothesis can be tested directly by sequencing both long and short virus RNA populations from infected mosquitoes or flies in wild type and Dicer2 null backgrounds. If RNAi serves to restrict the replication of spontaneously arising variants, one would anticipate an increase in the number and diversity of variants observed.

What are the downstream effectors of anti-viral signaling mediated by RNA-interference in insects? Are they the same for each virus or do distinct viruses elicit distinct responses? If the latter is the case, what are the molecular determinants of those distinct responses and how are they recognized? Presently, little is known of the molecular requirements necessary to activate classical insect immune signaling pathways in response to virus infection and the current state of knowledge lacks a complete synthesis of concepts [225]. Recent studies have identified genes involved in endocytosis as important components of insect anti-viral signaling, but functional information is lacking [226]. To that end, how does a large single-stranded RNA come to be taken up without being degraded by a live mosquito? How frequent is this uptake? This could be directly addressed by injecting serial dilutions of infectious virus and observing the resulting infection prevalence and the frequency of the event may give important clues as to its physiological relevance.

In the second study presented, it was determined that the cellular death factor Reaper from *Drosophila* was capable of causing killing by an otherwise innocuous virus, but that the killing was incomplete by 21 days post-infection. Furthermore, the insect-adapted strain used in the study was less effective at killing mosquitoes than

the vertebrate-adapted strain. However, the capacity of vertebrate-adapted strains to infect and disseminate after acquisition in a bloodmeal is reduced relative to the insect-adapted strain, MRE16 [206]. This gives rise to a paradox where the effective virus cannot infect through the natural route and the virus adapted to infect naturally does not cause sufficient killing to be used in an insect control strategy. Therefore, it seems that the greatest barrier to the development of an effective and practical biopesticide based on SV is the virus strain itself rather than the virus-encoded effector, especially given the remarkable killing capacity of FHV B2. Barriers to the implementation of an SV-based biopesticide include the wide tropism of Sindbis virus, which may give rise to unwanted off-target effects on species other than the mosquito vector. Importantly, killing by MRE16-B2 was also complete when the virus was injected, but did not occur until several days later than the killing by B2 in the vertebrate-adapted virus dsTE12Q. This quality, and perhaps more importantly its underlying biology, may prove useful for the development of “late life acting” or “evolution proof” biopesticides based on alphaviruses [163, 188].

Expression of the NSs virulence factor from San Angelo virus is toxic to vertebrate cells and enhances the virulence of Sindbis virus in neonatal mice. Although SV is capable of causing translational shut-off in host cells on its own [221], co-expression of an inhibitor of gene expression by recombinant SV may serve to enhance this capability, resulting in greater virus replication and neuronal cell death. A recent report implicates the region of homology shared by NSs and *Drosophila* Reaper in self association to form homo- and hetero-dimers with other IAP inhibitors [150]. Does NSs also associate with IAP inhibitors during bunyavirus infection or does it simply form functional homo-dimers with itself? Does NSs expression provide a replicative advantage to SV or is its expression simply toxic to infected cells? Perhaps most importantly, what is the mechanism of NSs toxicity during infection?

Together, these studies address functional requirements underlying virulence during

alphavirus infection in two distinct infection models. The use of recombinant viruses for heterologous expression of virulence determinants sheds light on the basic cellular processes co-opted by Sindbis virus during the parasitic process of virus infection and underscores important differences between virulence studies performed *in vitro* and those carried out in the complex environment of susceptible and refractory host tissues *in vivo*.

References

- [1] J. H. Strauss and E. G. Strauss, “The alphaviruses: gene expression, replication, and evolution,” *Microbiol. Rev.*, vol. 58, pp. 491–562, 1994.
- [2] S. C. Weaver, “Evolutionary influences in arboviral disease,” *Curr. Top. Microbiol. Immunol.*, vol. 299, pp. 285–314, Jan 2006.
- [3] J. L. Hardy, E. J. Houk, L. D. Kramer, and W. C. Reeves, “Intrinsic factors affecting vector competence of mosquitoes for arboviruses,” *Annu. Rev. Entomol.*, vol. 28, pp. 229–62, Jan 1983.
- [4] “CDC | Arborvirus transmission,” <http://www.cdc.gov/ncidod/dvibd/arbor/schemat.pdf>.
- [5] E. G. Strauss and J. H. Strauss, “Structure and Replication of the Alphavirus Genome,” in *The Togaviridae and Flaviviridae*. Boston, MA: Springer New York, 1986, pp. 35–90.
- [6] D. E. Griffin, “Chapter 30. Alphaviruses,” in *Fields Virol.*, 4th ed., D. M. Knipe and P. M. Howley, Eds. Lippincott Williams & Wilkins, 2001, pp. 917–962.
- [7] L. W. Enquist, R. M. Krug, V. R. Racaniello, A. M. Skalka, and S. Flint, *Principles of Virology: Molecular Biology, Pathogenesis, and Control*. American Society Microbiology, 1999.
- [8] M. Marsh, E. Bolzau, and A. Helenius, “Penetration of semliki forest virus from acidic prelysosomal vacuoles,” *Cell*, vol. 32, no. 3, pp. 931–940, Mar 1983.
- [9] H. Garoff, M. Sjöberg, and R. H. Cheng, “Budding of alphaviruses,” *Virus Res.*, vol. 106, no. 2, pp. 103–16, Dec 2004.
- [10] J. M. Smit, R. Bittman, and J. Wilschut, “Low-pH-dependent fusion of Sindbis virus with receptor-free cholesterol- and sphingolipid-containing liposomes,” *J. Virol.*, vol. 73, no. 10, pp. 8476–84, Oct 1999.
- [11] D. L. Sawicki, S. Perri, J. M. Polo, and S. G. Sawicki, “Role for nsP2 proteins in the cessation of alphavirus minus-strand synthesis by host cells,” *J. Virol.*, vol. 80, no. 1, p. 360, 2006.
- [12] J. Hertz and H. V. Huang, “Utilization of heterologous alphavirus junction sequences as promoters by Sindbis virus,” *J. Virol.*, vol. 66, no. 2, pp. 857–864, 1992.
- [13] C. Xiong, R. Levis, P. Shen, S. Schlesinger, C. M. Rice, and H. V. Huang, “Sindbis virus: an efficient, broad host range vector for gene expression in animal cells,” *Science (80-.)*, vol. 243, no. 4895, p. 1188, 1989.

- [14] J. M. Hardwick and B. Levine, "Sindbis virus vector system for functional analysis of apoptosis regulators," *Methods Enzymol.*, vol. 322, no. 1996, pp. 492–508, Jan 2000.
- [15] R. E. Kissling, R. W. Chamberlain, R. K. Sikes, and M. E. Eidson, "Studies on the North American arthropod-borne encephalitides. III. Eastern equine encephalitis in wild birds," *Am. J. Hyg.*, vol. 60, no. 3, pp. 237–250, Nov 1954.
- [16] S. C. Weaver, A. M. Powers, A. C. Brault, and A. D. Barrett, "Molecular epidemiological studies of veterinary arboviral encephalitides," *Vet. J.*, vol. 157, no. 2, pp. 123–38, Mar 1999.
- [17] S. A. Hackbarth, A. B. Reinartz, and B. P. Sagik, "Age-dependent resistance of mice to sindbis virus infection: reticuloendothelial role," *J. Reticuloendothel. Soc.*, vol. 14, no. 5, pp. 405–25, Nov 1973.
- [18] D. E. Griffin, B. Levine, W. R. Tyor, P. C. Tucker, and J. M. Hardwick, "Age-dependent susceptibility to fatal encephalitis: alphavirus infection of neurons," *Arch. Virol. Suppl.*, vol. 9, pp. 31–39, 1994.
- [19] S. Ubol, P. C. Tucker, D. E. Griffin, and J. M. Hardwick, "Neurovirulent strains of Alphavirus induce apoptosis in bcl-2-expressing cells: role of a single amino acid change in the E2 glycoprotein," *Proc. Natl. Acad. Sci. U. S. A.*, vol. 91, no. 11, pp. 5202–5206, May 1994.
- [20] B. Levine, Q. Huang, J. T. Isaacs, J. C. Reed, D. E. Griffin, and J. M. Hardwick, "Conversion of lytic to persistent alphavirus infection by the bcl-2 cellular oncogene," *Nature*, vol. 361, no. 6414, pp. 739–742, Feb 1993.
- [21] B. Levine, J. E. Goldman, H. H. Jiang, D. E. Griffin, and J. M. Hardwick, "Bcl-2 protects mice against fatal alphavirus encephalitis," *Proc. Natl. Acad. Sci. U. S. A.*, vol. 93, no. 10, pp. 4810–4815, May 1996.
- [22] S. Ubol, S. Park, I. Budihardjo, S. Desnoyers, M. H. Montrose, G. G. Poirier, S. H. Kaufmann, and D. E. Griffin, "Temporal changes in chromatin, intracellular calcium, and poly(ADP-ribose) polymerase during Sindbis virus-induced apoptosis of neuroblastoma cells," *J. Virol.*, vol. 70, no. 4, pp. 2215–2220, Apr 1996.
- [23] D. Bowers, B. A. Abell, and D. T. Brown, "Replication and tissue tropism of the alphavirus Sindbis in the mosquito *Aedes albopictus*," *Virology*, vol. 212, no. 1, pp. 1–12, Sep 1995.
- [24] A. R. Karpf and D. T. Brown, "Comparison of Sindbis virus-induced pathology in mosquito and vertebrate cell cultures," *Virology*, vol. 240, no. 2, pp. 193–201, Jan 1998.
- [25] D. Bowers, C. G. Coleman, and D. T. Brown, "Sindbis virus-associated pathology in *Aedes albopictus* (Diptera: Culicidae)," *J. Med. Entomol.*, vol. 40, no. 5, pp. 698–705, 2003.
- [26] G. R. Parikh, J. D. Oliver, and L. C. Bartholomay, "A haemocyte tropism for an arbovirus," *J. Gen. Virol.*, pp. 292–296, 2009.
- [27] T. W. Scott and L. H. Lorenz, "Reduction of *Culiseta melanura* fitness by eastern equine encephalomyelitis virus," *Am. J. Trop. Med. Hygiene*, vol. 59, no. 2, p. 341, 1998.
- [28] M. E. Faran, M. J. Turell, W. S. Romoser, R. G. Routier, P. H. Gibbs, T. L. Cannon, and C. L. Bailey, "Reduced survival of adult *Culex pipiens* infected with Rift Valley fever virus," *Am. J. Trop. Med. Hygiene*, vol. 37, no. 2, pp. 403–9, Sep 1987.

- [29] M. J. Turell, T. P. Gargan, and C. L. Bailey, “Culex pipiens (Diptera: Culicidae) morbidity and mortality associated with Rift Valley fever virus infection,” *J. Med. Entomol.*, vol. 22, no. 3, pp. 332–7, May 1985.
- [30] S. C. Weaver, T. W. Scott, and L. H. Lorenz, “Patterns of eastern equine encephalomyelitis virus infection in Culiseta melanura (Diptera: Culicidae),” *J. Med. Entomol.*, vol. 27, no. 5, pp. 878–91, Sep 1990.
- [31] T. W. Scott, S. W. S. Hildreth, and B. J. Beaty, “The distribution and development of eastern equine encephalitis virus in its enzootic mosquito vector , Culiseta melanura,” *Am. J. Trop. Med. Hyg.*, vol. 33, no. 2, pp. 300–310, Mar 1984.
- [32] T. W. Scott and S. C. Weaver, “Eastern equine encephalomyelitis virus: epidemiology and evolution of mosquito transmission,” *Adv. Virus Res.*, vol. 37, pp. 277–328, Jan 1989.
- [33] C. A. Mims, M. F. Day, and I. D. Marshall, “Cytopathic effect of Semliki Forest virus in the mosquito Aedes aegypti,” *Am. J. Trop. Med. Hygiene*, vol. 15, no. 5, pp. 775–784, Sep 1966.
- [34] B. Jobling, *Anatomical Drawings of Biting Flies*. Brit. Museum (Nat. Hist.), 1987.
- [35] I.-C. Huang, W. Li, J. Sui, W. Marasco, H. Choe, M. Farzan, and Others, “Influenza A virus neuraminidase limits viral superinfection,” *J. Virol.*, vol. 82, no. 10, p. 4834, May 2008.
- [36] P. Ellenberg, F. N. Linero, and L. A. Scolaro, “Superinfection exclusion in BHK-21 cells persistently infected with Junin virus,” *J. Gen. Virol.*, vol. 88, no. 10, pp. 2730–2739, Oct 2007.
- [37] G. Zou, B. Zhang, P.-Y. Lim, Z. Yuan, K. A. Bernard, and P.-Y. Shi, “Exclusion of West Nile Virus Superinfection through RNA Replication,” *J. Virol.*, vol. 83, no. 22, pp. 11 765–11 776, Nov 2009.
- [38] R. E. Johnston, K. Wan, and H. R. Bose, “Homologous Interference Induced by Sindbis Virus,” *J. Virol.*, vol. 14, no. 5, pp. 1076–1082, Nov 1974.
- [39] W. T. McAllister and C. L. Barrett, “Superinfection exclusion by bacteriophage T7,” *J. Virol.*, vol. 24, no. 2, pp. 709–11, Nov 1977.
- [40] L. Christen, J. Seto, and E. G. Niles, “Superinfection exclusion of vaccinia virus in virus-infected cell cultures,” *Virology*, vol. 174, no. 1, pp. 35–42, Jan 1990.
- [41] P. Whitaker-Dowling, J. S. Youngner, C. C. Widnell, and D. K. Wilcox, “Superinfection exclusion by vesicular stomatitis virus,” *Virology*, vol. 131, no. 1, pp. 137–43, Nov 1983.
- [42] W. R. Hardy, Y. S. Hahn, R. D. Groot, E. G. Strauss, and JH, “Synthesis and processing of the nonstructural polyproteins of several temperature-sensitive mutants of Sindbis virus,” *Virology*, vol. 177, no. 1, pp. 199–208, 1990.
- [43] Y. S. Hahn, E. G. Strauss, and J. H. Strauss, “Mapping of RNA- temperature-sensitive mutants of Sindbis virus: assignment of complementation groups A, B, and G to nonstructural proteins.” *J. Virol.*, vol. 63, no. 7, pp. 3142–50, Jul 1989.
- [44] R. H. Adams and D. T. Brown, “BHK cells expressing Sindbis virus-induced homologous interference allow the translation of nonstructural genes of superinfecting virus,” *J. Virol.*, vol. 54, no. 2, pp. 351–7, May 1985.

- [45] L. D. Condreay and D. T. Brown, “Exclusion of superinfecting homologous virus by Sindbis virus-infected *Aedes albopictus* (mosquito) cells,” *J. Virol.*, vol. 58, no. 1, pp. 81–86, Apr 1986.
- [46] V. Stollar and T. Shenk, “Homologous Viral Interference in *Aedes albopictus* Cultures Chronically Infected with Sindbis Virus,” *J. Virol.*, vol. 11, no. 4, pp. 592–595, Jul 1973.
- [47] A. R. Karpf, E. Lanches, E. G. Strauss, J. H. Strauss, and D. T. Brown, “Superinfection exclusion of alphaviruses in three mosquito cell lines persistently infected with Sindbis virus,” *J. Virol.*, vol. 71, no. 9, pp. 7119–7123, Sep 1997.
- [48] A. M. Powers, A. C. Brault, Y. Shirako, and E. G. Strauss, “Evolutionary relationships and systematics of the alphaviruses,” *J. Virol.*, vol. 75, no. 21, pp. 10118–10131, 2001.
- [49] S.-W. Ding, “RNA-based antiviral immunity,” *Nat. Rev. Immunol.*, vol. 10, no. 9, pp. 632–644, Sep 2010.
- [50] S. Deddouche, N. Matt, A. Budd, S. Mueller, C. Kemp, D. Galiana-Arnoux, C. Dostert, C. Antoniewski, J. A. Hoffmann, and J.-L. Imler, “The DExD/H-box helicase Dicer-2 mediates the induction of antiviral activity in drosophila,” *Nat. Immunol.*, vol. 9, no. 12, pp. 1425–1432, 2008.
- [51] N. N. Danial and S. J. Korsmeyer, “Cell Death:: Critical Control Points,” *Cell*, vol. 116, no. 2, pp. 205–219, 2004.
- [52] J. Kerr, A. Wyllie, and A. Currie, “Apoptosis: a basic biological phenomenon with wide-ranging implications in tissue kinetics,” *Br. J. Cancer*, vol. 258, no. 6, pp. 479–517, Dec 1972.
- [53] R. Lockshin and C. Williams, “Programmed cell death—I. Cytology of degeneration in the intersegmental muscles of the Pernyi silkworm,” *J. Insect Physiol.*, vol. 11, pp. 123–33, Mar 1965.
- [54] P. Vandenabeele, L. Galluzzi, T. Vanden Berghe, and G. Kroemer, “Molecular mechanisms of necroptosis: an ordered cellular explosion,” *Nat. Rev. Mol. Cell Biol.*, no. September, Sep 2010.
- [55] A. Degterev, J. Hitomi, M. Germscheid, I. L. Ch'en, O. Korkina, X. Teng, D. Abbott, G. D. Cuny, C. Yuan, G. Wagner, S. M. Hedrick, S. A. Gerber, A. Lugovskoy, and J. Yuan, “Identification of RIP1 kinase as a specific cellular target of necrostatins,” *Nat. Chem. Biol.*, vol. 4, no. 5, pp. 313–321, May 2008.
- [56] J. M. Hardwick, “Apoptosis in viral pathogenesis,” *Cell Death Differ.*, vol. 8, no. 2, pp. 109–110, Feb 2001.
- [57] R. J. Youle and M. Karbowski, “Mitochondrial fission in apoptosis,” *Nat. Rev. Mol. Cell Biol.*, vol. 6, no. 8, pp. 657–663, Aug 2005.
- [58] G. Nuñez, M. A. Benedict, Y. Hu, and N. Inohara, “Caspases: the proteases of the apoptotic pathway.” *Oncogene*, vol. 17, no. 25, p. 3237, 1998.
- [59] H. Y. Chang and X. Yang, “Proteases for cell suicide: functions and regulation of caspases,” *Microbiol. Mol. Biol. Rev.*, vol. 64, no. 4, pp. 821–46, Dec 2000.
- [60] A. Nadiri, M. K. M. Wolinski, and M. Saleh, “The inflammatory caspases: key players in the

- host response to pathogenic invasion and sepsis,” *J. Immunol.*, vol. 177, no. 7, pp. 4239–45, Oct 2006.
- [61] D. E. Griffin and J. M. Hardwick, “Apoptosis in Alphavirus Encephalitis,” in *Semin. Virol.*, vol. 8, no. 6, 1998, pp. 481–489.
 - [62] R. J. Clem, “Baculoviruses and apoptosis: the good, the bad, and the ugly,” *Cell Death Differ.*, vol. 8, no. 2, pp. 137–43, Feb 2001.
 - [63] J. M. Hardwick, “Viral interference with apoptosis,” *Semin. Cell Dev. Biol.*, vol. 9, no. 3, pp. 339–349, Jun 1998.
 - [64] B. A. Beutler, C. Eidenschenk, K. Crozat, and J.-L. Imler, “Genetic analysis of resistance to viral infection,” *Nat. Rev. Immunol.*, vol. 7, no. 10, pp. 753–766, 2007.
 - [65] Y.-B. Chen, S. Y. Seo, D. G. Kirsch, T. T. Sheu, W.-C. Cheng, and J. M. Hardwick, “Alternate functions of viral regulators of cell death,” *Cell Death Differ.*, vol. 13, no. 8, pp. 1318–1324, 2006.
 - [66] G. N. Barber, “Host defense, viruses and apoptosis,” *Cell Death Differ.*, vol. 8, no. 2, pp. 113–26, Feb 2001.
 - [67] C. Benedict, P. Norris, C. Ware, and Others, “To kill or be killed: viral evasion of apoptosis,” *Nat. Immunol.*, vol. 3, no. 11, pp. 1013–1018, 2002.
 - [68] R. C. Budd, W.-c. Yeh, and J. Tschopp, “cFLIP regulation of lymphocyte activation and development,” *Nat. Rev. Immunol.*, vol. 6, no. 3, pp. 196–204, 2006.
 - [69] M. Muzio, A. M. Chinnaiyan, F. C. Kischkel, K. O’Rourke, A. Shevchenko, J. Ni, C. Scaffidi, J. D. Bretz, M. Zhang, R. Gentz, M. Mann, P. H. Krammer, M. E. Peter, and V. M. Dixit, “FLICE, a novel FADD-homologous ICE/CED-3-like protease, is recruited to the CD95 (Fas/APO-1) death-inducing signaling complex,” *Cell*, vol. 85, no. 6, pp. 817–27, Jun 1996.
 - [70] J. R. Clayton and J. M. Hardwick, “Apoptosis and Virus Infection,” in *Encycl. Virol.*, 3rd ed., B. W. J. Mahy and M. H. V. Van Regenmortel, Eds. Oxford: Academic Press, 2008, ch. Apoptosis, pp. 154–162.
 - [71] A. L. Blasius and B. A. Beutler, “Intracellular toll-like receptors,” *Immunity*, vol. 32, no. 3, pp. 305–15, Mar 2010.
 - [72] K. R. Bortoluci and R. Medzhitov, “Control of infection by pyroptosis and autophagy: role of TLR and NLR,” *Cell. Mol. Life Sci.*, vol. 67, no. 10, pp. 1643–51, May 2010.
 - [73] A. Sabbah, T. H. Chang, R. Harnack, V. Frohlich, K. Tominaga, P. H. Dube, Y. Xiang, and S. Bose, “Activation of innate immune antiviral responses by Nod2,” *Nat. Immunol.*, vol. 10, no. 10, pp. 1073–80, Oct 2009.
 - [74] M. H. Shaw, T. Reimer, Y.-G. Kim, and G. Nuñez, “NOD-like receptors (NLRs): bona fide intracellular microbial sensors,” *Curr. Opin. Immunol.*, vol. 20, no. 4, pp. 377–82, Aug 2008.
 - [75] O. Takeuchi and S. Akira, “MDA5/RIG-I and virus recognition,” *Curr. Opin. Immunol.*, vol. 20, no. 1, pp. 17–22, 2008.
 - [76] T. Kawai and S. Akira, “Antiviral signaling through pattern recognition receptors,” *J.*

Biochem., vol. 141, no. 2, pp. 137–45, Mar 2007.

- [77] K. Schroder and J. Tschopp, “The inflammasomes,” *Cell*, vol. 140, no. 6, pp. 821–32, Mar 2010.
- [78] M. Yoneyama, M. Kikuchi, T. Natsukawa, N. Shinobu, T. Imaizumi, M. Miyagishi, K. Taira, S. Akira, and T. Fujita, “The RNA helicase RIG-I has an essential function in double-stranded RNA-induced innate antiviral responses,” *Nat. Immunol.*, vol. 5, no. 7, pp. 730–737, 2004.
- [79] T. Bergsbaken, S. L. Fink, and B. T. Cookson, “Pyroptosis: host cell death and inflammation,” *Nat. Rev. Microbiol.*, vol. 7, no. 2, pp. 99–109, Feb 2009.
- [80] Q. Sun, L. Sun, H.-H. Liu, X. Chen, R. B. Seth, J. Forman, and Z. J. Chen, “The specific and essential role of MAVS in antiviral innate immune responses,” *Immunity*, vol. 24, no. 5, pp. 633–642, 2006.
- [81] R. B. Seth, L. Sun, C. K. Ea, and Z. J. Chen, “Identification and characterization of MAVS, a mitochondrial antiviral signaling protein that activates NF- κ B and IRF3,” *Cell*, vol. 122, no. 5, pp. 669–682, 2005.
- [82] X. Li, L. Sun, R. B. Seth, and G. Pineda, “Hepatitis C virus protease NS3/4A cleaves mitochondrial antiviral signaling protein off the mitochondria to evade innate immunity,” *Proc. Natl. Acad. Sci. U. S. A.*, vol. 102, no. 49, pp. 17717–22, Dec 2005.
- [83] E. Meylan, J. Curran, K. Hofmann, D. Moradpour, M. Binder, R. Bartenschlager, and J. Tschopp, “Cardif is an adaptor protein in the RIG-I antiviral pathway and is targeted by hepatitis C virus,” *Nature*, vol. 437, no. 7062, pp. 1167–72, Oct 2005.
- [84] K. Li, E. Foy, J. C. Ferreon, M. Nakamura, A. C. M. Ferreon, M. Ikeda, S. C. Ray, M. Gale, and S. M. Lemon, “Immune evasion by hepatitis C virus NS3/4A protease-mediated cleavage of the Toll-like receptor 3 adaptor protein TRIF,” *Proc. Natl. Acad. Sci. U. S. A.*, vol. 102, no. 8, pp. 2992–7, Mar 2005.
- [85] J. Stack, I. R. Haga, M. Schröder, N. W. Bartlett, G. Maloney, P. C. Reading, K. A. Fitzgerald, G. L. Smith, and A. G. Bowie, “Vaccinia virus protein A46R targets multiple Toll-like-interleukin-1 receptor adaptors and contributes to virulence,” *J. Exp. Med.*, vol. 201, no. 6, pp. 1007–18, Mar 2005.
- [86] A. G. Bowie, E. Kiss-Toth, J. Symons, G. Smith, S. Dower, and L. a. J. O’Neill, “A46R and A52R from vaccinia virus are antagonists of host IL-1 and toll-like receptor signaling,” *Proc. Natl. Acad. Sci. U. S. A.*, vol. 97, no. 18, p. 10162, Aug 2000.
- [87] B. Dauber, J. Schneider, and T. Wolff, “Double-stranded RNA binding of influenza B virus nonstructural NS1 protein inhibits protein kinase R but is not essential to antagonize production of alpha/beta interferon,” *J. Virol.*, vol. 80, no. 23, pp. 11667–77, Dec 2006.
- [88] M. Mibayashi, L. Martínez-Sobrido, Y.-M. Loo, W. B. Cárdenas, M. Gale, and A. García-Sastre, “Inhibition of retinoic acid-inducible gene I-mediated induction of beta interferon by the NS1 protein of influenza A virus,” *J. Virol.*, vol. 81, no. 2, pp. 514–24, Jan 2007.
- [89] W. B. Cárdenas, Y.-M. Loo, M. Gale, A. L. Hartman, C. R. Kimberlin, L. Martínez-Sobrido, E. O. Saphire, and C. F. Basler, “Ebola virus VP35 protein binds double-stranded RNA

- and inhibits alpha/beta interferon production induced by RIG-I signaling,” *J. Virol.*, vol. 80, no. 11, pp. 5168–78, Jun 2006.
- [90] D. W. Leung, K. C. Prins, D. M. Borek, M. Farahbakhsh, J. M. Tufariello, P. Ramanan, J. C. Nix, L. A. Helgeson, Z. Otwinowski, R. B. Honzatko, C. F. Basler, and G. K. Amarasinghe, “Structural basis for dsRNA recognition and interferon antagonism by Ebola VP35,” *Nat. Struct. Mol. Biol.*, vol. 17, no. 2, pp. 165–172, Feb 2010.
- [91] J. Haasnoot, W. D. Vries, E. Geutjes, M. Prins, and P. De, “The Ebola virus VP35 protein is a suppressor of RNA silencing,” *PLoS Pathog.*, vol. 3, no. 6, p. e86, Jun 2007.
- [92] A. Olland, J. Jané-Valbuena, L. Schiff, and M. Nibert, “Structure of the reovirus outer capsid and dsRNA-binding protein σ 3 at 1.8 Å resolution,” *EMBO J.*, vol. 20, no. 5, pp. 979–989, 2001.
- [93] B. Perdiguer and M. Esteban, “The interferon system and vaccinia virus evasion mechanisms,” *J. Interf. Cytokine Res.*, vol. 29, no. 9, pp. 581–98, Sep 2009.
- [94] A. Elia, K. G. Laing, A. Schofield, V. J. Tilleray, and M. J. Clemens, “Regulation of the double-stranded RNA-dependent protein kinase PKR by RNAs encoded by a repeated sequence in the Epstein-Barr virus genome,” *Nucleic Acids Res.*, vol. 24, no. 22, pp. 4471–8, Nov 1996.
- [95] A. Gupta, J. J. Gartner, P. Sethupathy, A. G. Hatzigeorgiou, and N. W. Fraser, “Anti-apoptotic function of a microRNA encoded by the HSV-1 latency-associated transcript,” *Nature*, vol. 442, no. 7098, pp. 82–85, 2006.
- [96] J. Poppers, M. Mulvey, D. Khoo, and I. Mohr, “Inhibition of PKR activation by the proline-rich RNA binding domain of the herpes simplex virus type 1 Us11 protein,” *J. Virol.*, vol. 74, no. 23, pp. 11215–21, Dec 2000.
- [97] M. Andersson, P. Haasnoot, N. Xu, S. Berenjian, B. Berkhout, and G. Akusjärvi, “Suppression of RNA interference by adenovirus virus-associated RNA,” *J. Virol.*, vol. 79, no. 15, p. 9556, 2005.
- [98] N. Xu, B. Segerman, X. Zhou, and G. Akusjärvi, “Adenovirus virus-associated RNAII-derived small RNAs are efficiently incorporated into the RNA-induced silencing complex and associate with polyribosomes,” *J. Virol.*, vol. 81, no. 19, pp. 10540–9, Oct 2007.
- [99] M. Sano, Y. Kato, and K. Taira, “Sequence-specific interference by small RNAs derived from adenovirus VAI RNA,” *FEBS Lett.*, vol. 580, no. 6, pp. 1553–64, Mar 2006.
- [100] X. Liu, C. N. Kim, J. Yang, R. Jemmerson, and X. Wang, “Induction of apoptotic program in cell-free extracts: requirement for dATP and cytochrome c,” *Cell*, vol. 86, no. 1, pp. 147–57, Jul 1996.
- [101] S. J. Riedl and G. S. Salvesen, “The apoptosome: signalling platform of cell death,” *Nat. Rev. Mol. Cell Biol.*, vol. 8, no. 5, pp. 405–13, May 2007.
- [102] X. Teng and J. M. Hardwick, “The apoptosome at high resolution,” *Cell*, vol. 141, no. 3, pp. 402–404, Apr 2010.
- [103] A. Saleh, S. Srinivasula, S. Acharya, R. Fishel, and E. S. Alnemri, “Cytochrome c and

- dATP-mediated oligomerization of Apaf-1 is a prerequisite for procaspase-9 activation,” *J. Biol. Chem.*, vol. 274, no. 25, p. 17941, Jul 1999.
- [104] Y. Shi, “Caspase Activation:: Revisiting the Induced Proximity Model,” *Cell*, vol. 117, no. 7, pp. 855–858, Jun 2004.
- [105] H. Zou, W. J. Henzel, X. Liu, A. Lutschg, and X. Wang, “Apaf-1, a human protein homologous to *C. elegans* CED-4, participates in cytochrome c-dependent activation of caspase-3,” *Cell*, vol. 90, no. 3, pp. 405–13, Aug 1997.
- [106] J. M. Hardwick and R. J. Youle, “SnapShot: BCL-2 proteins.” *Cell*, vol. 138, no. 2, pp. 404, 404.e1, Jul 2009.
- [107] D. R. Green and G. Kroemer, “The pathophysiology of mitochondrial cell death,” *Science (80-.).*, vol. 305, no. 5684, p. 626, 2004.
- [108] M. G. Annis, E. L. Soucie, P. J. Dlugosz, J. A. Cruz-Aguado, L. Z. Penn, B. Leber, and D. W. Andrews, “Bax forms multispanning monomers that oligomerize to permeabilize membranes during apoptosis,” *EMBO J.*, vol. 24, no. 12, pp. 2096–2103, Jun 2005.
- [109] E. H.-Y. Cheng, M. C. Wei, S. Weiler, R. A. Flavell, T. W. Mak, T. Lindsten, and S. J. Korsmeyer, “BCL-2, BCL-X(L) sequester BH3 domain-only molecules preventing BAX- and BAK-mediated mitochondrial apoptosis,” *Mol. Cell*, vol. 8, no. 3, pp. 705–11, Oct 2001.
- [110] S. N. Willis, J. I. Fletcher, T. Kaufmann, M. F. van Delft, L. Chen, P. E. Czabotar, H. Ierino, E. F. Lee, W. D. Fairlie, P. Bouillet, A. Strasser, R. M. Kluck, J. M. Adams, and D. C. S. Huang, “Apoptosis Initiated When BH3 Ligands Engage Multiple Bcl-2 Homologs, Not Bax or Bak,” *Science (80-.).*, vol. 315, no. 5813, pp. 856–859, Feb 2007.
- [111] H. Kim, M. Rafiuddin-Shah, H.-C. Tu, J. R. Jeffers, G. P. Zambetti, J. J.-D. Hsieh, and E. H.-Y. Cheng, “Hierarchical regulation of mitochondrion-dependent apoptosis by BCL-2 subfamilies,” *Nat. Cell Biol.*, vol. 8, no. 12, pp. 1348–1358, 2006.
- [112] J. K. Brunelle and A. Letai, “Control of mitochondrial apoptosis by the Bcl-2 family,” *J. Cell Sci.*, vol. 122, no. Pt 4, pp. 437–41, Feb 2009.
- [113] S. Y. Seo, Y.-B. Chen, I. Ivanovska, A. M. Ranger, S. J. Hong, V. L. Dawson, S. J. Korsmeyer, D. S. Bellows, Y. Fannjiang, and J. M. Hardwick, “BAD is a pro-survival factor prior to activation of its pro-apoptotic function,” *J. Biol. Chem.*, vol. 279, no. 40, pp. 42240–42249, 2004.
- [114] H. Li, H. Zhu, C. J. Xu, and J. Yuan, “Cleavage of BID by caspase 8 mediates the mitochondrial damage in the Fas pathway of apoptosis,” *Cell*, vol. 94, no. 4, pp. 491–501, Aug 1998.
- [115] X. Luo, I. Budihardjo, H. Zou, C. Slaughter, and X. Wang, “Bid, a Bcl2 interacting protein, mediates cytochrome c release from mitochondria in response to activation of cell surface death receptors,” *Cell*, vol. 94, no. 4, pp. 481–90, Aug 1998.
- [116] E. H.-Y. Cheng, D. G. Kirsch, R. J. Clem, R. Ravi, M. B. Kastan, A. Bedi, K. Ueno, and J. M. Hardwick, “Conversion of Bcl-2 to a Bax-like death effector by caspases,” *Science (80-.).*, vol. 278, no. 5345, pp. 1966–1968, Dec 1997.

- [117] R. J. Clem, E. H.-Y. Cheng, C. L. Karp, D. G. Kirsch, K. Ueno, A. Takahashi, M. B. Kastan, D. E. Griffin, W. C. Earnshaw, M. A. Veliuona, and J. M. Hardwick, “Modulation of cell death by Bcl-XL through caspase interaction,” *Proc. Natl. Acad. Sci. U. S. A.*, vol. 95, no. 2, pp. 554–559, Jan 1998.
- [118] D. G. Kirsch, A. Doseff, B. N. Chau, D. S. Lim, N. C. de Souza-Pinto, R. Hansford, M. B. Kastan, Y. A. Lazebnik, and J. M. Hardwick, “Caspase-3-dependent cleavage of Bcl-2 promotes release of cytochrome c,” *J. Biol. Chem.*, vol. 274, no. 30, pp. 21 155–21 161, Jul 1999.
- [119] D. S. Bellows, B. N. Chau, P. Lee, Y. Lazebnik, W. H. Burns, and J. M. Hardwick, “Antia apoptotic herpesvirus Bcl-2 homologs escape caspase-mediated conversion to proapoptotic proteins,” *J. Virol.*, vol. 74, no. 11, pp. 5024–5031, Jun 2000.
- [120] J. Lewis, G. A. Oyler, K. Ueno, Y. Fannjiang, B. N. Chau, J. Vornov, S. J. Korsmeyer, S. Zou, and J. M. Hardwick, “Inhibition of virus-induced neuronal apoptosis by Bax,” *Nat. Med.*, vol. 5, no. 7, pp. 832–835, Jul 1999.
- [121] J. Lewis, S. L. Wesselingh, D. E. Griffin, and J. M. Hardwick, “Alphavirus-induced apoptosis in mouse brains correlates with neurovirulence,” *J. Virol.*, vol. 70, no. 3, pp. 1828–1835, Mar 1996.
- [122] Y. Fannjiang, C. H. Kim, R. L. Huganir, S. Zou, T. Lindsten, C. B. Thompson, T. Mito, R. J. Traystman, T. Larsen, D. E. Griffin, A. S. Mandir, T. M. Dawson, S. Dike, A. L. Sappington, D. A. Kerr, E. A. Jonas, L. K. Kaczmarek, and J. M. Hardwick, “BAK alters neuronal excitability and can switch from anti- to pro-death function during postnatal development,” *Dev. Cell*, vol. 4, no. 4, pp. 575–585, Apr 2003.
- [123] E. H.-Y. Cheng, B. Levine, L. Boise, C. B. Thompson, and J. M. Hardwick, “Bax-independent inhibition of apoptosis by Bcl-XL.” *Nature*, vol. 379, no. 6565, p. 554, Feb 1996.
- [124] S. B. Berman, Y.-B. Chen, B. Qi, J. M. McCaffery, E. Rucker 3rd, S. Goebbels, K. A. Nave, B. A. Arnold, E. A. Jonas, F. J. Pineda, and J. M. Hardwick, “Bcl-x L increases mitochondrial fission, fusion, and biomass in neurons,” *J. Cell Biol.*, vol. 184, no. 5, pp. 707–719, Mar 2009.
- [125] S. M. Best, “Viral subversion of apoptotic enzymes: escape from death row,” *Annu. Rev. Microbiol.*, vol. 62, pp. 171–92, Jan 2008.
- [126] B. A. Callus and D. L. Vaux, “Caspase inhibitors: viral, cellular and chemical,” *Cell Death Differ.*, vol. 14, no. 1, pp. 73–8, Jan 2007.
- [127] R. J. Clem and L. K. Miller, “Control of programmed cell death by the baculovirus genes p35 and iap,” *Mol. Cell. Biol.*, vol. 14, no. 8, pp. 5212–22, Aug 1994.
- [128] R. J. Clem, M. Fechheimer, and L. K. Miller, “Prevention of apoptosis by a baculovirus gene during infection of insect cells,” *Science (80-.).*, vol. 254, no. 5036, pp. 1388–90, Nov 1991.
- [129] D. Beidler, M. Tewari, P. D. Friesen, and G. Poirier, “The baculovirus p35 protein inhibits Fas-and tumor necrosis factor-induced apoptosis,” *J. Biol. Chem.*, 1995.
- [130] N. E. Crook, R. J. Clem, and L. K. Miller, “An apoptosis-inhibiting baculovirus gene with a zinc finger-like motif,” *J. Virol.*, vol. 67, no. 4, pp. 2168–74, Apr 1993.
- [131] J. Huang, Q. Huang, X. Zhou, M. M. Shen, A. Yen, S. X. Yu, G. Dong, K. Qu, P. Huang,

- E. M. Anderson, S. Daniel-Issakani, R. M. L. Buller, D. G. Payan, and H. H. Lu, “The Poxvirus p28 Virulence Factor Is an E3 Ubiquitin Ligase,” *J. Biol. Chem.*, vol. 279, no. 52, pp. 54 110–6, Dec 2004.
- [132] R. Swanson, M. P. Raghavendra, W. Zhang, C. Froelich, P. G. W. Gettins, and S. T. Olson, “Serine and Cysteine Proteases Are Translocated to Similar Extents upon Formation of Covalent Complexes with Serpins,” *J. Biol. Chem.*, vol. 282, no. 4, pp. 2305–13, Jan 2007.
- [133] P. C. Turner, M. C. Sancho, S. Thoennes, A. Caputo, R. Bleackley, and R. W. Moyer, “Myxoma Virus Serp2 Is a Weak Inhibitor of Granzyme B and Interleukin-1b-Converting Enzyme In Vitro and Unlike CrmA Cannot Block Apoptosis in Cowpox Virus-Infected Cells,” *J. Virol.*, vol. 73, no. 8, pp. 6394–6404, 1999.
- [134] P. D. Friesen and L. K. Miller, “Chapter 20. Insect Viruses,” in *Fields Virol.*, 4th ed., D. M. Knipe and P. M. Howley, Eds. Lippincott Williams & Wilkins, 2001, pp. 917–962.
- [135] P. M. Van Wynsberghe, H.-R. Chen, and P. Ahlquist, “Nodavirus RNA replication protein a induces membrane association of genomic RNA,” *J. Virol.*, vol. 81, no. 9, pp. 4633–44, May 2007.
- [136] D. Galiana-Arnoux, C. Dostert, A. Schneemann, J. A. Hoffmann, and J.-L. Imler, “Essential function in vivo for Dicer-2 in host defense against RNA viruses in drosophila,” *Nat. Immunol.*, vol. 7, no. 6, pp. 590–597, 2006.
- [137] B. J. Fenner, W. Goh, and J. Kwang, “Sequestration and protection of double-stranded RNA by the betanodavirus B2 protein,” *J. Virol.*, vol. 80, no. 14, pp. 6822–6833, Jul 2006.
- [138] A. Lingel, B. Simon, E. Izaurralde, and M. Sattler, “The structure of the flock house virus B2 protein, a viral suppressor of RNA interference, shows a novel mode of double-stranded RNA recognition,” *EMBO Rep.*, vol. 6, no. 12, pp. 1149–55, Dec 2005.
- [139] J. Chao, J. Lee, B. Chapados, E. Debler, A. Schneemann, and J. Williamson, “Dual modes of RNA-silencing suppression by Flock House virus protein B2,” *Nat. Struct. Mol. Biol.*, vol. 12, no. 11, pp. 952–957, 2005.
- [140] G. Singh, S. Popli, Y. Hari, P. Malhotra, S. Mukherjee, and R. K. Bhatnagar, “Suppression of RNA silencing by Flock house virus B2 protein is mediated through its interaction with the PAZ domain of Dicer,” *FASEB J.*, vol. 23, no. 6, pp. 1845–57, Jun 2009.
- [141] K. M. Myles, M. R. Wiley, E. M. Morazzani, and Z. N. Adelman, “Alphavirus-derived small RNAs modulate pathogenesis in disease vector mosquitoes,” *Proc. Natl. Acad. Sci. U. S. A.*, vol. 105, no. 50, p. 19938, 2008.
- [142] C. M. Cirimotich, J. C. Scott, A. T. Phillips, B. J. Geiss, and K. E. Olson, “Suppression of RNA interference increases alphavirus replication and virus-associated mortality in *Aedes aegypti* mosquitoes,” *BMC Microbiol.*, vol. 9, p. 49, Jan 2009.
- [143] K. White, E. Tahaoglu, and H. Steller, “Cell killing by the *Drosophila* gene reaper,” *Science (80-.)*, vol. 271, no. 5250, p. 805, 1996.
- [144] J. Chai, N. Yan, J. R. Huh, J.-W. Wu, W. Li, B. A. Hay, and Y. Shi, “Molecular mechanism of Reaper-Grim-Hid-mediated suppression of DIAP1-dependent Dronc ubiquitination,” *Nat.*

Struct. Biol., vol. 10, no. 11, pp. 892–898, Nov 2003.

- [145] H. D. Ryoo, A. Bergmann, H. Gonen, A. Ciechanover, and H. Steller, “Regulation of Drosophila IAP1 degradation and apoptosis by reaper and ubcD1,” *Nat. Cell Biol.*, vol. 4, no. 6, pp. 432–438, 2002.
- [146] I. Muro, B. A. Hay, and R. J. Clem, “The Drosophila DIAP1 protein is required to prevent accumulation of a continuously generated, processed form of the apical caspase DRONC,” *J. Biol. Chem.*, vol. 277, no. 51, pp. 49 644–50, Dec 2002.
- [147] M. Orme and P. Meier, “Inhibitor of apoptosis proteins in Drosophila: gatekeepers of death,” *Apoptosis*, vol. 14, no. 8, pp. 950–60, Aug 2009.
- [148] C. Holley, M. R. Olson, D. A. Colón-Ramos, and S. Kornbluth, “Reaper eliminates IAP proteins through stimulated IAP degradation and generalized translational inhibition,” *Nat. Cell Biol.*, vol. 4, no. 6, pp. 439–444, 2002.
- [149] E. Abdelwahid, T. Yokokura, R. J. Krieser, S. Balasundaram, W. H. Fowle, and K. White, “Mitochondrial disruption in Drosophila apoptosis,” *Dev. Cell*, vol. 12, no. 5, pp. 793–806, 2007.
- [150] C. Sandu, H. D. Ryoo, and H. Steller, “Drosophila IAP antagonists form multimeric complexes to promote cell death,” *J. Cell Biol.*, vol. 190, no. 6, pp. 1039–1052, Sep 2010.
- [151] C. B. Jonsson, L. T. M. Figueiredo, and O. Vapalahti, “A Global Perspective on Hantavirus Ecology, Epidemiology, and Disease,” *Clin. Microbiol. Rev.*, vol. 23, no. 2, pp. 412–441, Apr 2010.
- [152] Ö. Ergönül, “Crimean-Congo haemorrhagic fever,” *Lancet Infect. Dis.*, vol. 6, no. 4, pp. 203–14, Apr 2006.
- [153] X. Shi, A. Kohl, V. H. J. Léonard, P. Li, A. McLees, and R. M. Elliott, “Requirement of the N-terminal region of orthobunyavirus nonstructural protein NSm for virus assembly and morphogenesis,” *J. Virol.*, vol. 80, no. 16, pp. 8089–99, Aug 2006.
- [154] D. H. L. Bishop, K. G. Gould, H. Akashi, and C. M. Clerx-van Haaster, “The complete sequence and coding content of snowshoe hare bunyavirus small (S) viral RNA species,” *Nucleic Acids Res.*, vol. 10, no. 12, pp. 3703–3713, Jun 1982.
- [155] F. Fuller, A. S. Bown, and D. H. L. Bishop, “Bunyavirus Nucleoprotein, N, and a Non-structural Protein, NSS, Are Coded by Overlapping Reading Frames in the S RNA,” *J. Gen. Virol.*, vol. 64, no. 8, pp. 1705–1714, Aug 1983.
- [156] A. Bridgen, F. Weber, J. K. Fazakerley, and R. M. Elliott, “Bunyamwera bunyavirus nonstructural protein NSs is a nonessential gene product that contributes to viral pathogenesis,” *Proc. Natl. Acad. Sci. U. S. A.*, vol. 98, no. 2, pp. 664–9, Jan 2001.
- [157] D. A. Colón-Ramos, P. M. Irusta, E. C. Gan, M. R. M. Olson, J. Song, R. I. Morimoto, R. M. Elliott, M. Lombard, R. Hollingsworth, J. M. Hardwick, G. K. Smith, S. Kornbluth, and Others, “Inhibition of translation and induction of apoptosis by Bunyaviral nonstructural proteins bearing sequence similarity to reaper,” *Mol. Biol. Cell*, vol. 14, no. 10, pp. 4162–4172, Oct 2003.

- [158] K. Thress, J. Song, R. I. Morimoto, and S. Kornbluth, “Reversible inhibition of Hsp70 chaperone function by Scythe and Reaper,” *EMBO J.*, vol. 20, no. 5, pp. 1033–1041, Mar 2001.
- [159] C. F. Curtis, “Possible Use of Translocations to fix Desirable Genes in Insect Pest Populations,” *Nature*, vol. 218, no. 5139, pp. 368–369, Apr 1968.
- [160] C. A. Hill, F. C. Kafatos, S. K. Stansfield, and F. H. Collins, “Arthropod-borne diseases: vector control in the genomics era,” *Nat. Rev. Microbiol.*, vol. 3, no. 3, pp. 262–268, Feb 2005.
- [161] L. A. Moreira, A. K. Ghosh, E. G. Abraham, and M. Jacobs-Lorena, “Genetic transformation of mosquitoes: a quest for malaria control,” *Int. J. Parasitol.*, vol. 32, no. 13, pp. 1599–1605, Dec 2002.
- [162] S. Blanford, B. H. K. Chan, N. Jenkins, D. Sim, R. J. Turner, A. F. Read, and M. B. Thomas, “Fungal pathogen reduces potential for malaria transmission,” *Science (80-.)*, vol. 308, no. 5728, pp. 1638–1641, Jun 2005.
- [163] A. F. Read, P. A. Lynch, and M. B. Thomas, “How to Make Evolution-Proof Insecticides for Malaria Control,” *PLoS Biol.*, vol. 7, no. 4, p. e1000058, Apr 2009.
- [164] L. A. Moreira, I. Iturbe-Ormaetxe, J. a. Jeffery, G. Lu, A. T. Pyke, L. M. Hedges, B. C. Rocha, S. Hall-Mendelin, A. Day, M. Riegler, L. E. Hugo, K. N. Johnson, B. H. Kay, E. A. McGraw, A. F. van Den Hurk, P. a. Ryan, and S. L. O’Neill, “A Wolbachia symbiont in *Aedes aegypti* limits infection with dengue, Chikungunya, and *Plasmodium*,” *Cell*, vol. 139, no. 7, pp. 1268–78, Dec 2009.
- [165] C. McMeniman, R. Lane, B. Cass, A. Fong, M. Sidhu, Y. Wang, and S. L. O’Neill, “Stable introduction of a life-shortening Wolbachia infection into the mosquito *Aedes aegypti*,” *Science (80-.)*, vol. 323, no. 5910, p. 141, 2009.
- [166] A. Z. Fire, S. S. Xu, M. K. M. Montgomery, S. A. S. Kostas, S. E. Driver, and C. C. Mello, “Potent and specific genetic interference by double-stranded RNA in *Caenorhabditis elegans*,” *Nature*, vol. 391, no. 6669, pp. 806–811, Feb 1998.
- [167] G. J. Hannon, “RNA interference,” *Nature*, vol. 418, no. July, pp. 24–26, 2002.
- [168] M. Jinek and J. A. Doudna, “A three-dimensional view of the molecular machinery of RNA interference,” *Nature*, vol. 457, no. 7228, pp. 405–12, Jan 2009.
- [169] X. X.-h. Wang, R. Aliyari, W.-x. W. Li, H. H.-w. Li, K. Kim, R. Carthew, P. W. Atkinson, and S.-W. Ding, “RNA interference directs innate immunity against viruses in adult *Drosophila*,” *Science (80-.)*, vol. 312, no. 5772, pp. 452–454, 2006.
- [170] R. P. van Rij, M.-C. Saleh, B. Berry, C. Foo, A. Houk, C. Antoniewski, and R. Andino, “The RNA silencing endonuclease Argonaute 2 mediates specific antiviral immunity in *Drosophila melanogaster*.” *Genes Dev.*, vol. 20, no. 21, pp. 2985–95, Nov 2006.
- [171] U. Mudiganti, R. Hernandez, D. Ferreira, and D. T. Brown, “Sindbis virus infection of two model insect cell systems—A comparative study,” *Virus Res.*, vol. 122, no. 1-2, pp. 28–34, 2006.
- [172] R. M. Kinney, G. J. Chang, K. R. Tsuchiya, J. M. Sneider, J. T. Roehrig, T. M. Woodward, and D. W. Trent, “Attenuation of Venezuelan equine encephalitis virus strain TC-83 is

- encoded by the 5'-noncoding region and the E2 envelope glycoprotein," *J. Virol.*, vol. 67, no. 3, pp. 1269–77, Mar 1993.
- [173] B. D. Foy, K. M. Myles, D. J. Pierro, I. Sanchez-Vargas, M. Uhlírová, M. Jindra, B. J. Beaty, and K. E. Olson, "Development of a new Sindbis virus transducing system and its characterization in three Culicine mosquitoes and two Lepidopteran species," *Insect Mol. Biol.*, vol. 13, no. 1, pp. 89–100, Feb 2004.
- [174] A. S. Xiong, Q. H. Yao, R. H. Peng, H. Duan, X. Li, H. Q. Fan, Z. M. Cheng, and Y. Li, "PCR-based accurate synthesis of long DNA sequences," *Nat. Protoc.*, vol. 1, no. 2, pp. 791–797, 2006.
- [175] J. Sambrook, E. Fritsch, and T. Maniatis, *Molecular Cloning: A Laboratory Manual*. Cold Spring Harbor Laboratory Press, 1989.
- [176] E. L. Kaplan and P. Meier, "Nonparametric Estimation from Incomplete Observations," *J. Am. Stat. Assoc.*, vol. 53, no. 282, pp. 457–481, Jun 1958.
- [177] D. Cox, "Regression models and life-tables," *J. R. Stat. Soc. Ser. B*, vol. 34, no. 2, pp. 187–220, 1972.
- [178] M.-C. Saleh, M. Tassetto, R. P. van Rij, B. Goic, V. Gausson, B. Berry, C. Jacquier, C. Antoniewski, and R. Andino, "Antiviral immunity in Drosophila requires systemic RNA interference spread." *Nature*, vol. 458, no. 7236, pp. 346–50, Mar 2009.
- [179] A. J. Luers, S. D. Adams, J. V. Smalley, and J. J. Campanella, "A phylogenomic study of the genus alphavirus employing whole genome comparison," *Comp. Funct. Genomics*, vol. 6, no. 4, pp. 217–27, Jan 2005.
- [180] L. L. Coffey, N. Vasilakis, A. C. Brault, A. M. Powers, F. Tripet, and S. C. Weaver, "Arbovirus evolution in vivo is constrained by host alternation," *Proc. Natl. Acad. Sci. U. S. A.*, vol. 105, no. 19, pp. 6970–5, May 2008.
- [181] M. L. Miller and D. T. Brown, "Morphogenesis of Sindbis virus in three subclones of *Aedes albopictus* (mosquito) cells," *J. Virol.*, vol. 66, no. 7, pp. 4180–90, Jul 1992.
- [182] B. F. Eldridge and J. D. Edman, Eds., *Medical Entomology: A Textbook on Public Health and Veterinary Problems Caused by Arthropods*. Dordrecht: Springer Netherlands, 2004.
- [183] "WHO | Malaria," <http://www.who.int/mediacentre/factsheets/fs094/en/index.html>.
- [184] "History | CDC Malaria," <http://www.cdc.gov/malaria/history/index.htm>.
- [185] F. Moscardi, "Assessment of the application of baculoviruses for control of Lepidoptera," *Annu. Rev. Entomol.*, vol. 44, pp. 257–289, Jan 1999.
- [186] E.-J. Scholte, K. Ng'habi, J. Kihonda, W. Takken, K. Paaijmans, S. Abdulla, G. F. Killeen, and B. G. J. Knols, "An entomopathogenic fungus for control of adult African malaria mosquitoes," *Science (80-.).*, vol. 308, no. 5728, pp. 1641–1642, Jun 2005.
- [187] J. J. Becnel, "Prospects for the mosquito baculovirus CuniNPV as a tool for mosquito control," *J. Am. Mosq. Control Assoc.*, vol. 22, no. 3, pp. 523–6, Sep 2006.
- [188] X. Ren and J. L. Rasgon, "Potential for the *Anopheles gambiae* densonucleosis virus to act as

- an "evolution-proof" biopesticide." *J. Virol.*, vol. 84, no. 15, pp. 7726–9, Aug 2010.
- [189] A. F. Read and M. B. Thomas, "Mosquitoes Cut Short," *Science (80-.)*, vol. 323, no. 5910, pp. 51–52, Jan 2009.
- [190] M. J. Thomenius and S. Kornbluth, "Multifunctional reaper: sixty-five amino acids of fury," *Cell Death Differ.*, vol. 13, no. 8, pp. 1305–1309, 2006.
- [191] P. M. Irusta, E. Lamos, H. L. Galonek, M. A. V. Maten, M. C. Boersma, Y.-B. Chen, and J. M. Hardwick, "Regulation of apoptosis by viruses that infect insects," *Arch. Virol. Suppl.*, vol. (18), no. 18, pp. 171–178, 2004.
- [192] R. Taylor and H. S. Hurlbut, "The isolation of Coxsackie-like viruses from mosquitoes," *J. Egypt. Med. Assoc.*, vol. 36, no. 9, pp. 489–94, Jan 1953.
- [193] R. M. Taylor, H. S. Hurlbut, T. H. Work, J. R. Kingston, and T. E. Frothingham, "Sindbis virus: a newly recognized arthropod-transmitted virus." *Am. J. Trop. Med. Hygiene*, vol. 4, no. 5, pp. 844–62, Sep 1955.
- [194] P. C. Tucker, E. G. Strauss, R. J. Kuhn, J. H. Strauss, and D. E. Griffin, "Viral determinants of age-dependent virulence of Sindbis virus for mice." *J. Virol.*, vol. 67, no. 8, pp. 4605–10, Aug 1993.
- [195] A. Grishok, "Role of the immune response in age-dependent resistance of mice to encephalitis due to Sindbis virus," *J. Infect. Dis.*, vol. 133, no. 4, pp. 456–64, Apr 1976.
- [196] C. M. Rice, R. Levis, J. H. Strauss, and H. V. Huang, "Production of infectious RNA transcripts from Sindbis virus cDNA clones: mapping of lethal mutations, rescue of a temperature-sensitive marker, and in vitro mutagenesis to generate defined mutants." *J. Virol.*, vol. 61, no. 12, p. 3809, Dec 1987.
- [197] M. G. Varma, M. Pudney, and C. J. Leake, "Cell lines from larvae of Aedes (Stegomyia) malayensis Colless and Aedes (S) pseudoscutellaris (Theobald) and their infection with some arboviruses," *Trans. R. Soc. Trop. Med. Hyg.*, vol. 68, no. 5, pp. 374–82, Jan 1974.
- [198] K. E. Olson, K. M. Myles, R. C. Seabaugh, S. Higgs, J. Carlson, and B. J. Beaty, "Development of a Sindbis virus expression system that efficiently expresses green fluorescent protein in midguts of Aedes aegypti following per os infection," *Insect Mol. Biol.*, vol. 9, no. 1, pp. 57–65, Feb 2000.
- [199] U. K. Laemmli, "Cleavage of Structural Proteins during the Assembly of the Head of Bacteriophage T4," *Nature*, vol. 227, no. 5259, pp. 680–685, Aug 1970.
- [200] H. Schägger, "Tricine-SDS-PAGE," *Nat. Protoc.*, vol. 1, no. 1, pp. 16–22, Jun 2006.
- [201] N. Sarver and V. Stollar, "Sindbis virus-induced cytopathic effect in clones of Aedes albopictus (Singh) cells," *Virology*, vol. 80, no. 2, pp. 390–400, Jul 1977.
- [202] P. M. Irusta and J. M. Hardwick, "Neuronal apoptosis pathways in Sindbis virus encephalitis," *Prog. Mol. Subcell. Biol.*, vol. 36, pp. 71–93, 2004.
- [203] A. W. E. Franz, I. Sanchez-Vargas, Z. N. Adelman, C. D. Blair, B. J. Beaty, A. A. James, and K. E. Olson, "Engineering RNA interference-based resistance to dengue virus type 2 in genetically modified Aedes aegypti," *Proc. Natl. Acad. Sci. U. S. A.*, vol. 103, no. 11, pp.

4198–4203, Mar 2006.

- [204] L. Zhou, G. Jiang, G. Chan, C. P. Santos, D. W. Severson, and L. Xiao, “Michelob_x is the missing inhibitor of apoptosis protein antagonist in mosquito genomes.” *EMBO Rep.*, vol. 6, no. 8, pp. 769–74, Aug 2005.
- [205] D. A. Colón-Ramos, C. C. L. Shenvi, D. H. D. Weitzel, E. C. E. Gan, R. Matts, J. Cate, and S. Kornbluth, “Direct ribosomal binding by a cellular inhibitor of translation,” *Nat. Struct. Mol. Biol.*, vol. 13, no. 2, pp. 103–11, Feb 2006.
- [206] D. J. Pierro, K. M. Myles, B. D. Foy, B. J. Beaty, and K. E. Olson, “Development of an orally infectious Sindbis virus transducing system that efficiently disseminates and expresses green fluorescent protein in *Aedes aegypti*,” *Insect Mol. Biol.*, vol. 12, no. 2, pp. 107–116, 2003.
- [207] L. Labrada, X. H. Liang, W. Zheng, C. Johnston, and B. Levine, “Age-dependent resistance to lethal alphavirus encephalitis in mice: analysis of gene expression in the central nervous system and identification of a novel interferon-inducible protective gene, mouse ISG12,” *J. Virol.*, vol. 76, no. 22, p. 11688, 2002.
- [208] M. K. Borucki, B. J. Kempf, B. J. Blitvich, C. D. Blair, and B. J. Beaty, “La Crosse virus: replication in vertebrate and invertebrate hosts,” *Microbes Infect.*, vol. 4, no. 3, pp. 341–350, Mar 2002.
- [209] V. H. J. Léonard, A. Kohl, T. J. Hart, and R. M. Elliott, “Interaction of Bunyamwera Orthobunyavirus NSs protein with mediator protein MED8: a mechanism for inhibiting the interferon response.” *J. Virol.*, vol. 80, no. 19, pp. 9667–75, Oct 2006.
- [210] D. Thomas, G. Blakqori, V. Wagner, M. Banholzer, N. Kessler, R. M. Elliott, O. Haller, and F. Weber, “Inhibition of RNA polymerase II phosphorylation by a viral interferon antagonist,” *J. Biol. Chem.*, vol. 279, no. 30, pp. 31471–7, Jul 2004.
- [211] I. van Knippenberg, C. Carlton-Smith, and R. M. Elliott, “The N-terminus of Bunyamwera orthobunyavirus NSs protein is essential for interferon antagonism,” *J. Gen. Virol.*, vol. 91, no. 8, pp. 2002–2006, Aug 2010.
- [212] A. Kohl, R. F. Clayton, F. Weber, A. Bridgen, R. E. Randall, and R. M. Elliott, “Bunyamwera Virus Nonstructural Protein NSs Counteracts Interferon Regulatory Factor 3-Mediated Induction of Early Cell Death,” *J. Virol.*, vol. 77, no. 14, pp. 7999–8008, Jul 2003.
- [213] K. White, M. M. E. Grether, J. M. Abrams, L. Young, K. Farrell, and H. Steller, “Genetic control of programmed cell death in *Drosophila*,” *Science (80-.).*, vol. 264, no. 5159, pp. 677–683, Apr 1994.
- [214] M. R. Olson, C. L. Holley, E. C. Gan, D. a. Colón-Ramos, B. Kaplan, and S. Kornbluth, “A GH3-like domain in reaper is required for mitochondrial localization and induction of IAP degradation.” *J. Biol. Chem.*, vol. 278, no. 45, pp. 44758–68, Nov 2003.
- [215] C. S. Hahn, Y. S. Hahn, T. J. Braciale, and C. M. Rice, “Infectious Sindbis virus transient expression vectors for studying antigen processing and presentation.” *Proc. Natl. Acad. Sci. U. S. A.*, vol. 89, no. 7, pp. 2679–83, Apr 1992.
- [216] C. D. Freel, D. A. Richardson, M. J. Thomenius, E. C. Gan, S. R. Horn, M. R. Olson, and

- S. Kornbluth, “Mitochondrial localization of Reaper to promote inhibitors of apoptosis protein degradation conferred by GH3 domain-lipid interactions,” *J. Biol. Chem.*, vol. 283, no. 1, pp. 367–379, 2008.
- [217] C. Clavería, E. Caminero, C. Martínez-A, S. Campuzano, and M. Torres, “GH3, a novel proapoptotic domain in Drosophila Grim, promotes a mitochondrial death pathway,” *EMBO J.*, vol. 21, no. 13, p. 3327, 2002.
- [218] E. H.-Y. Cheng, J. Nicholas, D. S. Bellows, G. S. Hayward, H. G. Guo, M. S. Reitz, and J. M. Hardwick, “A Bcl-2 homolog encoded by Kaposi sarcoma-associated virus, human herpesvirus 8, inhibits apoptosis but does not heterodimerize with Bax or Bak.” *Proc. Natl. Acad. Sci. U. S. A.*, vol. 94, no. 2, pp. 690–4, Jan 1997.
- [219] M. D. Abramoff, P. J. Magelhaes, and S. J. Ram, “Image Processing with ImageJ,” *Biophotonics Int.*, vol. 11, no. 7, pp. 36–42, 2004.
- [220] M. R. Schlabach, J. K. Hu, M. Li, and S. J. Elledge, “Synthetic design of strong promoters,” *Proc. Natl. Acad. Sci. U. S. A.*, vol. 107, no. 6, pp. 2538–43, Feb 2010.
- [221] R. Toribio and I. Ventoso, “Inhibition of host translation by virus infection *in vivo*,” *Proc. Natl. Acad. Sci. U. S. A.*, vol. 107, no. 21, May 2010.
- [222] R. Gorchakov, E. I. Frolova, and I. Frolov, “Inhibition of transcription and translation in Sindbis virus-infected cells,” *J. Virol.*, vol. 79, no. 15, p. 9397, 2005.
- [223] E. E. Ravkov and R. Compans, “Hantavirus nucleocapsid protein is expressed as a membrane-associated protein in the perinuclear region,” *J. Virol.*, vol. 75, no. 4, pp. 1808–1815, 2001.
- [224] F. W. Nietzsche, *Twilight of the idols, or, How to philosophize with a hammer*, 1998th ed. New York: Oxford University Press, 1889.
- [225] L. R. Sabin, S. L. Hanna, and S. Cherry, “Innate antiviral immunity in Drosophila.” *Curr. Opin. Immunol.*, vol. 22, no. 1, pp. 4–9, Mar 2010.
- [226] M.-C. Saleh, R. P. van Rij, A. Hekele, A. Gillis, E. Foley, P. H. O’Farrell, and R. Andino, “The endocytic pathway mediates cell entry of dsRNA to induce RNAi silencing.” *Nat. Cell Biol.*, vol. 8, no. 8, pp. 793–802, 2006.

Appendix I

Oligonucleotide and probe sequences

129

Table I-I. Oligonucleotide and probe sequences

Nº	Name	Note	Sequence
B2			
1	B2***-F	<i>For mutating first three methionines to STOP</i>	TAGCCAAGCAAACTCGCGCTAATCCAGGAACTTCCCGACCGCATTCAAACGGCGGT GGATAGAGCCTAGGGATAGAGCTACCAAGACGCACCGAACAAACG
2	B2.1	<i>Oligo used for B2 synthesis</i>	ATCGAGATCTCACCATGCCAACGAAACTCGCGCTAATCCAGGAACTTCCCGACCGC ATTCAAACGGCGGTGGAAGCAGCCATGGGAATGAGCTACC
3	B2.2	<i>Oligo used for B2 synthesis</i>	CCATCCGACTTACCGTTAGTTGCCTTGTAGGCAAGCGTGCAGGTTGTCGAGG TCCCTGCGCACGTTGTCGGTGCCTTGTAGCTCATTCC
4	B2.3	<i>Oligo used for B2 synthesis</i>	GGTAAGTCGGATGGTAACATCACTGCTGGAGAAACCCAGCGTGGTGGCATAACCTAG AGGGAAAGGCCCGAGGAGGCAAACACACTCGAAGAA

Table I-I. Oligonucleotide and probe sequences

Nº	Name	Note	Sequence
5	B2.4	<i>Oligo used for B2 synthesis</i>	ATCGAGATCTCTACAGTTGCGGGTGGGGGTCACTCCGGTTGGAAAGGCTG TGGCTGAGCTCCAGCTTCGGAGGCCTTCGAGTGT
6	B2_161-186-R		ATGTTACCATCCGACTTACCGTTAGT
7	B2_167-203-F		GGTAAGTCGGATGGAACATCACTGCTGGAGAACCC
8	B2_1M*-F	<i>Changes Met1 to STOP</i>	TAGCCAAGCAAACCTCGCGCTAATCC
9	B2_C44Y-F	<i>C44 Y mutagenesis</i>	GCACGCTTACCTAAACAAGGC
10	B2_C44Y-R	<i>C44 Y mutagenesis</i>	GTTTAGGTAAGCGTGCAGGTTGTCG
11	B23X_1-F		GAATTCGCGGCCGCGGTACCTAGCCAAGCAAACCTCGCGCTAATCC
12	B23X_1-R		GCTAGCAAGCTTGGATCCAGTACTCTACAGTTTGCAGGGTGGGGGTAC
13	B23X_2-F		AGTACTGGATCCAAGCTTGCTAGCTAGCCAAGCAAACCTCGCGCTAATCC
14	B23X_2-R		AGTACTGTCGACCTGCAGGCATGCCTACAGTTTGCAGGGTGGGGGTAC
15	B23X_3-F		GCATGCCCTGCAGGTCGACAGTACTTAGCCAAGCAAACCTCGCGCTAATCC
16	B23X_3-R	<i>For making 3X-B2 Construct</i>	GAATTCGCGGCCGCGGTGACCCCTACAGTTTGCAGGGTGGGGGTAC
17	B23X-F	<i>For making 3X-B2 Construct - END</i>	GAATTCGCGGCCGCGGTACCTAG
18	B23X-R	<i>For making 3X-B2 Construct - END</i>	GAATTCGCGGCCGCGGTGACCCCTAC
19	B2-R		CTACAGTTTGCAGGGTGGGGGTAC
20	BglII_B2-R		AGATCTCTACAGTTTGCAGGG
21	BglII_Kozak_B2-F		AGATCTCACCATGCCAAGCA
22	BstEII-Met→STOP-B2-F	<i>Changes Met1 to STOP</i>	GGTCACCTAGCCAAGCAAACCTCGCGCTAATCC
23	N4_BstEII_B2-F	<i>For cloning into dsTE12Q and without a tag</i>	ATCAGGGTCACCATGCCAAGCAAAC
24	N4_BstEII_B2-R		ATCAGGGTGACCCCTACAGTTTGCAGGG
—			Reaper
25	EcoNotRpr6-F		CCTCGAATTGCGGCCGCACCATGGCAGTGGCATTCTACATAACCC

Table I-I. Oligonucleotide and probe sequences

Nº	Name	Note	Sequence
26	EcoNotRpr-F	<i>First Version of Reaper Primer</i>	ATCGGAATTCGCGGCCGCGCCACCATGGCAGTGGCATTCTAC
27	Reaper_dN-F	<i>Reaper deleted IBM AVAF</i>	ATCGCGCCGCCAACATGTACATACCCGATCAGGCAG
28	Reaper_dNHA-F	<i>Reaper deleted IBM "AVAF" with HA-epitope</i>	ATCGCGCCGCCAACATGTACCCCTACGACGTCCCCGACTACGCCTACATACCCG ATCAGGCAG
—			NSs
29	NSs_113-134-F		GGATCTTCTTCCTCAATGCCGC
30	NSs_154-170-F		TCGCGTAAACCAGAGAGGAAA
31	NSs_157-176-F	<i>For mutating Q51A, forward</i>	CGTAAACGCGAGAGGAAAGC
32	NSs_170-154-R	<i>For mutating Q51A, reverse</i>	TTCCCTCTCGCGTTACCGCA
33	NSs_Bgl_ACC-F	<i>For cloning into DB59</i>	ATATAGATCTACCATGATGTCGCATCAACCGG
34	NSs_Bgl-R	<i>For cloning into DB59</i>	TTAGAGATCTCTAGAACCCATCTAGCCAGG
35	NSs_Bst-F	<i>For cloning into dsTE12Q</i>	GGTCACCATGATGTCGCATCAACCGG
36	NSs_Bst-HA-F	<i>For cloning into dsTE12Q with HA-tag w/o DB59 linker</i>	GGTCACCATGTACCCATACGATGTTCCAGATTACGCTATGATGTCGCATCAACCGG
37	NSs_Bst-R	<i>For cloning into dsTE12Q</i>	GGTGACCCCTAGAACCCATCTAGCCAGG
38	NSs_dN38		AGATCTACCATGCGCAAAGCCAAG
39	NSs_dN51		AGATCTACCATGCGCGTAAACCAGAGAGGAAAGC
40	NSs_dN71		AGATCTACCATGCTGAAACAGGAACAATC
41	NSs_fs-F	<i>Early frameshift</i>	AGATCTACCATGATGATCGCATCAACCGGTGCAAATGGATTGATCCTGATGACAG GGTATCTGGCATTCTGTGTTAACATGAAGGGAGTCGATCAG
42	NSs_Met2Leu-F	<i>For mutating Mets to Leus</i>	AGATCTACCTTGTGTCGCATCAACCGGTGCAAATTGGATTGATCCTGTTGCAGGG TATCTGGCATTCTGTGTTAACATTGGGGAGTCGATCAG
43	NSs_QR-F	<i>For mutating Q51A;R52A, forward</i>	CGTAAACGCGGCAGGAAAGC
44	NSs_QR-R	<i>For mutating Q51A;Q52A, reverse</i>	GGATTGCTTCCTGCAGCGTTTAC
45	NSs_STOPs-F	<i>Adds STOPs to all frames</i>	AGATCTACCATGATGTCGCATCAACCGGTGCAAATTGATTAGATCCTGATG

Table I-I. Oligonucleotide and probe sequences

Nº	Name	Note	Sequence
46	NSs-F		ATGATGTCGCATCAACCGG
47	NSs-R		CTAGAACCCATCTAGCCAGG
—			
			Viruses
48	dsTE12Q1-F		TCAAGCCGCCATCTCAAAAACATC
49	dsTE12Q1-R		TTGGCGTCCGCTAGATAATGGT
50	MRE16-F		CGAGTGGCGGACCCCCTAAAA
51	MRE16-R		TTCGCCTGCTTCATTCTCACATC
52	TC83_1688*-F	<i>Forward primer for mutating BstEII site</i>	GGTTACAAGCTACGATGGCG
53	TC83_1688*-R	<i>Reverse primer for mutating BstEII site</i>	CGTAGCTTGTAAACCTTATCAAGCC
54	TC83_1688*_long-R	<i>Reverse primer for mutating BstEII site</i>	TCGCCATCGTAGCTTGTAAACCTTATCAAGCCACG
55	TC83_Sall-F	<i>Forward primer, amplicon 1</i>	GTCGACTTGATGTTACAAGAGGC
56	TC83_Sall_long-F	<i>Forward primer, amplicon 1</i>	AAGCCGATGTCGACTTGATGTTACAAGAGGCTGGG
57	TC83_EcoRI-R	<i>Reverse primer, amplicon 2</i>	GGCGAATTCATGGAAGGG
58	TC83_ApaI-F	<i>For adding BstEII site in place of GFP</i>	GGGCCCCATAACTCTACGGCTAACCTGAATGGACTACGACATAGTCTAGTCCG CCAAGTCTAGAGCTTGCCGCCACCATGGTGAGC
59	TC83_ApaI-R	<i>Reverse complement of above to dimerize</i>	GCTCACCATGGTGGCGGCAAGCTCTAGACTGGCGGACTAGACTATGTCGTAGTCC ATTCAAGGTTAGCCGTAGAGAGTTATAGGGGCC
60	TC83_AflII-F	<i>For Afl amplicon, forward</i>	GGTCACCAGCGGCCAACATGATCCGACCAGC
61	TC83_AflII-R		CTTAAGCGCGCCAGAACG
62	pTC83-F_1512	<i>For sequence verification of Bst1683*</i>	CTAAGTGCAGCCGATGAGG
63	pTC83-R_2305		CAGGGTCTCTACGGGGTGTGTTG

Table I-I. Oligonucleotide and probe sequences

Nº	Name	Note	Sequence
64	pTC83-F_7398	<i>For sequencing TC-83-based constructs</i>	GCAAGGCAGTAGAACATCAAGGTAT
65	pTC83-R_9196	<i>For verifying Apa/AfII insert</i>	GGGAACGTCACATTGGCGAGCAGA
66	pTC83-R_8274	<i>For sequencing TC-83 based constructs, reverse</i>	AGGGGCCTTATGCACATCAGTTCC
–		General	
67	SP6-F	<i>SP6 Promoter Primer</i>	GATTTAGGTGACACTATAG
68	T7-F	<i>T7 Promoter Primer</i>	TAATACGACTCACTATAGG
–		qPCR oligos & probes	
69	B2-48F		AACGGCGGTGGAAGCA
70	B2-98R		TTGTTCCGTGCCCTTTGGT
71	B2-65T	<i>B2 probe</i>	CCATGGGAATGAGC
72	EGFP-615F		GTCCCGCCCTGAGCAAAGA
73	EGFP-668R		TCCAGCAGGACCATGTGATC
74	EGFP-634T	<i>EGFP probe</i>	CCCAACGAGAAAGCG

Appendix II

Perl script for comparing identity blocks

Perl script for comparing identity blocks

```
#!/usr/bin/perl

#COMPARE AND TALLY BLOCKS OF IDENTITY
#INPUT = PRE-ALIGNED PAIRWISE ALIGNMENT AS SINGLE FASTA FILE
#OUTPUT = FILE "OUTPUT" IN WORKING DIRECTORY, SINGLE LINE OF CSV WITH HEADER

use strict;
#use warnings;
use Bio::SeqIO;

my $seqio_obj = Bio::SeqIO->new(-file => '12QvMRE16.fas', -format => 'fasta');

my $seq1 = $seqio_obj->next_seq;
#print $seq1->seq, "\n\n";

my $seq2 = $seqio_obj->next_seq;
#print $seq2->seq, "\n\n";

my @seqA = split(undef, $seq1->seq);
my @seqB = split(undef, $seq2->seq);

if (scalar @seqA >= scalar @seqB){
    my $length = scalar @seqB;
    our @choice = @seqB;
    our @unchosen = @seqA;
    #print "\nThe choice was @seqB, length: ". scalar @choice ."\n";
} else {
    my $length = scalar @seqA;
    our @choice = @seqA;
    our @unchosen = @seqB;
    #print "\nThe choice was @seqA, length: ". scalar @choice ."\n";
}

my $end = scalar our @choice;
my $longer = scalar our @unchosen;

#print "\nThe chosen sequence was $end bp in length.";
#print "\nThe unchosen sequence was $longer bp in length.\n\n";

#print "Sequence 1 Length (including gaps): ", scalar @seqA, "\n";
```

```

#print "Sequence 2 Length (including gaps): ", scalar @seqB, "\n\n";
#the idea here was to make an array filled
#with 1s and 0s to be counted later

my $i = 0;
foreach (@choice){

    if ($unchosen[$i] eq $_){
        my $block = 1;
        our @output;
        push (@output, $block);
        #print $block;
        $i++;
    }

} else {
    my $block = 0;
    our @output;
    push (@output, $block);
    $i++;
    #print $block;

}

}

#print "\nThis is the output from the foreach loop:\n";
#print our @output, "\n\n";
#print "The binary array is ". scalar our @output. " bp long.\n\n";

my $idblock = 0;

foreach $_ (our @output){
    our @counts;
    if ($_ == 1){
        $idblock++;
    } else {
        push (@counts, $idblock);
        $idblock = 0;
    }
}

#print "This is the output of the second foreach loop:\n";
#print our @counts, "\n";

my $blocks = join(',', our @counts); #places commas between values into string
$blocks =~ s/,0//g; #remove zeroes

my @commas = split("", $blocks); #puts them back into an array

#print "Here is the new output:\n";
#print @commas, "\n";

my $header = "Block_length";

open (FILE, ">output");
print FILE $header, "\n";
foreach (@commas){

    print FILE $_;

}

print FILE "\n";

```

```

close (FILE);

print "Script executed successfully!\n";

exit;

#####

```

R script for analyzing and plotting perl script output

```

#sourcing in data from idblocks.pl and creating a nice histogram from it

data1 = scan("/media/INTERNAL/Personal_Items/JHSPH/Hardwick_Lab_Items/Thesis_U
Research/Mosquito_Project/Alphavirus_Alignments/ID_Block_Comparison/12QvTC83",
sep = ",",
skip = 1)
data2 = scan("/media/INTERNAL/Personal_Items/JHSPH/Hardwick_Lab_Items/Thesis_U
Research/Mosquito_Project/Alphavirus_Alignments/ID_Block_Comparison/12QvMRE16",
sep = ",",
skip = 1)
data3 = scan("/media/INTERNAL/Personal_Items/JHSPH/Hardwick_Lab_Items/Thesis_U
Research/Mosquito_Project/Alphavirus_Alignments/ID_Block_Comparison/MRE16vTC83
", sep = ",",
skip = 1)

summary (data1)
summary (data2)
summary (data3)

#Count the number of possible siRNAs based on the alignment

sub.data1 = data1[data1 >=21]
sub.data2 = data2[data2 >=21]
sub.data3 = data3[data3 >=21]

potential1 = sum(sub.data1-20)
potential2 = sum(sub.data2-20)
potential3 = sum(sub.data3-20)

#make a nice plot

par(las = 1, mfrow = c(3,2))
plot(data1,
      xlab = "Block_Uposition",
      ylab = "Block_ULength_(bp)",
      main = "SV_UdsTE12Q_vs._VEE_TC-83\nIdentity_UBlocks",
      ylim = c(0,30),
      pch = 16,
      col=ifelse(abs(data1) >= 21, 2, 1)
)
abline(h=21, lty = 2, col = "blue")

hist(data1,
      xlab = "Block_ULength_(bp)",
      ylab = "#_of_blocks",
      breaks = (max(data1)),
      main = "SV_UdsTE12Q_vs._VEE_TC-83\nNumber_of_blocks",
      ylim = c(0,200),
      xlim = c(0,25),
      col = "gray",
      pch = 2
)

```

```

)
plot(data2,
      xlab = "Block_position",
      ylab = "Block_Length_(bp)",
      main = "SV.dsTE12Q_vs._SV.MRE16\nIdentity_blocks",
      ylim = c(0,50),
      pch = 16,
      col=ifelse(abs(data2) >= 21, 2, 1))

abline (h=21, lty = 2, col = "blue")

hist (data2,
      xlab = "Block_Length_(bp)",
      ylab = "#_of_blocks",
      breaks = (max(data2)),
      main = "SV.dsTE12Q_vs._SV.MRE16\nNumber_of_blocks",
      ylim = c(0,200),
      xlim = c(0,50),
      col = "gray",
      pch = 2
)

plot(data3,
      xlab = "Block_position",
      ylab = "Block_Length_(bp)",
      main = "SV.MRE16_vs._VEE.TC-83\nIdentity_blocks",
      ylim = c(0,30),
      pch = 16, col=ifelse(abs(data3) >= 21, 2, 1))

abline (h=21, lty = 2, col = "blue")

hist(data3,
      xlab = "Block_Length_(bp)",
      ylab = "#_of_blocks",
      main = "SV.MRE16_vs._VEE.TC-83\nNumber_of_blocks",
      ylim = c(0,200),
      xlim = c(0,25),
      col = "gray",
      pch = 2
)

print("The_number_of_theoretical_siRNAs_for.dsTE12Q_compared_to_TC-83_is:")
print (potential1)
print ("The_number_of_theoretical_siRNAs_for.dsTE12Q_compared_to_MRE16_is:")
print (potential2)
print ("The_number_of_theoretical_siRNAs_for.MRE16_compared_to_TC-83_is:")
print (potential3)

```



John R Clayton

SCIENTIST · VECTOR-BORNE DISEASES

2525 North Filbert Road, Exeter, California 93221 USA

+1 (559) 769-7805 | jrclayton@yahoo.com | [jrclayton](https://www.linkedin.com/in/jrclayton/) | [johnrandyclayton](https://www.facebook.com/johnrandyclayton) | [jrclayton](https://www.instagram.com/jrclayton/) | [John-Clayton-6](https://www.google.com/search?q=John+Clayton+6)

"Time flies like an arrow. Fruit flies like a banana."



Summary

I am a molecular biologist by training with 15 years of experience working on the genetics of disease vector mosquitoes. I have a PhD in Molecular Microbiology & Immunology from Johns Hopkins University. A California native, I was born and raised near Blythe, in the remote expanses of the Sonoran desert. Over the years, I've held more than a dozen positions in the US States of California, Georgia and Maryland as well as Heidelberg, Germany and Strasbourg, France. In addition to being a native speaker of English, I have a working knowledge of French, Spanish & German.

Education

Johns Hopkins Bloomberg School of Public Health

Baltimore, MD

Department of Molecular Microbiology & Immunology

DOCTORATE

2003-2010

Dissertation: *Transduction of Virulence Factors by Alphaviruses in Vertebrate and Invertebrate Models of Infection*

Johns Hopkins Bloomberg School of Public Health

Baltimore, MD

Department of International Health

CERTIFICATE, VACCINE SCIENCE & POLICY

2003-2005

University of California

Berkeley, CA

Department of Molecular & Cell Biology

BACCALAUREATE

1996-2000

Emphasis: *Genetics & Development*

Work Experience

Université de Strasbourg

Strasbourg, France

Institut de Biologie Moléculaire et Cellulaire

POST-DOCTORAL RESEARCHER

2011-2015

As a fellow with the French *Institut national de la santé et de la recherche médicale* (INSERM), I successfully developed reagents to silence single alleles of polymorphic genes in *An. gambiae* to determine the contribution of each allele to susceptibility to *Plasmodium* infection in the mosquito. My other main research project involved the characterization of a transgenic strain of *An. gambiae* that produces small piwi-like RNAs derived from its integrated transgene locus, causing them to become hyper-susceptible to *Plasmodium* infection.

Johns Hopkins Bloomberg School of Public Health

Baltimore, MD

Department of Molecular Microbiology & Immunology

PRE-DOCTORAL RESEARCHER

2003-2010

My dissertation research largely involved the characterization of and acquired, sequence-specific anti-viral resistance phenotype observed in *Aedes aegypti* during Alphavirus infection. I also developed a recombinant, mosquitocidal Alphavirus expressing the pro-apoptotic gene *reaper* and evaluated its suitability as a potential biocontrol agent. Another project involved comparative analysis of the Bunyavirus virulence factor NSs in mice and mosquitoes.

European Molecular Biology Laboratory

Heidelberg, Germany

Kafatos Group

POST-BACCALAUREATE RESEARCHER

2002-2003

While working in the Kafatos lab I developed a transgenic strain of *An. gambiae* expressing a fluorescent reporter specifically in midgut epithelial cells that had been invaded by the malaria parasite. In parallel, I performed functional analysis of immunity genes and identified a role for the mosquito NF-κB-like transcription factor *REL2* during *Plasmodium* infection.

Centers for Disease Control & Prevention

Atlanta, GA

Entomology Branch

EMERGING INFECTIOUS DISEASES FELLOW

2000-2002

While an EID fellow at the CDC, I invented the breakthrough transformation method for *An. gambiae* still in use today. I also characterized the transgenic strains we obtained while working with both *P. vivax* and *P. falciparum* malaria parasites in a BSL-2 environment. Field work opportunities included surveillance for West Nile Virus and assisting in CDC's emergency response during the 2001 Anthrax bioterror crisis.

University of California

Berkeley, CA

Department of Integrative Biology

RESEARCH ASSISTANT

1998-1999

While in the Brent Mishler's laboratory I evaluated the utility of RNA secondary structures to reconstruct deep phylogenies of green plants.

Languages

Spoken	<ul style="list-style-type: none"> English French Spanish German 	

Programming	<ul style="list-style-type: none"> R LaTeX Python Bash 	

Skills

Laboratory

- Expert at a wide array of molecular biology, biochemistry & genetics techniques
-

Entomology

- Expert at all aspects of cultivating and maintaining colonies of *Anopheles* & *Aedes* mosquitoes

-

Software

- Expert user of the Microsoft Windows, Apple Mac OS X, Darwin/BSD Unix and Linux operating systems

-

Teaching Experience

Université de Strasbourg

Strasbourg, France

Institut de Biologie Moléculaire et Cellulaire

MASTER'S STUDENT MENTOR

2011-2015

Technical oversight of three master's level students with projects related to functional analysis of *Anopheles* genes during malaria infection and *in vivo* RNA interference in *Anopheles* and *Drosophila*.

Johns Hopkins Bloomberg School of Public Health

Baltimore, MD

Department of Molecular Microbiology & Immunology

TEACHING ASSISTANT

2005

Graduate student instructor for Molecular Entomology. Lead exam reviews for students before midterm and final.

University of California

Berkeley, CA

TEACHING ASSISTANT

2000

Undergraduate student instructor for Health and Medical ethics.

Honors & Awards

2004	Scholarship	Dr. Lloyd and Mae Rozeboom Scholarship in Medical Entomology	Baltimore, MD
2000	Fellowship	Emerging Infectious Diseases Laboratory Research Fellowship	Atlanta, GA
1999	Travel Grant	Deep Green Travel Grant for the XVI International Botanical Congress	Berkeley, CA
1996	Scholarship	Blythe Jaycees Scholarship	Blythe, CA

Training Courses

- Ethics & Safety**
- Chemical and biological waste disposal practices and safety training
 - Radioactive isotope certification and safety training
 - Ethical use of vertebrate animals in research training

Extracurricular Activities

Phi Kappa Tau Fraternity

Berkeley, CA

MEMBER, NU CHAPTER

1997-2000

As member of the fraternity, I held the positions of Scholarship Chair and Secretary as well as serving on the chapter Executive Committee.

The Daily Californian

Berkeley, CA

PRODUCTION INTERN

1998

Responsible for daily page layout

UC Berkeley Intercollegiate Bowling Team

Berkeley, CA

MEMBER

1996-1997

Selected for the university bowling team as a first semester freshman

PVHS Class of 1996

Blythe, CA

PRESIDENT

1995-1996

Elected to serve as Senior class president

PVHS Yellowjackets Golf Team

Blythe, CA

VARSITY LETTERMAN

1993-1996

Played on varsity golf team for four years

The Stinger

Blythe, CA

EDITOR

1993-1994

Features Editor and Advertisement Sales for our student newspaper

Personal Interests

In my spare time, I like to travel and visit monuments, museums and parks. Activities I enjoy include bowling, cycling, golf, tennis, volleyball and poker. I also enjoy dining, cinema, theater and classical as well as contemporary live music performances.

Published Research

Lamacchia, Marina, **Clayton, John R**, Rui Wang-Sattler, Lars M Steinmetz, Elena A Levashina, and Stéphanie Blandin (2013). "Silencing of Genes and Alleles by RNAi in Anopheles gambiae". In: *Methods in Molecular Biology* 923.2, pp. 161–176.

Clayton, John R (2010). "Transduction of Virulence Factors by Alphaviruses in Vertebrate and Invertebrate Models of Infection". Dissertation. Johns Hopkins University, p. 193.

Clayton, John R and J Marie Hardwick (2008). "Apoptosis and Virus Infection". In: *Encyclopedia of Virology*. Ed. by BWJ Mahy and MHV Van Regenmortel. 3rd. Oxford: Academic Press. Chap. Apoptosis, pp. 154–162.

Lobo, Neil F, **Clayton, John R**, Malcolm J Fraser, Fotis C Kafatos, and Frank H Collins (2006). "High efficiency germ-line transformation of mosquitoes." In: *Nature Protocols* 1.3, pp. 1312–1317.

Meister, Stephan, Stefan M Kanzok, Xue-Li Zheng, Coralia Luna, Tong-Ruei Li, Ngo T Hoa, **Clayton, John R**, Kevin P White, Fotis C Kafatos, George K Christophides, and Liangbiao Zheng (2005). "Immune signaling pathways regulating bacterial and malaria parasite infection of the mosquito Anopheles gambiae." In: *Proceedings of the National Academy of Sciences of the United States of America* 102.32, pp. 11420–11425.

Grossman, Genelle L, Cristina S Rafferty, **Clayton, John R**, Theresa K Stevens, Odette Mukabayire, and Mark Q Benedict (2001). "Germline transformation of the malaria vector, Anopheles gambiae, with the piggyBac transposable element." In: *Insect molecular biology* 10.6, pp. 597–604.

Photographs

Enserink, Martin (2002). *Ecologists see flaws in transgenic mosquito.*

Jasny, Barbara R and Orla M Smith (2002). Poster: MOSQUITO Anopheles gambiae.

Enserink, Martin (2001). *Two New Steps Toward a 'Better Mosquito'.*

Patents

Levashina, Helena, Stéphanie Blandin, Fotis Kafatos, **Clayton, John**, Shin-Hong Shiao, and Luis Moita (2004). "Use of Thioester-Containing Proteins (TEPs) for triggering/inducing an immune response in mosquitoes of Anopheles against Plasmodium."

Research Presentations

Clayton, John R (2002). *Transgenesis in Anopheles gambiae*. Strasbourg, France.

Bendik, Jean, **Clayton, John R**, Andrew Hopkins, Lauren Singer, and Fernando Torres (2001). *EID Roundtable – Q and A Session From Current EID Fellows*. Atlanta, GA USA.

Clayton, John R and Mark Q Benedict (2001). *Germline Transformation of Anopheles gambiae with the piggyBac transposable element*. Atlanta, GA USA.

Courses Attended

Clayton, John R and Stéphanie A Blandin (2011). *Identifying Loci Controlling Resistance to Plasmodium Infection in the Mosquito Anopheles gambiae*. Heidelberg, Germany.

International Bioinformatics Workshop on Malaria Vectors, Sponsored by The Johns Hopkins Malaria Research Institute (2003). Baltimore, MD USA.

Posters

Clayton, John R, Julien Pompon, Elena A Levashina, and Stéphanie A Blandin (2014). *An immunodeficient transgenic Anopheles gambiae line to study the mosquito complement system*. New Orleans, LA USA.

Clayton, John R and J Marie Hardwick (2009). *Potent Acquired Antiviral Immunity in the Yellow Fever Mosquito Aedes aegypti*. Baltimore, MD USA.

Clayton, John R, Heidi L Galonek, Beth Lamos, Mary Vander-Maten, Pablo Irusta, and J Marie Hardwick (2006). *Effects of Drosophila reaper in Mosquitoes*. Big Sky, MT USA.

Benedict, Mark Q, **Clayton, John R**, and Genelle L Grossman (2001). *Mobility of piggyBac in Anopheles gambiae*. Barcelona, Spain.

Clayton, John R and John A Wheeler (1999). *Phylogenetic significance of rbcL secondary structures*. St. Louis, MO USA.